National Library of Canada
Bibliothèque nationale du Canada

Canadian Theses Service
Service des thèses canadiennes

Ottawa, Canada
K1A 0N4

NOTICE

The quality of this microform is heavily dependent upon the quality of the original thesis submitted for microfilming. Every effort has been made to ensure the highest quality of reproduction possible.

If pages are missing, contact the university which granted the degree.

Some pages may have indistinct print especially if the original pages were typed with a poor typewriter ribbon or if the university sent us an inferior photocopy.

Previously copyrighted materials (journal articles, published tests, etc.) are not filmed.

Reproduction in full or in part of this microform is governed by the Canadian Copyright Act, R.S.C. 1970, c. C-30.

AVIS

La qualité de cette microforme dépend grandement de la qualité de la thèse soumise au microfilmage. Nous avons tout fait pour assurer une qualité supérieure de reproduction.

S'il manque des pages, veuillez communiquer avec l'université qui a conféré le grade.

La qualité d'impression de certaines pages peut laisser à désirer, surtout si les pages originales ont été dactylographiées à l'aide d'un ruban usé ou si l'université nous a fait parvenir une photocopie de qualité inférieure.

Les documents qui font déjà l'objet d'un droit d'auteur (articles de revue, tests publiés, etc.) ne sont pas microfilmés.

La reproduction, même partielle, de cette microforme est soumise à la Loi canadienne sur le droit d'auteur, SRC 1970, c. C-30.

NL-339 (r. 88/04)

Canada

THE UNIVERSITY OF ALBERTA

SODIUM-DRIVEN NUCLEOSIDE TRANSPORT IN MOUSE LEUKEMIA L1210 CELLS

by

LINA DAGNINO

(C)

A THESIS

SUBMITTED TO THE FACULTY OF GRADUATE STUDIES AND RESEARCH

IN PARTIAL FULFILLMENT OF THE REQUIREMENTS FOR THE DEGREE

DOCTOR OF PHILOSOPHY

DEPARTMENT OF PHARMACOLOGY

EDMONTON, ALBERTA

FALL, 1988

Permission has been granted to the National Library of Canada to microfilm this thesis and to lend or sell copies of the film.

The author (copyright owner) has reserved other publication rights, and neither the thesis nor extensive extracts from it may be printed or otherwise reproduced without his/her written permission.

L'autorisation a été accordée à la Bibliothèque nationale du Canada de microfilmer cette thèse et de prêter ou de vendre des exemplaires du film.

L'auteur (titulaire du droit d'auteur) se réserve les autres droits de publication; ni la thèse ni de longs extraits de celle-ci ne doivent être imprimés ou autrement reproduits sans son autorisation écrite.

ISBN 0-315-45748-1

THE UNIVERSITY OF ALBERTA

RELEASE FORM

NAME OF AUTHOR: Lina Dagnino

TITLE OF THESIS: Sodium-Driven Nucleoside Transport in Mouse Leukemia L1210 Cells

DEGREE FOR WHICH THESIS WAS PRESENTED: DOCTOR OF PHILOSOPHY

YEAR THIS DEGREE GRANTED: FALL, 1988

Permission is hereby granted to THE UNIVERSITY OF ALBERTA LIBRARY to reproduce single copies of this thesis and to lend or sell such copies for private, scholarly or scientific research purposes only.

The author reserves other publication rights, and neither the thesis, nor extensive extracts from it may be printed of otherwise reproduced without the author's written permission.

Lina Dagnino

Apdo. Postal 590

Toluca, Mexico

25 July 1988

THE UNIVERSITY OF ALBERTA

FACULTY OF GRADUATE STUDIES AND RESEARCH

The undersigned certify that they have read, and recommend to the Faculty of Graduate Studies and Research for acceptance, a thesis entitled **Sodium-Driven Nucleoside Transport in Mouse Leukemia L1210 Cells**, submitted by **Lina Dagnino** in partial fulfillment of the requirements for the degree of DOCTOR OF PHILOSOPHY.

ARP Paterson

Supervisor

A Clanachan

Carl E Cass

J. Francis Henderson

J D Young

External Examiner

25 July 1988

To my parents
and to A.R.P. Paterson

They guided my thought,
and inspired my pursuit of life

ABSTRACT

The nucleoside transport (NT) inhibitor dipyridamole enhanced the antiproliferative activity of 2'-deoxyadenosine and 9-beta-D-arabinofuranosyladenine (araA) towards cultured mouse leukemia L1210/C2. Increased araA antiproliferative activity occurred with enhancement of the cellular content and retention of araA and its 5'-triphosphate (araATP). AraA and araATP accumulation was also induced by the NT inhibitors, dilazep and nitrobenzylthioinosine (NBMPR). These effects arose from inhibition of non-concentrative, reversible NT systems, without effect on a sodium-dependent, concentrative, and inwardly-directed NT system.

The sodium-linked NT system of L1210/AM cells (i) translocated some purine nucleosides and uridine, but not thymidine, (ii) was impaired when alkali metal or N-methyl-D-glucammonium ions replaced extracellular Na^+ (Na^+_o), or transmembrane Na^+ gradients were abolished, and (iii) was unaffected by substitution of extracellular Cl^- by SCN^- or SO_4^{-2} ions.

When Na^+_o was 100 mM, the K_m and V_{max} for adenosine (Ado) transport were, respectively, 10 uM and 1.7 pmol/ul cell water.sec. $K_{0.5}$ values for Ado-coupled Na^+ fluxes decreased from 30 mM to 3 mM when Ado was increased from 0.5 uM to 100 uM. Hill analysis of the dependence of Ado fluxes on Na^+_o yielded an Na^+:Ado stoichiometry of 1:1.

Sodium-dependent Ado transport was inhibited by N-

ethylmaleimide, showdomycin and *p*-chloromercuri-phenylsulphonate (*p*CMBS). Partial protection of sodium-driven Ado transport from inhibition by *p*CMBS occurred (i) when Ado was present during cell incubation with *p*CMBS, or (ii) by sequential cell treatment with *p*CMBS and 2-mercaptoethanol. *p*CMBS possibly reacted with thiol groups essential for transport activity.

A NT variant clone, L1210/B23.1, was isolated from L1210/MC5-1 cells (a NT mutant of wild type L1210 cells). L1210/B23.1 cells apparently lack sodium-dependent NT activity because (i) initial rates of formycin B (FB) influx were similar in cells suspended in Na^+-containing, and in Na^+-free medium (0-10 uM NBMPR present), and (ii) NBMPR induced FB accumulation in L1210/MC5-1, but not in L1210/B23.1 cells.

Co-administration of NBMPR phosphate (NBMPR-P) and 2-fluoro-araA phosphate (FAMP) to mice bearing L1210/C2 leukemia enhanced (i) the increase in life span of animals that died leukemic deaths, and (ii) 60-day survivorship. Several leukemic mice receiving FAMP developed fatal, delayed neurotoxicity (evident as hind limb paralysis), which was reduced or prevented by NBMPR-P.

ACKNOWLEDGEMENTS

My deepest gratitude is reserved for Dr. A.R.P. Paterson. Without his guidance, patience and encouragement, the last three years would not have been so fulfilling and accomplished. It was my good fortune to benefit from his willingness to share a wealth of experience and insight.

I would like to thank Drs. W.P. Gati and E.S. Jakobs for their assistance and friendship. Thanks are due to Dr. C.E. Cass for her advice, and M. Selner, whose help with cell culture was invaluable. I extend my gratitude to the staff of the McEachern Laboratory for their companionship, and Friday afternoon goodies.

I am indebted to Dr. L.L. Bennett, Jr. for his generous gift of the L1210/AM clone, instrumental in the development of this project. I also thank Dr. J.A. Belt, who kindly provided L1210/B2 and L1210/MC5-1 cells, in addition to a manuscript prior to publication describing the latter cells.

I wish to acknowledge the assistance of H. El-Sharkawi and Dr. L.W. Brox, and J. Chlebek and Dr. A.R. Morgan in experiments of DNA extraction, and Dr. J.D. Harrison and the Department of Chemistry in atomic spectrophotometric measurements. Thanks to A.A. Adjei for his input in chemotherapy experiments, and to B. Hunter for literary advice.

Financial support from the Alberta Heritage Foundation for Medical Research and the National Cancer Institute of Canada is gratefully acknowledged.

TABLE OF CONTENTS

	Page
ABSTRACT	v
ACKNOWLEDGEMENTS	vii
LIST OF TABLES	xv
LIST OF FIGURES	xvii
LIST OF ABBREVIATIONS	xxiv
INTRODUCTION	1
1. Nucleoside permeation in mammalian cells	1
2. The simple carrier model for non-concentrative transport	2
3. Nucleoside transport in erythrocytes	4
a) Substrate specificity and kinetic properties	4
b) Inhibitors of NT in erythrocytes	5
c) Structural properties of NT systems in erythrocytes	7
4. Non-concentrative NT in mammalian nucleated cells	8
a) Substrate specificity and kinetic properties	8
b) Inhibitors of non-concentrative NT systems	9
c) Structural studies	11
5. Secondary-active NT systems	12

Page

6. Modulation of nucleoside analogue toxicity by transport inhibitors 15
7. Cellular metabolism of dAdo, araA and 2-F-araA 19
8. Research proposal 21

METHODS 24

I. CHEMICALS 24

II. CELL CULTURE PROCEDURES 25
1. Cell lines 25
a) L1210/C2 25
b) L1210/araC/MeMPR (L1210/AM) 26
c) L1210/MC5-1 26
d) L1210/B23.1 27
2. Measurement of clonogenic viability 27
3. Measurement of proliferation rates 28
4. Mutagenesis and mutant isolation techniques 28
III. ANALYTICAL PROCEDURES 29
1. Purification of radiochemicals 29
2. Preparation of PEI(borate) cellulose plates 29
3. Analysis of intracellular anabolites of nucleosides 31
a) Preparation of cell extracts 31
b) Effects of ADA inhibitors on nucleoside deamination 31

Page

c) TLC analysis of dAdo and araA anabolites 32

4. Extracellular products derived from nucleoside anabolites 34

5. Isolation of nucleic acids 35

a) Composition of solutions utilized . . . 35

b) Procedure 36

6. Measurement of intracellular sodium 38

7. Measurement of cellular ATP concentrations 40

IV. EXPERIMENTS WITH CULTURED CELLS 40

1. Cellular accumulation of nucleosides or nucleoside analogues and their anabolites 40

2. Cellular retention of nucleoside 5'-triphosphates 42

3. Cellular depletion of ATP 42

4. Transport measurements 42

a) Composition of transport media 42

b) Transport assay protocol 45

5. Binding assays 47

a) Time courses of ^{3}H-NBMPR binding 47

b) Equilibrium binding of ^{3}H-NBMPR 48

V. CHEMOTHERAPY EXPERIMENTS 48

Page

RESULTS 47

I. EFFECTS OF NT INHIBITORS ON THE TOXICITY AND CELLULAR METABOLISM OF NUCLEOSIDE ANALOGUES IN L1210/C2 CELLS 50

1. Enhancement by dipyridamole of the anti-proliferative activity, accumulation and retention of dAdo and dATP in L1210/C2 cells 50

2. Effect of NT inhibitors on accumulation, retention and antiproliferative activity of araA and araATP 55

3. Effect of NT inhibitors on retention of cellular araATP 64

4. Influence of dipyridamole and araA on cell proliferation rates and viability in cultures of L1210/C2 cells 69

5. Relationship between cellular formation of araATP and incorporation of araA into DNA 72

6. Enhancement by dipyridamole of the anti-proliferative activity of purine nucleoside analogues 77

7. Modulation by dipyridamole of araC toxicity and araCTP retention in L1210/C2 cells . . 79

II. NUCLEOSIDE TRANSPORT IN L1210 CELLS 87

1. *Influx of FB and araA in L1210/C2 cells* . . 87

Page

2. Transport of nucleosides in L1210/AM cells 94
   a) Concentrative NT in L1210/AM cells . . . 94
   b) Site-specific binding of NBMPR to L1210/AM cells 100
   c) Sensitivity of NT systems in L1210/AM cells to NBMPR, dipyridamole and dilazep 105
3. Dependence of the concentrative NT system in L1210/AM cells on sodium electrochemical gradientes 109
4. Anion requirements of sodium-driven Ado transport 116
5. Temperature dependence of sodium-driven NT activity in L1210/AM cells 116
6. Substrate specificity 120
7. Kinetic studies of sodium-linked Ado transport in L1210/AM cells 128
8. Stoichiometry of sodium-linked Ado transport in L1210/AM cells 135
9. Drug effects on sodium-dependent Ado transport 141
10. Effect of thiol-modifying reagents 145

Page

IV. SELECTION OF A CLONE OF L1210 CELLS DEFICIENT IN SODIUM-LINKED NUCLEOSIDE TRANSPORT . . . 153

V. CHEMOTHERAPY OF L1210 MOUSE LEUKEMIA WITH ARA-AMP OR FAMP AND INHIBITORS OF NUCLEOSIDE TRANSPORT 166

SUMMARY AND FUTURE DIRECTIONS 176

REFERENCES 187

LIST OF TABLES

Table		Page
1	HPLC elution times of nucleosides and nucleoside analogues	30
2	Mobilities of nucleosides and nucleoside 5'-phosphates on PEI-cellulose thin-layer chromatograms	33
3	HPLC elution system for ATP analysis	41
4	ATP concentration in L1210/AM cells after treatment with rotenone or DNP	43
5	TLC analysis of medium from suspensions of [^{3}H]dATP-ccntaining cells	58
6	TLC analysis of medium from suspensions of [^{3}H]araATP-containing cells	68
7	Effect of exposure to araA, dCF and dipyridamole on the clonogenic viability of L1210/C2 cells	73
8	Summary: modulation by dipyridamole of antiproliferative activity and accumulation of nucleoside analogues in L1210/C2 cells	86
9	Nucleoside metabolism in L1210 cells	97
10	Intracellular sodium concentrations	112

Table		Page
11	Inhibition of sodium-linked transport of Ado in L1210/AM cells by purine and pyrimidine nucleosides	125
12A	The sodium-linked NT system of L1210/AM cells: dependence of Ado transport characteristics (K_m, V_{max}) on the extracellular concentration of Na^+	131
12B	The sodium-linked NT system of L1210/AM cells: dependence of "Na^+/Ado" transport characteristics ($K_{0.5}$) on the extracellular concentration of Ado	132
13	Characteristics of the sodium-dependent NT system in L1210/AM cells	152
14	Treatment of mice implanted with leukemia L1210/C2 cells with combinations of araAMP, dCF and dipyridamole	167
15	Neurological toxicity of antimetabolites	169
16	Treatment of mice implanted with leukemia L1210/C2 cells with FAMP and NT inhibitors	172

LIST OF FIGURES

Fig.		Page
1	Standard plot for determination of sodium by atomic emission spectrophotometry	39
2	Enhancement by dipyridamole of antiproliferative effects of dAdo towards L1210/C2 cells	51
3	Enhancement by dipyridamole of the content of dAdo and dATP in L1210/C2 cells	53
4	Enhancement by dipyridamole of dATP retention in L1210/C2 cells	56
5	Extracellular decay products of cellular ^{3}H-dATP	57
6	Accumulation of araA and araATP in L1210/C2 cells.	60
7	Accumulation of araA and araATP in L1210/C2 cells treated with 1.5 uM EHNA and NT inhibitors	62

Fig.		Page
8	Decay of cellular levels of araATP in the presence of NT inhibitors	66
9	Decay product of cellular ^{3}H-araATP	67
10	Proliferation rates of L1210/C2 cells in medium containing araA	70
11	Effect of araA and dipyridamole on the proliferation of L1210/C2 cells	71
12	AraA incorporation into DNA and RNA in L1210/C2 cells	75
13	Relationship between cellular araATP concentrations and araA incorporation into DNA in L1210/C2 cells	76
14	Enhancement of antiproliferative effects of 2-F-araA in the presence of dipyridamole	78
15	Effects of dipyridamole on the anti-proliferative effects of 2-Br-2'-dAdo on L1210/C2 cells	80

Fig.		Page
16	Dipyridamole enhancement of the anti-proliferative activity of 2-Cl-2'-dAdo on L1210/C2 cells	81
17	Dipyridamole protection against the anti-proliferative effects of araC in L1210/C2 cells	83
18	Enhancement in the cellular retention of araCTP by NT inhibitors	84
19	Dipyridamole-insensitive FB influx in L1210/C2 cells	88
20	Sodium-dependence of dipyridamole-insensitive FB influx in L1210/C2 cells	90
21	Effect of NT inhibitors on inward fluxes of FB in L1210/C2 cells	92
22	Inhibition of araA uptake in L1210/C2 cells	95
23	Concentrative influx of 60 uM FB in L1210/AM cells	98
24	Sodium-dependence of concentrative dAdo transport in L1210/AM cells	99

Fig.		Page
25	Time courses of ^{3}H-NBMPR binding to L1210/AM cells at 22°C in sodium medium	101
26	Site-specific binding of ^{3}H-NBMPR to L1210/AM cells	102
27	Concentration-effect plots of inhibition by NBMPR of FB transport in L1210/AM cells	104
28	Concentration-effect plots for the inhibition by dipyridamole of Ado transport in L1210/AM cells	107
29	Concentration-effect plots of inhibition by dilazep of Ado transport in L1210/AM cells	108
30	Sodium dependence of Ado permeation in L1210/AM cells in medium containing dipyridamole	111
31	Effect of nystatin on Ado permeation in L1210/AM cells in dipyridamole-containing medium	113
32	Dipyridamole-insensitive transport of Ado in energy-depleted L1210/AM cells	115

Fig.		Page
33	Effect of chloride ion substitution on sodium-linked transport of dAdo in L1210/AM cells	117
34	Effects of temperature on sodium-linked transport of 20 uM Ado	119
35	Low rates of sodium-linked Ado influx in L1210/AM cells at 5°C	121
36	Concentrative influx of araA in dCF-treated L1210/AM cells	122
37	Permeant specificity of the sodium-linked NT system in L1210/AM cells	124
38	Dependence of sodium-driven Ado transport on extracellular concentrations of Ado and Na^+	129
39	Ado and ^{22}Na influx in sodium-depleted and ATP-depleted L1210/AM cells	138
40	Hill analysis of the dependence of Ado transport rates on the extracellular concentrations of Na^+ and Ado	140

Fig.		Page
41	Effect of agents that influence ion movements on inward Ado fluxes by the sodium-linked NT system in L1210/AM cells	142
42	Effect on NEM on the sodium-dependent transport of 10 uM Ado in L1210/AM cells	147
43	Effect of prior incubation of L1210/AM cells withshowdomycin on sodium-linked Ado (10 uM) transport	149
44	Effect of *p*CMBS on sodium-linked Ado transport in L1210/AM cells	150
45	Concentration-effect relationships for the inhibition of FB (10 uM) transport in L1210/MC5-1 cells	155
46	Effect of NBMPR on the influx of FB in L1210/MC5-1 cells	156
47	Enhancement by dipyridamole of the antiproliferative effects of araA towards L1210/MC5-1 cells	158

Fig.		Page
48	Effect of NBMPR on the influx of FB in L1210/B23.1 cells	161
49	Concentration-effect relationships for NBMPR inhibition of FB (10 uM) transport in L1210/B23.1 cells	163
50	Effect of dipyridamole on the antiproliferative activity of araA towards L1210/B23.1 cells	164

LIST OF ABBREVIATIONS

ADA	Adenosine deaminase
Ado	Adenosine
ATP	Adenosine 5'-triphosphate
araA	9-Beta-D-arabinofuranosyladenine
(araA)DNA	DNA containing araA residues
araADP	AraA 5'-diphosphate
araAMP	AraA 5'-monophosphate
araATP	AraA 5'-triphosphate
araC	1-Beta-D-arabinofuranosylcytosine
araCTP	AraC 5'-triphosphate
araH	9-Beta-D-arabinofuranosylhypoxanthine
2-Br-2'-dAdo	2-Bromo-2'-deoxyadenosine
2-Cl-2'-dAdo	2-Chloro-2'-deoxyadenosine
Cyd	Cytidine
dAdo	Deoxyadenosine
dADP	dAdo 5'-diphosphate
dAMP	dAdo 5'-monophosphate
dATP	dAdo 5'-triphosphate
dCF	2'-Deoxycoformycin
dCyd	2'-Deoxycytidine
ddAdo	2',3'-Dideoxyadenosine
dIno	2'-Deoxyinosine
Dip	Dipyridamole
DMF	N,N-demethylformamide
DMSO	Dimethylsulphoxide
DNP	2,3-Dinitrophenol
dThd	2'-Deoxythymidine
dUrd	2'-Deoxyuridine
EDTA	Ethylenediaminetetraacetic acid
EHNA	Erythro-9-(2-hydroxy-3-nonyl)adenine
2-F-Ado	2-Fluoro-Ado

2-F-araA	2-Fluoro-araA
FAMP	2-Fluoro-AraA 5'-monophosphate
FB	Formycin B
5-F-Urd	5-Fluoro-uridine
5-FU	5-Fluorouracil
Guo	Guanosine
HEPES	4-(2-hydroxyethyl)-1-piperazineethanesulphonic acid
HNBTGR	2-Amino-6-[(2-hydroxy-5-nitro)thio]-9-beta-D-ribofuranosylpurine
HPLC	High-performance liquid chromatography
IC_{50}	Concentration of drug(s) inhibiting the parameter measured in individual experiments by 50%
Ino	Inosine
kDa	Kilo-Dalton
MeMPR	Methylmercaptopurine ribonucleoside
MTX	Methotrexate
NBdAdo	N^6-(4-nitrobenzyl)-2'-dAdo
NBMPR	Nitrobenzylthioinosine; 6-[(4-nitrobenzyl)-thio)]-9-beta-D-ribofuranosylpurine
NBMPR-P	NBMPR 5'-monophosphate
NBTGR	Nitrobenzylthioguanosine; 2-amino-6-[(4-nitrobenzyl)thio]-9-beta-D-ribofuranosylpurine
NEM	N-ethylmaleimide
NMG	N-methyl-D-glucammonium
NT	Nucleoside transport
PBS	Phosphate-buffered saline solution
pCMBS	p-Chloromercuriphenylsulphonate
PEG	Polyethyleneglycol
PEI	Polyethyleneimine
SAH	S-Adenosylhomocysteine
S.D.	Standard deviation

SDS	Sodium dodecylsulphate
TBP	Tris-buffered phenol
TCA	Trichloroacetic acid
TLC	Thin-layer chromatography
Tris	Tris-(hydroxymethyl)aminomethane
Urd	Uridine
UV	Ultraviolet

INTRODUCTION

1. Nucleoside permeation in mammalian cells

Nucleosides enter mammalian cells by passive diffusion and/or mediated permeation. Mediated permeation of nucleosides, designated as transport (1), occurs *via* concentrative or facilitated diffusion mechanisms[1]. The relative contributions to influx of passive diffusion, non-concentrative and concentrative transport of a nucleoside vary depending on the cell type, the nature of the permeant and its concentration in the extracellular medium (2,3).

Lipophilic nucleoside analogues, such as 3'-deoxy-3'-azidothymidine and 2',3'-dideoxythymidine, permeate human erythrocytes by non-mediated processes (2,4). In some cells, such as mouse erythrocytes infected with *Plasmodium yoelii*[2] and in cultured HOC-7 human ovarian carcinoma cells (5), a substantial fraction of Ado permeation appears to occur by passive diffusion.

Passive diffusion contributes little to permeation of physiological nucleosides because the latter are hydrophilic molecules and diffuse poorly across the lipid

---

[1] NT down concentration gradients is designated as "facilitated diffusion" or "non-concentrative" transport throughout this study.

[2] W.P. Gati and A.R.P. Paterson, unpublished results

bilayer of the plasma membrane. This has been demonstrated in studies in which inhibition of nucleoside transport (NT) protected various cell lines against the cytotoxicity of nucleoside analogues (6-8). In addition, nucleoside permeation in NT-deficient mutants of S49 mouse lymphoma and HCT-8 carcinoma cells is markedly lower than in the parent lines (9-11).

Non-concentrative NT systems have been identified in human erythrocytes and in various types of mammalian nucleated cells. In the former, nucleoside permeation is mediated by a single system which has been extensively studied. Three types of non-concentrative NT systems have been described in other mammalian cells, and one of these types may be similar to that present in human erythrocytes (*vide infra*). Non-concentrative NT systems have been the subject of several reviews (1,3,12-18).

Sodium-dependent, concentrative NT systems have been recognized in various cell types, including rat enterocytes, rat renal epithelial cells, rabbit choroid plexus and mouse splenocytes. It would appear that many sodium-dependent NT systems in various species and tissues may have characteristic substrate specificity (*vide infra*).

2. The simple carrier model for non-concentrative NT

The kinetic behaviour of the non-concentrative NT system of the human erythrocyte is consistent with that proposed for a simple carrier mechanism (19-21). The fea-

tures of the NT system of human erythrocytes include saturability of permeation rate as a function of nucleoside concentration, competition between permeating nucleosides, inhibition by specific agents, and *trans* phenomena, such as *trans*-acceleration[3] of Urd fluxes induced by permeant nucleosides like dThd, and counter-transport[4] (19-21).

Saturability of permeation rates is not observed when permeation occurs by passive diffusion; however, saturability of permeation rates is not exclusive to carrier-mediated permeant translocation and has also been reported for ion movements through some channels (22).

The phenomenon of *trans*-acceleration of the flux of a permeant induced by another permeant has been considered indicative of carrier-mediated translocation (22,23), although

---

[3] By convention, the *cis* face of the plasma membrane denotes the face from which transport is measured. Thus, permeant fluxes occur from the *cis* to the *trans* face (22,23). *Trans*-acceleration is defined as the increase in the flux of a permeant *A* from the *cis* face to the *trans* face of the membrane, induced by the presence of another substrate *B* at the *trans* face. *A* may be an isotopically-labelled form of *B*, or a structurally related permeant. The *trans*-acceleration of *A* will occur if (i) both *A* and *B* use the same carrier, and (ii)the translocation rate of the empty carrier is lower than that of the complex formed between the carrier and *B* (22-24)

the absence of this phenomenon does not necessarily signify that a putative permeant is not recognized by the transporter. For example, 2-chloroadenosine, which enters human erythrocytes *via* the nucleoside-specific transport system, decreased Urd efflux from human erythrocytes that were "loaded" with ^{3}H-Urd (24). *Trans*-inhibition of Urd efflux by 2-chloroadenosine was attributed to a lower translocation rate of the 2-chloroadenosine-loaded carrier relative to that of the Urd-loaded carrier.

3. Nucleoside transport in erythrocytes

a) Substrate specificity and kinetic properties

The NT system of human erythrocytes has broad substrate specificity, as shown by (i) influx measurements of radiolabelled nucleosides, (ii) inhibition of Urd influx by other nucleosides, and (iii) acceleration of Urd efflux by permeant nucleosides (12).

---

[4] Counter-transport of two substrates, observed only when permeation is mediated by a reversible transport system, will occur if a nucleoside *A* is allowed to achieve identical concentrations on both sides of the plasma membrane, and a nucleoside *B* is then added only to one side of the membrane. Nucleoside *B* will flow down its concentration gradient, inducing uphill fluxes of *A* in the opposite direction. The counter-flow of *A* and *B* indicates that these permeants are substrates for the same carrier mechanism (19,20)

The kinetic behaviour of the erythrocyte NT system has been reported to change upon storage. Thus, the maximum velocity for zero-*trans* efflux of Urd in stored erythrocytes was four-fold higher than that for zero-*trans* influx; this directional asymmetry of Urd fluxes was also observed under equilibrium exchange conditions (19). However, similar experiments with fresh erythrocytes showed directional symmetry of Urd transport in those cells (25,26).

b) Inhibitors of NT in erythrocytes

Nucleoside permeation in human erythrocytes is selectively inhibited by *p*-nitrobenzylthiopurine nucleosides such as NBMPR, NBTGR and some N^6-nitrobenzyl analogues of Ado and dAdo (13) at concentrations between 1 and 10 nM. Inhibition of NT in erythrocytes by NBMPR is reversible and has been correlated with high-affinity binding of NBMPR to sites in the erythrocyte plasma membrane. The number of NBMPR binding sites in mammalian erythrocytes ranges between zero and 10,000 *per* cell, with K_D values of about 1 nM (27,28).

NBMPR appears to bind to sites located on the outer face of the erythrocyte plasma membrane, as shown by studies that measured the temperature-dependence of changes in rates of NBMPR binding to membrane vesicles and unsealed ghosts from pig erythrocytes (29). These studies demonstrated that the rate of NBMPR binding to inside-out membrane vesicles was substantially reduced by a decrease in temperature from 22°C to 4°C. However, temperature decreases did not affect the rate of NBMPR binding to inside-out vesicles in the

presence of the detergent, saponin, or in preparations containing either right side-out vesicles or unsealed ghosts. These results were interpreted suggesting that NBMPR diffusion through the plasma membrane was reduced by lowering the temperature in the absence of detergents. Accordingly, the decrease in the rates of NBMPR binding at 4°C to inside-out, but not to right side-out vesicles indicated that NBMPR-binding sites are located on the outer face of the erythrocyte plasma membrane (29).

The binding of NBMPR to erythrocytes was found to be competitively inhibited by Ado and Urd; the K_i values for inhibition of NBMPR binding by these nucleosides were similar to their K_m values for equilibrium-exchange influx (19,30-32). Conversely, NBMPR was a competitive inhibitor of the influx and equilibrium exchange efflux of Urd in erythrocytes, but a non-competitive inhibitor of Urd efflux (19,32). These findings were interpreted to mean that NBMPR was bound by sites associated with the permeation site, and located on the outer face of the plasma membrane (17,30,32). The nature of the interaction between NBMPR and the nucleoside permeation site has been interpreted in terms of a model which proposes that the nucleoside permeation site and the inhibitor binding site are identical or share common regions (17). According to this model, the permeation site and the NBMPR binding site possess overlapping regions (17); NBMPR binds to the permeation site when the latter faces the outer side of the plasma membrane, and this interaction is

strengthened by hydrophobic attraction between the nitrobenzyl moiety in NBMPR and a region in the transporter proximal to the permeation site (17,30,33,34).

It has also been suggested that the relationship between the NBMPR binding site and the nucleoside permeation site in erythrocytes may involve allosteric interactions between inhibitor and permeant sites. The asymmetric nature of NBMPR binding to the erythrocyte plasma membrane, but the directional symmetry of Urd influx in those cells, have been considered as evidence supporting the concept that the NBMPR binding site and the nucleoside permeation site may be physically dissociated (18).

c) Structural properties of NT systems in erythrocytes

When the site-bound ligands, ^{3}H-NBMPR or ^{3}H-[N^{6}-(4-azidobenzyl)]-adenosine, were subjected to UV irradiation, a polypeptide functionally, and perhaps physically, associated with the human erythrocyte NT system became covalently labelled (35,36). NBMPR-binding polypeptides, which have an approximate *Mr* 55,000 (36,37), constitute about 3% of the human erythrocyte band 4.5 proteins (Steck's nomenclature, ref. 38) (17). The functional transporter may be a dimer, since radiation-inactivation studies have indicated a molecular weight of 100-120 kDa for the functional transport system (39).

The NBMPR-binding polypeptides from human and pig erythrocytes showed apparent molecular weights of 55,000 and 64,000, respectively, and gave rise to different products

after endoglycosidase F and endo-beta-galactosidase treatment (40), indicating that the NBMPR-binding polypeptides are extensively glycosylated and that they may differ between species. Papain and *Staphylococcus aureus* V8 protease treatments of [^{3}H]NBMPR-labelled preparations of band 4.5 polypeptides yielded fragments with M_r 33,000 (37).

The nucleoside transporter in human erythrocytes appears to have essential thiol groups. Incubation with *p*CMBS of inside-out vesicles at 1°C inhibited Urd influx and NBMPR binding. Similar treatment with *p*CMBS of intact cells had no effect on Urd influx and NBMPR binding. Because diffusion of *p*CMBS across the plasma membrane appears to be reduced at 1°C, these results indicated that the groups modified by *p*CMBS may be located on the cytoplasmic face of the membrane (41). Inhibition of NT by *p*CMBS in erythrocytes was reduced when Urd was included in the medium during incubation with the organomercurial, implying that reactive thiol groups were involved in Urd permeation (41).

4. Non-concentrative NT in mammalian nucleated cells

a) Substrate specificity and kinetic properties

Non-concentrative NT systems in normal and transformed mammalian cells have been shown to recognize a number of nucleosides and nucleoside analogues. K_m values for Ado influx into various types of mammalian cells at room temperature range between 10 µM and 120 µM, while V_{max} values between 5 and 49 pmol/µl cell water.sec have been reported

(1,13,16,42-50). It should be noted, however, that the values of kinetic constants reported in these studies varied depending on the method utilized to measure nucleoside fluxes.

Various substituents on the purine or pyrimidine base moieties of nucleosides are tolerated by the NT system, as are deletion or changes in the configuration of hydroxyl groups at C-2 of the pentofuranosyl ring (1,13,42-50). In some cell types, NT systems participate in the translocation of nucleobases. For instance, in S49 mouse lymphoma cells, inward fluxes of hypoxanthine, guanine and adenine were inhibited by Ado, dThd, dipyridamole and NBMPR (51,52), and Urd transport in Chinese hamster ovary cells was inhibited by hypoxanthine (53). Ionized substrates do not serve as permeants for non-concentrative NT systems (21,54,55).

b) Inhibitors of non-concentrative NT systems

A number of structurally diverse agents inhibit non-concentrative NT systems in different mammalian cell types. These inhibitors include vasodilators (dipyridamole, dilazep, lidoflazine and hexobendine (13), papaverine (56), cytochalasin B (57), colchicine (58), phloretin (59), phloridzin (59), and podophyllotoxin (60).

S^6-Derivatives of 6-thioinosine and 6-thioguanosine, such as iodohydroxinitrobenzylthioinosine, HNBTGR and NBMPR, selectively inhibit non-concentrative NT in some nucleated cell types (16,61). NT inhibition by NBMPR is reversible and binding of NBMPR has been correlated with inhibition of

transport in several cell lines (15). The NBMPR-binding site and the nucleoside transporter of S49 cells appear to be functionally related, since AE_1 cells, a mutant clone of S49 cells virtually devoid of NT activity, lack high-affinity NBMPR binding sites (9).

K_D values for NBMPR binding, measured in various cell lines, range between 0.1 and 1 nM, and binding site densities of 10^5 to 10^6 sites *per* cell have been reported (3,13,62). Substitution of the purine ring by a pyrimidine moiety, as in 4-[(2-hydroxy-5-nitrobenzyl)thio]uridine, yielded a derivative with substantially reduced NT inhibitory properties (62).

NBMPR and *p*CMBS have revealed heterogeneity in the nonconcentrative NT systems present in mammalian cells. For instance, the NT systems of S49 and RPMI 6410 cells were completely inhibited by 100 nM NBMPR (42,45,63), whereas NBMPR concentrations greater than 10 uM were required to partially inhibit NT in cells of the following cultured lines: Walker 256 rat carcinosarcoma, Novikoff UASJ-2.9, Morris 3924A and Reuber H-35 rat hepatoma (3,15,42,63).

The co-existence of NT systems with high and low sensitivity to NBMPR has been shown in L1210 mouse leukemia (50) and HeLa cells (62). The isolation of L1210 mutants lacking the NT component of low sensitivity to NBMPR suggested that the two systems may be different gene products[5]. It has also been suggested that NBMPR-sensitive and NBMPR-insensitive NT systems could be different conformations of

the same polypeptide (64).

The NBMPR-sensitive NT systems present in L1210 cells and S49 cells were inhibited by concentrations of *p*CMBS greater than 200 uM (50,63), whereas the NT components of low sensitivity to NBMPR present in L1210 cells and in Walker 256 cells were inhibited by less than 25 uM *p*CMBS (50,63).

Dipyridamole and dilazep inhibit non-concentrative NT systems of high and low sensitivity to NBMPR (35,45,65), although NT systems of low sensitivity to both NBMPR and dipyridamole have been described (66). Since dipyridamole inhibits NT in some cell types devoid of NBMPR binding sites (63), the determinants for interaction of dipyridamole with the transporter may differ from those for NBMPR.

c) Structural studies

The photoactivation of site-bound ^{3}H-NBMPR resulted in labelling of proteins from mouse lymphoma and leukemia cells with M_r 55,000-60,000 (67-69). Similar results have been obtained with membranes from rat lung and guinea-pig heart, lung and liver (70-72), suggesting that NT systems similar to the nucleoside transporter of human erythrocytes may be present in cells of those tissues. Photoactivation of site-bound ^{3}H-NBMPR covalently labelled plasma membrane proteins with M_r 60,000 from rat liver, and M_r 55,000 from guinea-pig liver (71,73). This variation probably arose from

---

[5] J.A. Belt, personal communication

differences in glycosylation, since treatment with endoglycosidase F yielded polypeptides with M_r 45,000 in both preparations.

A polypeptide with M_r 72,000-80,000 was labelled by photoactivation of site-bound ^{3}H-NBMPR to wild type Novikoff rat hepatoma membranes (74). A cloned line of Novikoff cells, the UASJ-2.9 clone, has been shown to have high-affinity NBMPR binding sites, although NT in these cells has low sensitivity to NBMPR, suggesting that the NBMPR binding site and the permeation site are not functionally coupled in this cell line (18).

5. Secondary-active NT systems

Permeation of unmetabolized nucleosides against concentration gradients has been observed in a number of cell types, as outlined below.

1. Kessel and Shurin (75) reported that the presence of uranyl ions in the incubation medium of dCyd kinase-deficient L1210 cells resulted in a two-fold accumulation of cellular araC, relative to the extracellular concentration of that nucleoside analogue. While the presence of a concentrative NT system in L1210 cells was dismissed by the authors, the present report demonstrates the activity of such a system in L1210 cells (see "Results and Discussion").

2. Isolated rat hepatocytes accumulated unmetabolized dThd above extracellular levels via a high-affinity NT system, although no further characterization of this system has

been reported (76).

3. Le Hir and Dubach (77) described a sodium-dependent, concentrative NT system found in brush border vesicles from proximal tubules of rat kidney. This system, resistant to inhibition by NBMPR and NBTGR (78,79), showed high affinity for Ado, dAdo, Ino and Guo (K_m values of 1.48, 8.61, 2.02 and 3.48 μM, respectively) and recognized Cyd, dThd and Urd as permeants (80).

4. During incubation of mouse kidney slices in medium containing 2'-deoxytubercidin, intracellular levels of the free nucleoside reached levels 2- to 3-fold greater than the concentration in the medium. The accumulation of 2'-deoxytubercidin under these conditions was inhibited by sodium azide (81). Although the cellular accumulation of 2'-deoxytubercidin in this preparation was not attributed to the operation of nucleoside-specific transport systems, concentrative renal NT mechanisms appear to function in humans and mice. It was reported that average renal clearance values for dAdo and Ado in humans were 5-fold larger and 5-fold lower, respectively, than that of the creatinine cleared (61.9 ml/min/1.73 m^2, ref. 82). In the same study, it was observed that the renal clearance values for inulin, dAdo and Ado were 0.193 ml/min, 0.313 ml/min and 0.059 ml/min, respectively (82). Since creatinine and inulin are not significantly secreted or reabsorbed by renal tubules in mice and humans, clearance of a substance above that of creatinine or inulin indicates renal secretion of that

substance, whereas clearance below creatinine levels is suggestive of renal reabsorption (83). The results from dAdo and Ado clearance measurements suggest the presence in human and mouse kidneys of systems that actively secrete dAdo and reabsorb Ado.

5. In isolated epithelial cells (enterocytes) from guinea-pig jejunum, Schwenk *et al.* (84) measured a 13-fold accumulation of free Urd above the external nucleoside concentration. Rates of Ado transport measured in this system were saturable and nucleoside accumulation required a Na^+ gradient. The concentrative NT process in these cells was inhibited by ouabain and by antimycin A, an inhibitor of mitochondrial ATP production.

6. IEC-6 cells, a cultured line of rat intestinal epithelial cells, concentrated FB in a sodium-dependent, NBMPR-insensitive manner (85). These cells also exhibited NT activity that (i) had no sodium requirement, (ii) was susceptible to NBMPR inhibition, and (iii) also appeared to mediate nucleoside efflux from IEC-6 cells (85).

7. Rabbit choroid plexus was shown to have at least two different NT systems (86-89). One of these systems was non-concentrative, sensitive to inhibition by 10 uM NBMPR, and probably involved in nucleoside efflux. The other NT system was concentrative, insensitive to NBMPR inhibition, and energy- and sodium-dependent. The sodium-dependent system was inhibited by ouabain and NEM, but not by the non-penetrating thiol-reactive agent, 6,6'-dithiodinicotinic

acid, suggesting that thiol groups located in the inner face of the plasma membrane were involved in nucleoside permeation. This concentrative NT system recognized dUrd, dThd, Ado and dCyd, but not 3'-dAdo. Blockade of mediated efflux by NBMPR in choroid plexus resulted in enhanced accumulation of permeant nucleosides by the active system (86-89).

8. Darnowski and Handschumacher (90) have shown that systems capable of uphill translocation of nucleosides may be present in various murine tissues. The activity of these systems in mice was evident in the levels of free Urd found in intestine, liver, kidney and spleen, which were 4- to 12-fold higher than in plasma.

9. Uphill transport of Urd has also been demonstrated in dispersed mouse splenocytes. Concentrative Urd influx in these cells was sodium- and energy-dependent, and was inhibited by purine nucleosides, but not by pyrimidine nucleosides, NBMPR, glucose, dipyridamole or nucleobases. In these cells, an NT system that mediated non-concentrative permeation of both purine and pyrimidine nucleosides was also demonstrated (91).

6. Modulation of nucleoside analogue toxicity by transport inhibitors.

Inhibitors of NT have been shown to reduce the antiproliferative activity of toxic nucleoside analogues towards various types of cultured neoplastic cells. For instance, RPMI 6410 cells were protected from the growth inhibitory

effects of 5-azacytidine, 6-azauridine, araC, 2-F-Ado and showdomycin when 5 μM NBMPR was included in culture media (6). The presence of 10 μM NBMPR in the growth media of L5178Y lymphoma cells also protected these cells from the antiproliferative activity of formycin or tubercidin (7), and the inhibitory effects of araC on HL-60 cell proliferation were decreased when cells were cultured in the presence of dipyridamole (1 μM, ref. 8). The protection of cultured cells against the antiproliferative activity of nucleoside drugs by NBMPR or dipyridamole has been attributed to inhibition of cellular NT systems with consequent decrease in the influx of nucleoside drugs.

NT inhibitors have also been shown to decrease the toxic effects of some nucleoside analogues in animals. For instance, protection of normal mice from the lethal effects of nebularine, tubercidin and toyocamycin was achieved by co-administration with NBMPR, NBdAdo or dilazep. Such protection likely derives from decreased permeation of the nucleoside drugs into cells of dose-limiting tissues, subsequent to inhibition of nucleoside influx by NT inhibitors (15).

The inclusion of NBdAdo in therapy regimens in which otherwise lethal doses of nebularine were administered increased the number of long-term surviving mice implanted with Ehrlich ascites carcinoma (13). Increases in life-span were also observed when L1210 leukemia-bearing mice were treated with nebularine and dilazep (13). In these experi-

ments, NT inhibitors may have increased the therapeutic effectiveness of nebularine by decreasing the influx of the toxic nucleoside into host tissues to a greater extent than into the tumours.

In another application of the "host-protection" strategy, treatment of *P. yoelii*-infected mice with potentially lethal doses of tubercidin and host-protective doses of NBMPR-P did not produce long-term survivors, but increased median survival times (92). NBMPR was also shown to increase the therapeutic effectiveness of tubercidin in the treatment of mice infected with *S. japonicum* (93). In a similar therapeutic tactic, treatment regimens including nebularine and NBMPR or dilazep were effective in the treatment of mice infected with *Schistosoma mansoni* (94). NBMPR and dilazep may have increased the therapeutic effectiveness of tubercidin and nebularine by selectively reducing the influx and toxicity of the nucleoside drugs into host tissues. Selective host protection was probably achieved because nucleoside analogue permeation in erythrocytes infected with *P. yoelii* and in schistosomes includes inhibitor-insensitive components (92-94).

Protection of host tissues by an NT inhibitor against toxic nucleosides would appear to require the following conditions: (i) effective concentrations of the NT inhibitor must reach target tissues, and (ii) a significant proportion of nucleoside entry in those tissues must be mediated by an NT system sensitive to that NT inhibitor. In view of the

heterogeneity of NT systems, host protection in this context is likely to occur only in particular circumstances that provide the foregoing conditions.

In seeming contrast to the host protection phenomenon, inhibition of NT enhanced the cytotoxicity of certain nucleoside analogues. For example, the presence of dipyridamole increased the antiproliferative activity of dAdo/dCF combinations towards cultured L1210 cells (95). This effect of dipyridamole likely resulted from selective inhibition in L1210 cells of a route for dAdo efflux without blockade of dAdo influx (see "Results and Discussion"). In another example of enhancement of nucleoside analogue toxicity by NT inhibitors, araC inhibition of L5178Y cell proliferation was increased when incubation with that nucleoside analogue was followed by addition of dipyridamole (96). Dipyridamole may have reduced the efflux of araC from these cells, maintaining cellular levels of araC and its 5'-phosphates and, thereby, increasing araC cytotoxicity.

Decreases in the toxicity of nucleoside analogues by NT inhibitors have not always been observed in animals. One study reported that the toxicity of araC, 5-F-Urd and 5-azacytidine administered to normal mice was unaltered by NBMPR. It was also reported that the toxic activities of 5-azacytidine and 5-F-Urd were increased by co-administration with dilazep (15), perhaps because the latter agent inhibited efflux of nucleoside drugs from dose-limiting tissues. This hypothesis has yet to be tested.

7. Cellular metabolism of dAdo, araA and 2-F-araA.

A portion of the present study involved experiments that measured the antiproliferative activity or chemotherapeutic effects of dAdo, araA and 2-F-araA. A summary of the metabolic fates and apparent mechanisms of action of these nucleoside analogues is given below.

2'-Deoxyadenosine is a substrate of enzymes involved in Ado metabolism. The general features of dAdo metabolism are outlined in the scheme of p. 54. Adenosine deaminase (ADA) converts dAdo into deoxyinosine. Formation of the latter can be substantially reduced by dCF or EHNA, potent ADA inhibitors with K_i values of 2.5×10^{-12} M and 1.6×10^{-9} M, respectively (97).

2'-Deoxyadenosine is phosphorylated by both Ado and dCyd kinases in various mammalian cells (98-100). The 5'-monophosphate is converted to dADP, which, in turn, gives rise to dATP as the final phosphorylation product (98-100). The mechanisms of dAdo cytotoxicity are not clear, although contributory effects appear to be feedback inhibition of ribonucleotide reductase by dATP (101,102) and dAdo inhibition of SAH hydrolase; the latter effect may halt some methylation reactions (103,104).

Accumulation of dAdo and its 5'-phosphates in genetic or pharmacologically-induced ADA deficiency was accompanied by ATP depletion in erythrocytes, lymphocytes and CEM cultured cells (105). In CEM cells, dATP formation resulted in ATP degradation to ADP and AMP. The dATP so produced

stimulated AMP deamination to IMP. The degradation of AMP to IMP, and the utilization of ATP to produce dATP in these cells resulted in ATP depletion (105). The cellular metabolism of dAdo has been the subject of several reviews (106-109).

The nucleoside analogues, araA and 2-F-araA, are substrates for some of the enzymes that metabolize dAdo in mammalian cells. AraA is phosphorylated by dCyd kinase, Ado kinase and, possibly, by a deoxyribonucleoside kinase (110-112). AraAMP and araADP are phosphorylated by adenylate kinase and nucleoside diphosphate kinase, respectively (113). AraA is deaminated by ADA, and the product, araH, has little biological activity (114). Inhibition of ADA greatly enhances formation of araA 5'-phosphates in cells (115).

2-F-AraA is converted to FAMP primarily by dCyd kinase (116). The enzymes involved in subsequent phosphorylation steps have not been characterized, but 2-F-araATP is a major metabolite. 2-F-AraA is not as susceptible to deamination as araA (117,118), although deamination products have been detected after administration of [^{3}H]2-F-araA to mice, dogs and monkeys (119).

AraA and 2-F-araA appear to have multiple mechanisms of action, including inhibition of DNA synthesis. AraATP and 2-F-araATP have been reported to inhibit DNA polymerase alpha, but not DNA polymerase beta, by competing with the natural substrate, dATP. The affinity of araATP for mammalian DNA polymerase alpha is similar to that of dATP (110,118-122).

Ribonucleotide reductase is inhibited by araATP and its 2-fluoro derivative (123,124). Such inhibition would reduce dATP levels which, in turn, would probably enhance the effectiveness of both 5'-triphosphates to interfere with DNA synthesis (120).

The clonogenic viability of cultured L1210 cells has been related to the extent of araA incorporation into DNA (125). Similarly, the incorporation of 2-F-araA residues into the DNA and RNA of HL-60 cells has also been correlated with loss of clonogenic viability (126).

AraA and, to a lesser extent, 2-F-araA inhibit SAH hydrolase in several mammalian cell types, although the contribution of this effect to cytotoxicity has not been demonstrated (104,123,127-129).

8. Research proposal.

Permeation of nucleosides and their analogues across plasma membranes of mammalian cells occurs mainly *via* nucleoside-specific transport systems. Consequently, NT activity is a determinant of nucleoside analogue cytotoxicity in various cell types. As discussed in Section 6, inhibition of NT activity in cultured cells or *in vivo* may increase or decrease the toxicity of nucleoside analogues, depending on the cell type, inhibitor and analogue used (6-8,15,92-96). Protection of cells from nucleoside analogue toxicity by NT inhibitors appears to derive from reduction of mediated

nucleoside influx. In contrast, blockade of mediated nucleoside efflux by NT inhibitors may induce cellular accumulation of nucleoside analogues and/or their metabolites, and, thereby, enhance the toxicity of those analogues. For instance, the NT inhibitor, dipyridamole, enhanced the antiproliferative effects and cellular concentrations of dAdo and its anabolites in cultured L1210 mouse leukemia cells (95), probably by blocking transporter-mediated dAdo efflux.

The diversity of NT inhibitor effects on the biological activity of nucleoside analogues in various cell types suggests that the pharmacokinetics and pharmacodynamics of nucleoside drugs may be modulated by inhibition of NT *in vivo*. Inhibition of NT activity might be exploitable therapeutically if blockade of nucleoside efflux, with consequent enhancement of nucleoside drug toxicity, could be selectively achieved in target cells.

The present study initially aimed at (i) determining the effect of NT inhibitors on nucleoside efflux, (ii) investigating if cellular retention and cytotoxicity of nucleoside analogues could be enhanced or modulated by NT inhibitors, and (iii) evaluating the antineoplastic activity of nucleoside analogues when administered in combination with NT inhibitors. The model system first selected for this project, the L1210/C2 clone, offered the possibility to investigate if the effects of nucleoside analogues observed in cultured cells could also be obtained in therapeutic experiments with animals, since these cells proliferate both

in vivo and in culture.

METHODS

I. CHEMICALS

2'-Deoxycoformycin, 2-F-araA, 2-FAMP, araC and L-Ado were generous gifts from the Division of Cancer Treatment, National Cancer Institute, Bethesda, Maryland (USA). NBMPR was prepared in this laboratory (130), and NBMPR-P and NBdAMP were prepared by the Research Laboratory, Yamasa Shoyu Ltd., Chosi (Japan). AraA was purchased from Pfantstiehl Laboratories, Waukegan, Illinois (USA). Tricaprylylamine (alamine 336) and 1,1,2-trichloro-trifluoroethane (Freon TF), were obtained, respectively, from the Henkel Co., Kankakee, Illinois (USA), and from Dupont, Maitland, Ontario (Canada). Dilazep was a gift from Hoffman-LaRoche, Basel, (Switzerland). EHNA was kindly provided by Dr. H.J. Schaeffer, Wellcome Research Laboratories, Research Triangle Park, North Carolina (USA). Cell culture materials were purchased from GIBCO, Burlington, Ontario (Canada). PEI-cellulose TLC sheets were purchased from Brinkmann Instruments, Westbury, New York (USA). Tritium-labelled nucleosides were obtained from Moravek Biochemicals, Brea, California (USA). Proteinase K was purchased from Boehringer Ingleheim, Dorval, Quebec (Canada). [1,2-^{3}H]polyethyleneglycol (2 mCi/g) and ^{22}NaCl (>100 Ci/g) were obtained from NEN, Lachine, Quebec (Canada). DNP and paraffin oil (Saybolt viscosity 125-135)

were obtained from Fisher Scientific, Fair Lawn, New Jersey, (USA). Silicone 550 oil was purchased from Dow Corning, Mississauga, Ontario (Canada). FB was a generous gift from the late Professor Hamao Umezawa, Institute for Microbial Chemistry, Tokyo (Japan).

II. CELL CULTURE PROCEDURES

1. Cell lines

This study utilized cells derived from cultured lines of mouse leukemia L1210. The original L1210 cell line was isolated from the spleen and lymph nodes of a DBA/2 mouse following treatment with methylcholantrene by skin painting (131).

The L1210 sublines used in this study are described below. Stocks of these lines frozen in growth medium with 10% dimethylsulfoxide were stored under liquid nitrogen. Cultures started from the frozen stock were not passaged more than 35 sub-culture generations. The results reported in this study were obtained with cells from cultures in which cell proliferation was exponential; this was achieved by ensuring that cell densities in cultures did not exceed 6 x 10^5 cells/ml.

a) L1210/C2

This cloned line, capable of proliferation *in vivo* and *in vitro* (132), was obtained from Dr. C.E. Cass, McEachern Laboratory, University of Alberta. L1210/C2 cells were

cultured in Fischer's medium with 10% horse serum. The cells were maintained in exponential growth by dilution to 0.05 x 10^6 cells/ml with fresh medium every 2-3 days. The doubling time of L1210/C2 cells under these conditions was 15-18 h.

b) L1210/araC/MeMPR (L1210/AM)

This clone, designated here as L1210/AM, was kindly provided by Dr. L. L. Bennett Jr., Southern Research Institute, Birmingham, Alabama (USA). L1210/AM cells were developed in a two-step selection procedure in culture, the first of which established a line resistant to araC. The second step involved selection of cells capable of proliferation in culture medium containing MeMPR[6]. L1210/AM cells are deficient in Ado, dAdo and dCyd kinase activities (133) and were cultured as described for L1210/C2 cells. Exponentially growing L1210/AM cells doubled in 12-14 h.

c) L1210/MC5-1

L1210/MC5-1 cells were kindly provided by Dr. J.A. Belt, St. Jude Children's Research Hospital, Memphis, Tennessee (USA). L1210/MC5-1 cells, which were selected from a mutagenized population of L1210/B2[7] cells for resistance to

---

[6] L.L. Bennett Jr., personal communication

[7] L1210/B2 cells are a cloned line derived from wild-type cells from the Southern Research Institute, Birmingham, Alabama (USA) (J.A. Belt, personal communication)

araC and tubercidin in the presence of 1 μM NBMPR, possess NT characteristics that differ from those of the parent line, and from those of L1210/C2 and L1210/AM cells (*vide infra*). L1210/MC5-1 cells were propagated in RPMI 6410 growth medium with 10% horse serum, and were sub-cultured as described for L1210/C2 cells to maintain exponential growth. Doubling times during exponential growth ranged between 12 and 14 h.

d) L1210/B23.1

This clone was selected from a population of mutagenized L1210/MC5-1 cells for resistance to a combination of araA, EHNA and NBMPR. The NT characteristics of L1210/B23.1 cells differ markedly from those of the parental cells, as shown in the following chapter. The culture conditions for L1210/B23.1 cells were similar to those for the parent line. L1210/B23.1 cell population doubling times were 12-14 h during exponential growth.

2. Measurement of clonogenic viability (134)

Cells were cultured with drugs for 24 h and clonogenic viability was measured in drug-free, soft-agar medium as follows. Cells were suspended at graded densities between 16 and 200 cells/ml in drug-free cloning medium containing Fisher's medium with 0.13% agar, 10% horse serum, 10% conditioned medium (filtered growth medium from 24-h cultures) and 50 μg/ml gentamicin. Five-ml portions of the cell

suspensions were cultured in 10 mm x 130 mm test tubes at 37°C and, after 10-14 days, the content of each tube was poured into a Petri dish for enumeration of colonies under a dissecting microscope.

3. Measurement of proliferation rates

Cell proliferation rates were assayed as described by Cass *et al.*(134). Replicate cultures were prepared to contain 10^5 cells/ml and graded concentrations of test agents in growth medium with 100 units/ml penicillin G and 100 µg/ml streptomycin. Cell densities were determined after 48 h of culture at 37°C using an electronic particle counter. Cell population doublings (means from replicate samples) were expressed as percentages those in drug-free cultures.

4. Mutagenesis and mutant isolation techniques

In the selection of the L1210/B23.1 clone, a suspension of L1210/MC5-1 cells containing approximately 4.4 X 10^8 cells in 270 ml of growth medium was incubated with MNNG (3 µg/ml) at 37°C for 1 h. The cells were washed once with 200 ml of growth medium and cultured at 37°C under non-selective conditions to allow expression of mutant phenotypes. Judging from the cell concentration 24 h after treatment with MNNG, and assuming unaltered cell population doubling times, 20-30% of the cells survived the mutagenic treatment. After approximately 10 doublings, cells from the mutagenized culture

were treated for 1 h with 1.5 μM EHNA and suspended at 10^6 cells/ml in 350 ml of soft-agar cloning medium (*vide supra*) containing 1.5 μM EHNA, 7 μM araA and 10 μM NBMPR or 5 μM dipyridamole. Five-ml portions of this suspension were poured into 60-mm culture dishes and were incubated at 37°C. The selection procedure yielded 34 macroscopic colonies, which, when about 1 mm in diameter, were individually suspended in drug-free growth medium (RPMI 6410) to establish 34 clonal cultures. After 4-6 weeks in culture, the proliferation rates of these clones in growth medium containing 7 μM araA, 1.5 μM EHNA and 5 μM dipyridamole were determined to verify resistance to the drug combination.

III. ANALYTICAL PROCEDURES

1. Purification of radiochemicals

Tritium-labelled nucleosides were purified prior to use by HPLC using a Spectra Physics 8000A instrument equipped with a variable wavelength detector. Nucleosides were eluted from a C_{18} reversed-phase column (Whatman Partisil ODS-3) by a linear methanol-water gradient which flowed at 1 ml/min and changed from 0 to 25% methanol in 35 min. Retention times of the nucleosides and nucleoside analogues purified are listed in Table 1.

2. Preparation of PEI(borate) cellulose plates (135)

PEI cellulose sheets were washed with 10% NaCl, dried and soaked for 5 min in 0.4 M triethylammonium tetraborate

Table 1

HPLC elution times of nucleosides and nucleoside analogues

Compounds were purified by HPLC on a Whatman Partisil ODS-3 column using as eluant a methanol-water gradient (0 to 25% methanol in 35 min) at 1 ml/min.

Nucleoside	Retention time (min)
dAdo	28.6
Ado	20.5
araA	23.1
dThd	14.4
araC	11.0
FB	13.6*
Urd	7.0*

* Purified by elution with water

(99 g boric acid, 112 ml triethylamine and water to give a final volume of 1 l). The plates were drained, then immersed (without drying), first in water (1 min) and then in methanol (1 min), and dried overnight.

3. Analysis of intracellular anabolites of nucleosides

a) Preparation of cell extracts

Suspensions of cells in growth media with a ^{3}H-nucleoside were cooled to 4°C, centrifuged (150 x g, 2 min, 4°C), and the cell pellet was washed once with ice-cold, nucleoside-free growth medium. After centrifugation, cell pellets were mixed with 0.1 ml of 0.4 M TCA and kept for 20-30 min in an ice bath. The TCA-containing suspension was centrifuged (150 x g, 2 min, 4°C), acid extracts were transferred to microcentrifuge tubes containing 0.1 ml of 0.5 M alamine in Freon TF and the two solutions were thoroughly mixed. The upper, neutralized aqueous layers were stored at -20°C until analyzed (within 12-24 h).

b) Effects of ADA inhibitors on nucleoside deamination

Cells were incubated in growth medium containing 1.1 uM dCF or 1.5 μM EHNA for 1 h at 37°C prior to the addition of ^{3}H-dAdo or ^{3}H-araA and then were further incubated under culture conditions for 20 h. Cell extracts obtained as described in Section 3a were analyzed by TLC on PEI cellulose chromatograms developed with water. Rf values for dAdo and dIno in this system were 0.50 and 0.64, respec-

tively.

To determine if araH was formed from ^{3}H-araA deamination, cell extracts were analyzed on washed PEI cellulose sheets with development in acetic acid:2-propanol:water (65:22:13 v/v/v). This solvent system resolved araA (*Rf*=0.42) from araH (*Rf*=0.27). Less than 5% of the radioactivity applied to the chromatograms co-migrated with authentic dIno or araH.

c) TLC analysis of dAdo and araA anabolites

Formation of 5'-phosphates of ^{3}H-dAdo or ^{3}H-araA was assayed by TLC analysis of cell extracts using a procedure described by Schwartz and Drach (136) and modified by Lauzon *et al.* (137). Samples of cell extracts (5µl) and appropriate carrier compounds were applied to PEI cellulose sheets. The chromatograms were first run with 0.66 M acetic acid until the solvent front was 2 cm above the origin. Without drying, the chromatograms were developed in a second solvent system, 0.33 M LiCl in 0.66 M acetic acid, advancing the solvent front a further 6 cm. Again without drying, the chromatograms were developed a further 9 cm in the final solvent system, 0.66 M LiCl in 0.66 M acetic acid. This procedure resolved nucleosides and their tri-, di-, and monophosphates. *Rf* values are listed in Table 2.

Sections (0.5 cm) of the chromatograms were extracted with 0.5 M NaOH at room temperature for at least 3 h and, after neutralization (HCl), ^{3}H-activity in each section was

Table 2

Mobilities of nucleosides and nucleoside 5'-phosphates on PEI-cellulose thin-layer chromatograms.

PEI-cellulose chromatograms were developed sequentially with 0.66 M acetic acid, 0.33 M LiCl in 0.66 M acetic acid and 0.66 M LiCl in 0.66 M acetic acid.

Compound	*Rf*
dAdo	0.87
dAMP	0.66
dADP	0.20
dATP	0.03
araA	0.90
araAMP	0.68
araADP	0.23
araATP	0.04
araC	0.91
araCTP	0.03

determined by liquid scintillation counting. To establish the efficacy of the NaOH extraction step, 5-µl samples of cell extracts were added to scintillation vials containing a blank chromatogram segment and ^{3}H-activity was measured. Extraction efficiencies were ≥ 95%, and at least 95% of the applied ^{3}H-activity was accounted for on the chromatograms.

4. Extracellular products derived from nucleoside anabolites

During incubation at 37°C in growth medium containing ^{3}H-dAdo, ^{3}H-araA or ^{3}H-araC for intervals specified in individual experiments, L1210/C2 cells accumulated pools of ^{3}H-labelled dATP, araATP or araCTP. Monophosphate and diphosphate derivatives of the ^{3}H-nucleosides together represented 17% or less of the total cellular ^{3}H-activity. The cells were pelleted, washed once with cold growth medium and incubated at 37°C in nucleoside-free medium for 3 h. To identify extracellular products derived from catabolism of the ^{3}H-labelled nucleoside 5'-triphosphates, samples of culture medium were first freeze-dried to yield residues which were then extracted with 0.4 M TCA; after neutralization, the extracts were analyzed by TLC or HPLC. The following TLC analysis systems were used: (i) PEI (borate) cellulose developed with water, or with acetic acid:2-propanol:water (65:23:12 v/v/v), (ii) PEI cellulose developed with water, and (iii) silica gel developed with methanol:chloroform:3% acetic acid (2:3:1 v/v/v). HPLC analysis was performed as

described in Section III.1 for the purification of radiochemicals.

5. Isolation of nucleic acids (138-141)[8]

a) Composition of solutions utilized.

I. Washing PBS, pH 7.4 :

137.0 mM NaCl

16.0 mM Na_2HPO_4

1.2 mM KH_2PO_4

II. Tris-EDTA-SDS, pH 8.0 :

10 mM Tris.HCl

10 mM EDTA

10 mM NaCl

0.5% SDS

III. Tris-EDTA, pH 8.0 :

50 mM Tris.HCl

10 mM EDTA

10 mM NaCl

---

[8] The help of Mr. H. El-Sharkawi and the guidance of Dr. L.W. Brox in the extraction of cellular nucleic acids by the phenol method is gratefully acknowledged

IV. Tris-buffered phenol (TBP):

Equal volumes of DNA-grade phenol and 1.0 M Tris (pH 8.0) were thoroughly mixed and let stand a few minutes. The upper aqueous layer was removed and another portion of 1.0 M Tris was mixed. The aqueous layer was again removed and an equal volume of 0.1 M Tris was added. After shaking, the mixture was allowed to stand overnight at 4°C. The upper layer was then replaced with 0.25 volumes of 1.0 M Tris. This solution was stored at 4°C.

V. TBP-Chloroform:

This is a 1:1 (v/v) mixture of equal volumes of HPLC-grade chloroform and TBP which was stored at 4°C.

VI. Buffered Cesium Sulphate Solution:

65 g Cs_2SO_4

10 ml DMSO

Tris-EDTA buffer (ph 8.0) was added to give a final volume of 100 ml. The density of this solution is approximately 1.50 g/ml. The presence of urea or a polar solvent such as DMF or DMSO prevents RNA aggregation induced by cesium sulphate.

b) Procedure

Following culture in medium containing ^{3}H-araA, L1210/C2 cells were washed once with cold PBS (4°C),

suspended in polypropylene tubes containing 5 ml Tris-EDTA-SDS buffer and treated overnight with proteinase K (50 µg/ml) at 37°C. The digest was extracted once with 5 ml cold TBP and then extracted two or three times with 5 ml cold TBP-chloroform. To the resulting solution (5 ml), 0.5 ml of 2.5 M sodium acetate and 10 ml of cold ethanol (-20°C) were added and the mixture, placed in 30-ml Corex centrifuge tubes, was stored overnight at -20°C to induce nucleic acid precipitation. After centrifugation (8500 x g for 10 min at 4°C), the pellets were dissolved in 0.5 ml of Tris-EDTA, warmed to 80°C for 10 min to denature the nucleic acids and cooled in ice-water. The solutions so obtained were layered over 4 ml of buffered cesium sulphate solution; 0.5 ml paraffin oil were added and the samples were centrifuged in a Beckman VTi 65 vertical rotor at 7°C (150 000 x g for 50 h). These conditions established a cesium sulphate gradient that separated macromolecules according to their buoyant densities. RNA, DNA and proteins were located in gradient regions with densities of 1.62-1.68 g/ml, 1.42-1.48 g/ml, and ≤1.35 g/ml, respectively. To analyze the gradients, the centrifuge tubes were perforated at the bottom with a syringe needle, paraffin oil was added from the top at a rate of 1.0 ml/min (controlled by a peristaltic pump), and 0.2-ml fractions were collected from the bottom into microcentrifuge tubes. Fraction densities were determined pycnometrically. Nucleic acids in gradient fractions were precipitated by addition of 25 µl of 4.0 M TCA and recovered

by centrifugation. This was necessary to preclude precipitation of the scintillation cocktail by cesium sulphate during measurement of ^{3}H-activity in nucleic acid isolates. nucleic acid pellets were dissolved in 0.5 ml of 0.5 M NaOH and, after neutralization (HCl), the ^{3}H-activity of the samples was determined by liquid scintillation counting.

6. Measurement of intracellular sodium.[9]

Incubation mixtures containing approximately 1.6×10^{6} cells were centrifuged (150 x g, 2 min) and cell pellets were suspended in 0.35 ml of 0.4 M TCA. After 10 min, the mixtures were centrifuged and 0.3-ml portions of the extracts were transferred to polypropylene test tubes. Water (6.7 ml) was added to the sample extracts and the sodium content of each was determined by atomic emission spectrophotometry. Sample emissions of 589.4 nm light were amplified by adjusting photomultiplier voltage to 394.8 V and signals were integrated for 3 sec. Under these conditions, emission readings from 0.01-0.05 mM NaCl solutions were linear (Fig. 1). The sodium content of cell extracts was determined from the standard emission plot. Solutions in these experiments were prepared using 18-Mohm water, which

---

[9] The help of Dr. J.D. Harrison and the Department of Chemistry in the atomic emission spectrophotometry and in the use of the Varian Techtron 70 instrument is gratefully acknowledged

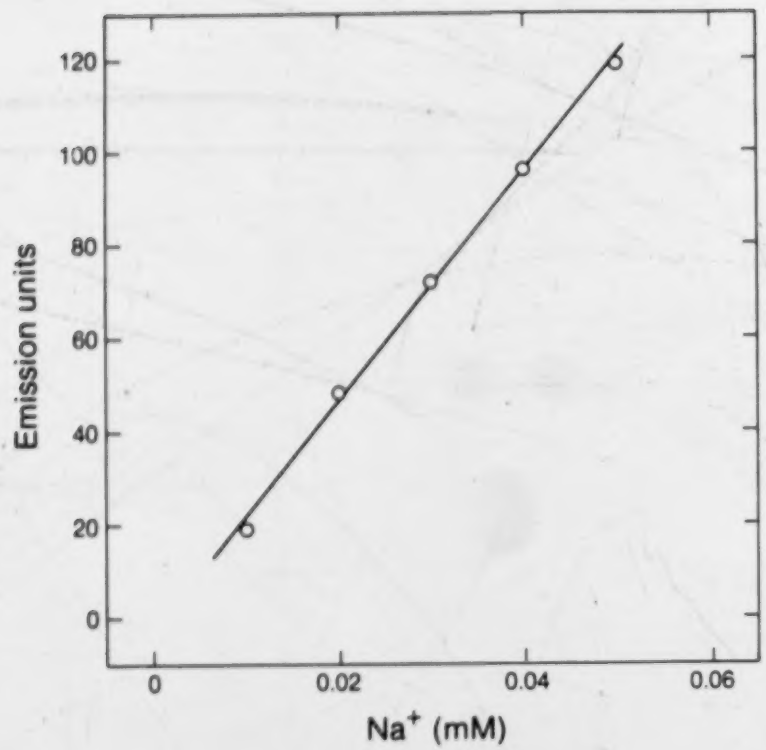

Fig. 1. Standard plot for determination of sodium by atomic emission spectrophotometry. The emission of 589.4 nm light by sodium-containing solutions was determined adjusting the photomultiplier voltage of the spectro-photometer 394.8 V, to give linear readings between 0.01 and 0.05 mM Na^+. A linear regression plot is fitted to the data shown, which are means of triplicate readings. Standard deviations were less than 5% in each of the triplicate measurements.

gave a background of 3-5 emission units. Pellet volumes were determined by adding ^{3}H-water to incubation mixtures that were then extracted in the same manner as in the determination of sodium. Extracellular pellet space was determined by using ^{3}H-PEG in place of ^{3}H-water.

7. Measurement of cellular ATP concentrations

Cellular ATP was determined by HPLC analysis of neutralized TCA extracts (0.13 ml) from cells prepared as described in Section 3a. In the HPLC analysis, 0.1-ml samples of cell extract were applied to a Whatman Partisil 10 SAX anion exchange column. The samples were eluted at 2 ml/min with the solvent gradient system defined in Table 3 (142). ATP eluted with a retention time of 24.13 min.

IV. EXPERIMENTS USING CULTURED CELLS

1. Cellular accumulation of nucleosides or nucleoside analogues and their anabolites.

After cell suspensions were incubated in growth medium containing 1.1 μM dCF or 1.5 μM EHNA for 1 h at 37°C, ^{3}H-dAdo or ^{3}H-araA was added to each mixture, with or without an NT inhibitor, and incubation was then continued under culture conditions. At specified time intervals, neutralized TCA extracts of the cells were prepared and analyzed by TLC, as described previously (Section III.3) .

Table 3

HPLC elution system for ATP analysis

The composition of the elution buffer used in the linear gradient for HPLC analysis of ATP is expressed as the percentage of each constituent in the final solution, and as a function of time.

time (min)	0.75 M $NH_4H_2PO_4$ pH 3.7 (%)	0.005 M $NH_4H_2PO_4$ pH 2.8 (%)
0	0	100
20	40	60
30	40	60
35	0	100

2. Cellular retention of nucleoside 5'-triphosphates.

Cells cultured as described in Section IV.1 and containing a ^{3}H-nucleoside and its corresponding 5'-triphosphate were separated from culture medium by centrifugation (100 x g, 4 min, 4°C), washed once with ice-cold, drug-free medium and suspended in medium with or without an NT inhibitor. After incubation under culture conditions for specified intervals, cell samples were extracted and prepared for TLC analysis of the acid-soluble fraction, as already described (Section III.3).

3. Cellular depletion of ATP.

Suspensions of L1210/AM cells in Tris medium (p.43) containing 0.5 x 10^{6} cells/ml were incubated at 37°C with 25 µM rotenone or 250 µM DNP for 15 min. Neutralized TCA extracts prepared from the cells were analyzed by HPLC for their ATP content. Water spaces in pellets and cells were determined as described in Section III.6. The effects of these treatments on cellular ATP levels have been summarized in Table 4.

4. Transport measurements

a) Composition of transport media

Cell suspension media differed depending on the transport assay performed. The pH value of all solutions was adjusted to 7.4 at 22°C and, unless otherwise indicated, all transport assays were conducted at 22°C.

Table 4

ATP concentrations in L1210/AM cells after treatment with rotenone or DNP

Cell suspensions were incubated at 37°C for 15 min under the conditions indicated and neutralized TCA extracts were analyzed by HPLC using the system shown in Table 3. Intracellular water space, necessary to express ATP content in concentration units, was determined as described in Section III.6.

Treatment		Cellular ATP concentration (mM)
Agent	Concentration	
None		3.7 ± 0.6[1]
Rotenone	25 µM	0.3 ± 0.1
DNP	250 µM	0.4 ± 0.2

[1] Mean ± S.D. of 3 determinations

I. Transport medium (TM):

Fischer's medium buffered with 20 mM HEPES in place of sodium bicarbonate (143).

II. Sodium medium:

2.6 mM KCl

1.4 mM KH_2PO_4

1.0 mM $CaCl_2$

138.0 mM NaCl

8.0 mM Na_2HPO_4

5.0 mM glucose

This medium is Dulbecco's salts medium (144), modified by the addition of glucose (5 mM, final). In some experiments, NaCl was replaced by equimolar amounts of NMG^+ chloride (NMG medium) or KCl (potassium medium). NMG^+ has been used as an "inert" cation in Na^+-free cell suspension media (145,146). In the present study, the difference in the volumes of cells suspended in sodium or in NMG medium did not exceed 5%. In those media, Na_2HPO_4 was replaced by 8.0 mM K_2HPO_4. In experiments where the sodium concentration was varied, mannitol was added to adjust the osmolality of the solutions to 300 $\pm$ 10 mOsm (determined with a Wescor vapour pressure osmometer, Model 5500).

III. Transport oil:

Prepared by mixing 75 ml paraffin oil with 425 ml

silicone 550 oil, to give a final density of 1.02-1.03 g/ml

IV. Tris medium:

132 mM Tris.HCl

30 mM KCl

1 mM $MgCl_2$ and 1 mM $CaCl_2$

V. Tris/ NaCl medium:

112 mM NaCl

30 mM KCl

20 mM Tris.HCl

Solutions IV and V were utilized in experiments measuring ^{22}Na fluxes. Cells were suspended in medium IV in experiments measuring cellular ATP content prior to and following treatment with metabolic inhibitors.

b) Transport assay protocol

Cells were suspended in a transport medium with or without an NT inhibitor at 1-2 x 10^7 cells/ml. Unless otherwise stated, cell suspensions were maintained at room temperature for 10-35 min prior to transport assays. Incubation of cells under these conditions for periods not exceeding 1 h preserved cell viability and NT function. Portions (0.1 ml) of such cell suspensions were layered over 0.10 ml of transport oil in 1.5-ml microcentrifuge tubes and sets of five tubes were placed in the rotor of an Eppendorf Model

5412 microcentrifuge. To start intervals of permeant influx, 0.1-ml volumes of ^{3}H-permeant solution were added counting metronome signals or using a stop-watch (for influx intervals greater than 30 sec). Since specific inhibitors of sodium-linked NT in L1210 cells have not been identified, periods of nucleoside influx were ended by centrifugal pelleting of cells under the oil. Cellular permeant uptake during pelleting was considered to be equivalent to permeant influx during an interval of 2 sec (143). In rapid sampling assays, 2 sec were added to nominal uptake intervals, that is, between permeant addition and centrifuge switch-on.

The "oil-stop" method for measurement of cellular permeant uptake does not enable direct determination of the cellular permeant content at time-zero (permeant association with the cells arising from adsorption to the plasma membrane or any process other than interaction with NT systems). Time-zero nucleoside uptake was determined by adding cell suspension to permeant solutions (in the presence of 10-20 μM dipyridamole) at 0°C to -2°C, followed by immediate centrifugation. This tactic was supported by the experiment of Fig. 34, which showed that Ado transport *via* the sodium-dependent system in L1210/AM cells was virtually abolished at 5°C. The presence of dipyridamole eliminated nucleoside permeation *via* non-concentrative systems. In figures illustrating time courses of nucleoside influx, cellular nucleoside content at time-zero is shown and has not been subtracted from cellular nucleoside content at indivi-

dual time intervals.

Aqueous layers in the assay tubes were removed by aspiration and tube walls above the oil layers were washed with distilled water. The aqueous and oil layers were then removed and cell pellets were dissolved in 0.2 ml 5% Triton X-100. The tubes were placed in scintillation vials, 8-ml portions of scintillation fluid (147) were added and ^{3}H-activity was measured.

Intracellular water volumes were estimated by subtracting the extracellular space (determined with ^{3}H-PEG in place of permeant) from total pellet water. The intracellular water constituted 80-90% of the pellet space. Time courses of nucleoside influx plotted in appropriate figures show nucleoside content associated with the intracellular spaces.

In the present study, nucleoside influx mediated by sodium-driven systems in L1210 cells were approximately linear for at least 10 sec (e.g. Fig. 30), and transport rates was readily determined from the slopes of time courses of nucleoside influx. Transport assays were done in triplicate and experiments were repeated 2-4 times.

5. Binding assays.

a) Time courses of ^{3}H-NBMPR binding

Portions (0.5 ml) of cell suspensions (4×10^{6} cells/ml) in sodium medium were added to microcentrifuge containing transport oil (0.15 ml) and 0.5 ml of ^{3}H-NBMPR (20 nM, final) in the presence or absence of 20 μM NBTGR.

These reaction mixtures were kept at 22°C for specified intervals until cells were pelleted under oil. Subsequent sample work-up to determine the ^{3}H-content of cells was similar to that described for transport experiments. Site-specific binding of NBMPR was determined by subtracting the cell content of ^{3}H-NBMPR obtained in the presence of NBTGR ("non-specific binding") from that in the absence of NBTGR ("total binding").

b) Equilibrium binding of ^{3}H-NBMPR

Binding assays were performed as described in the preceding section, except that NBMPR concentrations were varied (0.04-40 nM) and all samples were incubated for 30 min before centrifugation. Concentrations of free (unbound) ligand were determined from the ^{3}H-NBMPR content of the cell-free medium. The cell content of ^{3}H-NBMPR bound specifically and non-specifically was estimated as described in the preceding section.

V. CHEMOTHERAPY EXPERIMENTS

For chemotherapy experiments, 21-25 g female B6D2F_1 mice (F_1 hybrids between DBA/2 males and C57Bl/B6 females) were obtained from the Health Sciences Small Animal Program, University of Alberta. The animals were intraperitoneally implanted each with 10^6 L1210/C2 cells (0.2 ml of a suspension containing 5 x 10^6 cells/ml in 0.9% NaCl) obtained from ascitic fluid of donor mice. Drugs were dissolved in 0.9%

NaCl (pH 7.4, unless otherwise indicated) and administered 24 h after tumour implantation by i.p. injection. The volumes of drug solutions administered were proportional to 0.1 ml per 10 g body weight. Chemotherapy treatments followed schedules specified in individual experiments.

RESULTS AND DISCUSSION

I. EFFECTS OF NT INHIBITORS ON THE TOXICITY AND CELLULAR METABOLISM OF NUCLEOSIDE ANALOGUES IN L1210/C2 CELLS.[10]

1. Enhancement by dipyridamole of the antiproliferative activity, accumulation and retention of dAdo and dATP in L1210/C2 cells.

The presence of dAdo in the culture medium of L1210/C2 cells decreased cell proliferation rates in a concentration-dependent manner, with an IC_{50} value of 26 μM (Fig. 2). The antiproliferative effects of dAdo increased when dipyridamole was included in the medium. IC_{50} values for the inhibition of cell proliferation by dAdo in the presence of 1 or 10 μM dipyridamole were 9 and 1.5 μM, respectively (Fig. 2).

Kang and Kimball (95) reported that, in L1210 cells, the cellular accumulation of dAdo and its 5'-phosphates was increased by dipyridamole, an effect accompanied by enhancement of dAdo antiproliferative activity. To examine the effect of dipyridamole on the accumulation of dAdo and dATP in L1210/C2 cells, cells were cultured at 37°C in medium containing 40 μM ^{3}H-dAdo with or without 10 μM dipyridamole.

---

[10] Unless otherwise indicated, dCF (1.1 μM, final) was added to cell suspensions at least 1 h prior to the addition of dAdo or araA in these experiments. The data reported in Section I are means of replicate samples. All experiments were repeated two or three times with a variation of 5-7%.

Pathways of dAdo metabolism in mammalian cells

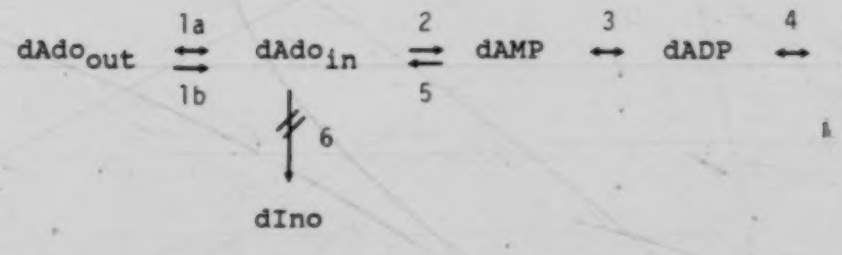

Step	Enzyme[12]	Ref.
1	NT systems:	
	(a) non-concentrative	148-150
	(b) Dipyridamole-insensitive	
2	Ado kinase, dCyd kinase, deoxyribonucleoside kinase	151-153
3	Deoxyribonucleotide kinase	154,155
4	Deoxyribonucleoside 5'-diphosphate kinase	154,155
5	5'-Nucleotidase	156-159
6	Adenosine deaminase	160

[12] Many of the enzymes involved in deoxyribonucleoside metabolism have not been characterized. While these activites are recognized, their presence in L1210 cells has not been demonstrated for all.

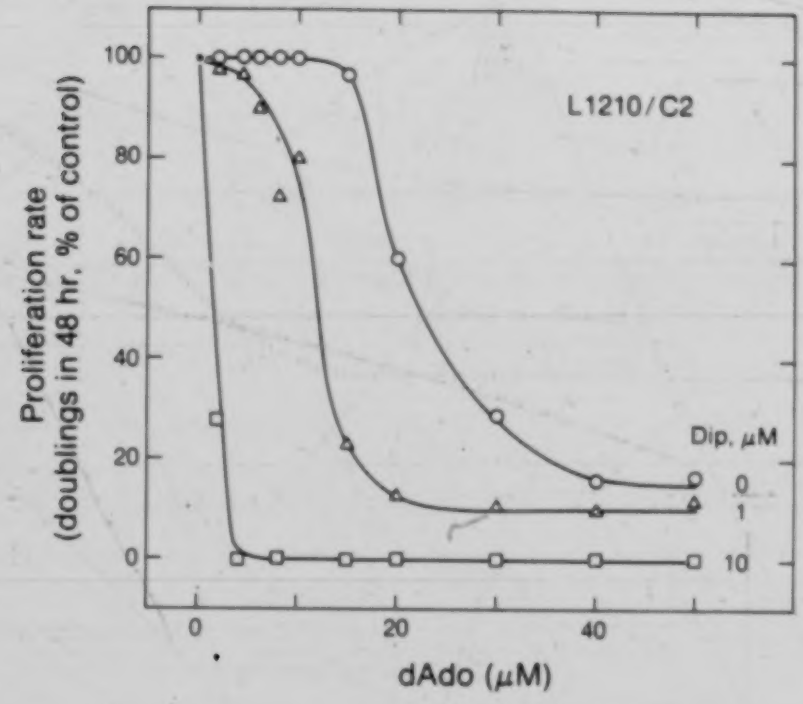

Fig. 2. Enhancement by dipyridamole of the anti-proliferative effect of dAdo towards L1210/C2 cells. Cultures (10^5 cells/ml) were incubated with dCF (1.1 μM, final) for 1 h prior to the addition of dAdo and dipyridamole. In growth medium without additives, the cell population doubling time was 19.2 h. Final concentrations of dipyridamole were (○) 0, (△) 1 μM, or (□) 10 μM.

Figure 3 shows that, after 3 h of incubation, cellular levels of dAdo and dATP[11] were increased about 12-fold by the presence of dipyridamole in the culture medium. The metabolism of dAdo in L1210/C2 cells under these conditions probably involved the reaction sequences oulined in the scheme of p. 51. In this scheme, the passage of dAdo across the plasma membrane is primarily transporter-mediated, a concept supported by this study. It is a conclusion of this study that multiple NT systems participate in dAdo translocation, one such system being a non-concentrative transporter. In the scheme outlined on p. 51, cytoplasmic dAdo may be phosphorylated, or, because of reversibility of the facilitated diffusion system, may leave the cell. Blockade of dAdo efflux would be expected to increase cellular accumulation and retention of dAdo and its 5'-phosphates. Accordingly, the accumulation of dAdo and dATP in the presence of dipyridamole in L1210/C2 cells shown in Fig. 3 may be attributable to inhibition of dAdo efflux.

The metabolic scheme of p. 51 suggests that, if cells containing dAdo and its 5'-phosphates were in dAdo-free medium, cytoplasmic dAdo would leave the cells down a

---

11 With the exception of cells cultured in the presence of dipyridamole for 3 h, in which the amount of dAMP+dADP constituted 17% of total ^{3}H-labelled material, cellular levels of dAMP+dADP did not exceed 9% of total ^{3}H-activity (data not shown)

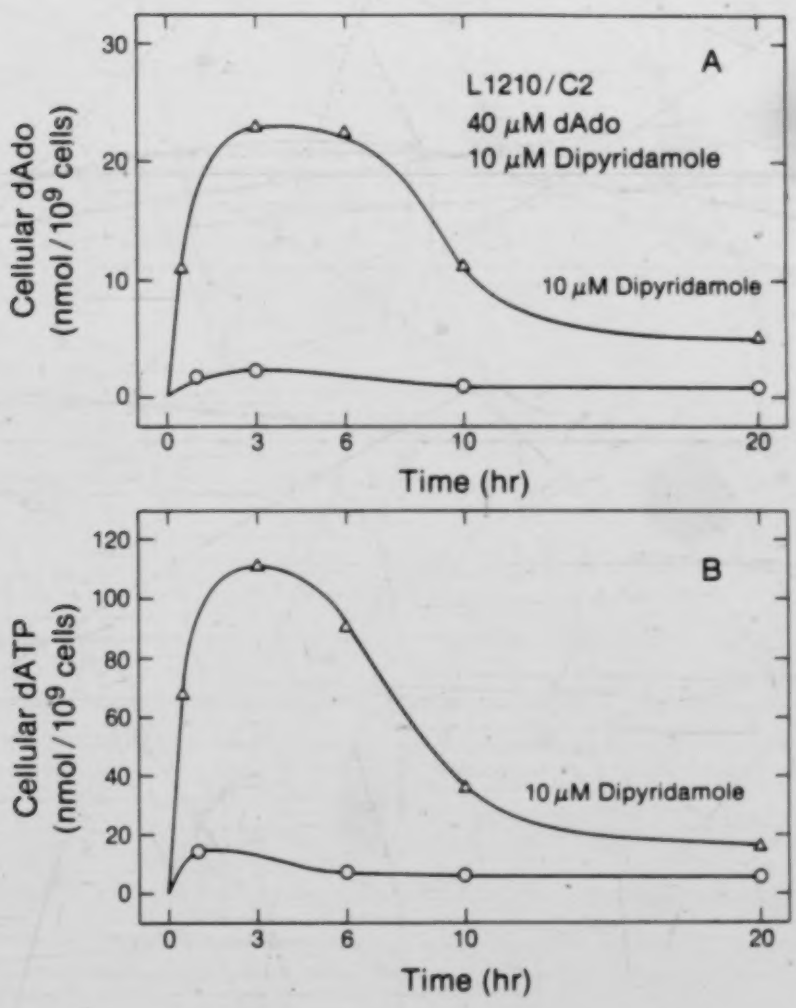

Fig. 3. Enhancement by dipyridamole of the cellular content of dAdo (Panel A) and dATP (Panel B) in L1210/C2 cells. Cells suspended at a density of 5 x 10^5 cells/ml were cultured at 37°C in medium containing 40 μM ^{3}H-dAdo. dCF (1.1 μM, final) was added to cultures 1 h prior to addition of dAdo and dipyridamole (10 μM, final). Cultures were prepared with (△) or without (○) dipyridamole. After indicated intervals, cells were pelleted and TCA extracts were prepared for TLC analysis of cellular dAdo and dATP content as described in "Materials and Methods".

BLANK PAGE INSERTED

concentration gradient. Loss of cytoplasmic dAdo might be followed by dephosphorylation of dAMP, dADP and dATP, which would result in further outward movement of dAdo down its concentration gradient.

When L1210/C2 cells containing ^{3}H-dATP were suspended in dAdo-free medium, dATP levels diminished with time, with a half-life of 87 min (Fig. 4). Such decreases were accompanied by the appearance in the extracellular medium of ^{3}H-activity, which was shown by HPLC and TLC analyses to be mainly dAdo (Fig. 5, Table 5). Thus, appearance of ^{3}H-dAdo in the suspension medium coordinately related decreases in cellular dATP with dAdo efflux.

The presence of 10 uM dipyridamole during incubation of cells containing ^{3}H-dATP in dAdo-free medium increased the half-life of dATP to 140 min (Fig. 4), and decreased the fraction of ^{3}H-activity appearing in the medium (data not shown). Thus, the increase in cellular retention of dATP was consistent with blockade by dipyridamole of dAdo exit from the cells, but did not preclude the possibility of dipyridamole effects on dAdo phosphorylation and/or on dephosphorylation pathways.

2. Effect of NT inhibitors on accumulation, retention and antiproliferative activity of araA and araATP.

To further explore the enhancement of nucleoside anabolism and retention in L1210/C2 cells, experiments similar to those described in the preceding section were

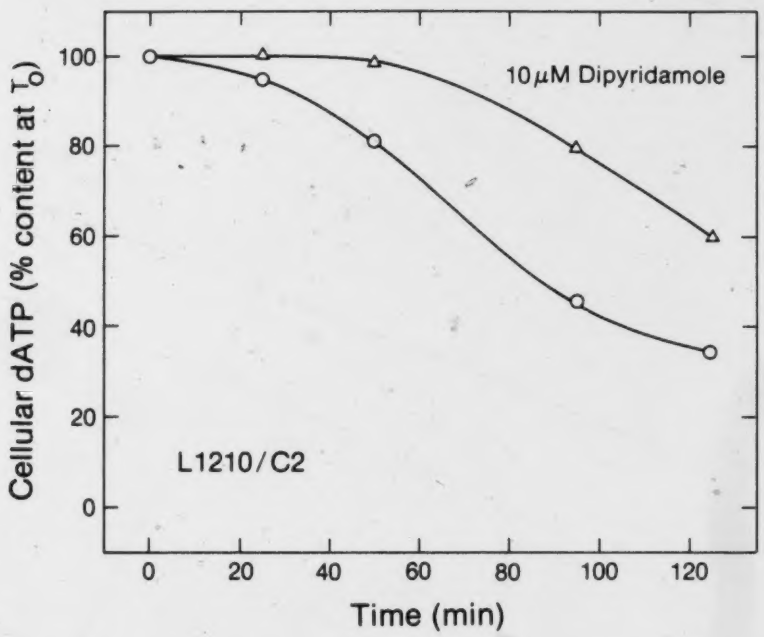

Fig. 4. Enhancement by dipyridamole of dATP retention in L1210/C2 cells. Cell suspensions (5 x 10^5 cells/ml in roller bottles (1.5 rpm)) were incubated at 37°C with 1.1 μM dCF for 1 h prior to the addition of ^{3}H-dAdo (40 μM, final). After incubating for a further 3.3 h, the cellular dATP content was 100 nmol/10^9 cells. Cells were then washed once with ice-cold growth medium without additives, suspended in warm medium with (△) or without (○) 10 μM dipyridamole and incubated at 37°C. At the times indicated, cells were collected and neutralized TCA cell extracts were prepared; dATP concentrations in the extracts were determined by TLC analysis.

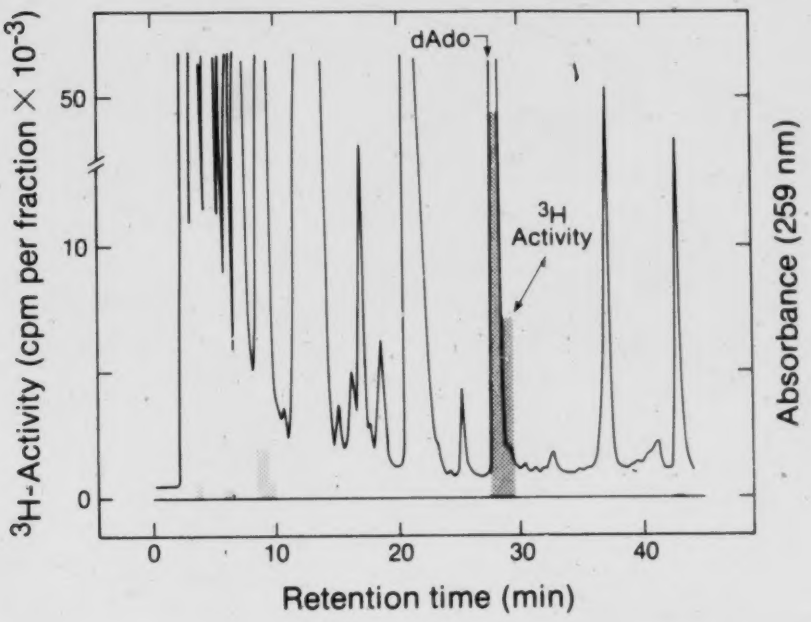

Fig. 5. Extracellular decay products of cellular ^{3}H-dATP. L1210/C2 cells containing ^{3}H-dATP, prepared as described in Fig. 4, were washed once, suspended in growth medium and incubated at 37°C for 3 h. Medium samples were freeze-dried, the residues were extracted with ice-cold 0.4 M TCA, and, after neutralization, the extracts were analyzed by HPLC. Shaded areas represent ^{3}H-activity above background. The absorbance peak designated as dAdo (retention time, 28.6 min) was present only when authentic dAdo was added as a marker.

Table 5

TLC analysis of medium from suspensions of ^{3}H-dATP-containing L1210/C2 cells

Samples of suspension medium from cells containing ^{3}H-dATP were freeze-dried and extracted with 0.4 M TCA. After neutralization with alamine/Freon, cell extracts were analyzed by TLC. ^{3}H-Activity accompanying added non-isotopic dAdo ("carrier") is expressed as a percentage of the total ^{3}H-activity applied to chromatograms.

Stationary phase	Developing solvent	^{3}H-activity accompanying dAdo
Cellulose	Water	83.6 %
PEI(borate) cellulose	0.1 M H_3BO_3	94.0 %
PEI cellulose	Water	91.4 %

undertaken with araA and the NT inhibitors, NBMPR, dilazep and dipyridamole. Dipyridamole alters cellular processes other than NT (161,162). Thus, the inclusion of NBMPR and dilazep tested the possibility that the enhancement of nucleoside accumulation and retention (Figs. 3 and 4) was a particular property of dipyridamole. The inhibitor concentrations used (10 μM dipyridamole, 15 μM dilazep, 8 μM NBMPR) were thought to decrease nucleoside influx in L1210/C2 cells to about the same extent (however, see Section II.1).

In cells cultured at 37°C in medium containing 20 μM ^{3}H-araA (without NT inhibitors), araA and araATP reached peak concentrations of approximately 5 nmol/10^{9} cells and 16 nmol/10^{9} cells in 21 h (Fig. 6). AraAMP and araADP were not found in these cells, likely because their cellular levels were below the detection limit of the analytical technique used.

The presence of 10 μM dipyridamole in cell suspension medium containing ^{3}H-araA, increased cellular araA and araATP pools as much as 12- and 5.6-fold, respectively (Fig. 6). The maximum concentrations of araA and araATP observed in cell suspensions containing dilazep were similar to those reached in dipyridamole-containing cultures. However, cells cultured in medium containing dilazep maintained high levels of araA and araATP for shorter time intervals (Fig. 6), and by the end of the 21-h incubation period, the concentration of araATP in these cells was not significantly different from that in inhibitor-free cultures. Decreases in cellular levels

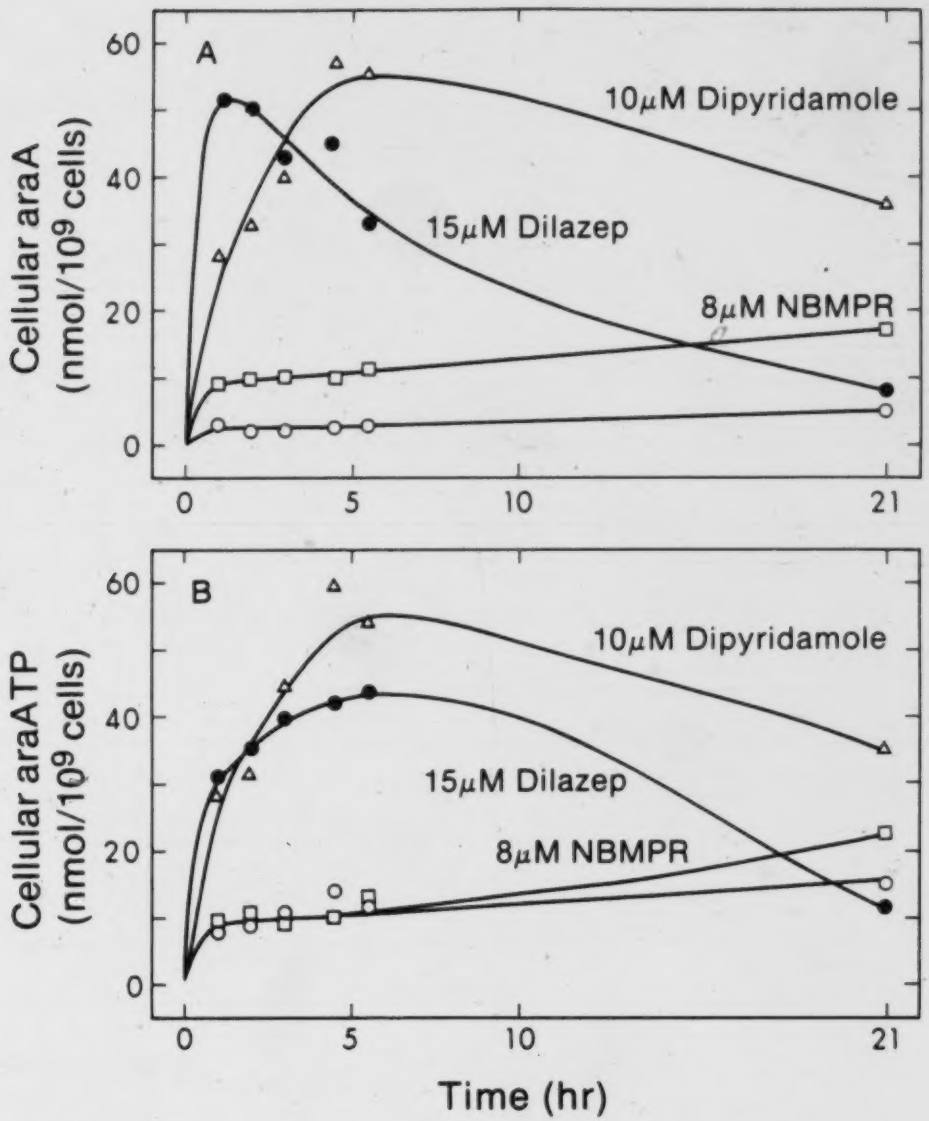

Fig. 6. Accumulation of araA (Panel A) and araATP (Panel B) in L1210/C2 cells. Cells suspended at a density of 5 x 10^5 cells/ml were incubated at 37°C with 1.1 μM dCF for 1 h prior to addition of ^{3}H-araA (20 μM, final) alone (○), or in combination with 10 μM dipyridamole (△), 15 μM dilazep (●) or 8 μM NBMPR (□) for the intervals indicated. Cellular contents of araA or araATP were measured by TLC analysis of neutralized TCA extracts.

of araA and araATP, which probably reflected araA efflux from the cells, were not attributable to degradation of dilazep during the interval of culture. The stability of that NT inhibitor was evident in parallel experiments with ^{3}H-dilazep, which showed that 90% of the ^{3}H-activity in the incubation mixture co-migrated with authentic dilazep on silica gel thin-layer chromatograms after 20 h of incubation at 37°C (data not shown).

Dilazep has two basic nitrogen atoms and, in solutions at pH 7.4, approximately 3% of dilazep molecules are uncharged. Inhibition of NT activity in human erythrocytes apparently occurs by interaction of uncharged dilazep molecules with the NT system of these cells [2]. Since culture of L1210/C2 cells for periods of over 4 h significantly acidified the growth medium (in the experiments of Figs. 6 and 7), the fraction of dilazep molecules capable of inhibiting NT may have been reduced. Accordingly, a pH-related reduction in the inhibition by dilazep of araA efflux mediated by non-concentrative systems may have influenced the kinetics of araA retention in those cultures (Figs. 6 and 7).

The increase in cellular accumulation of araA and araATP observed in the presence of 8 μM NBMPR was markedly smaller than the increases observed in the presence of dilazep or dipyridamole. The maximum concentration of araA achieved in these cell suspensions was approximately 3-fold greater than that in inhibitor-free cultures. AraATP concentrations in the presence and in the absence of NBMPR were similar (Fig. 6).

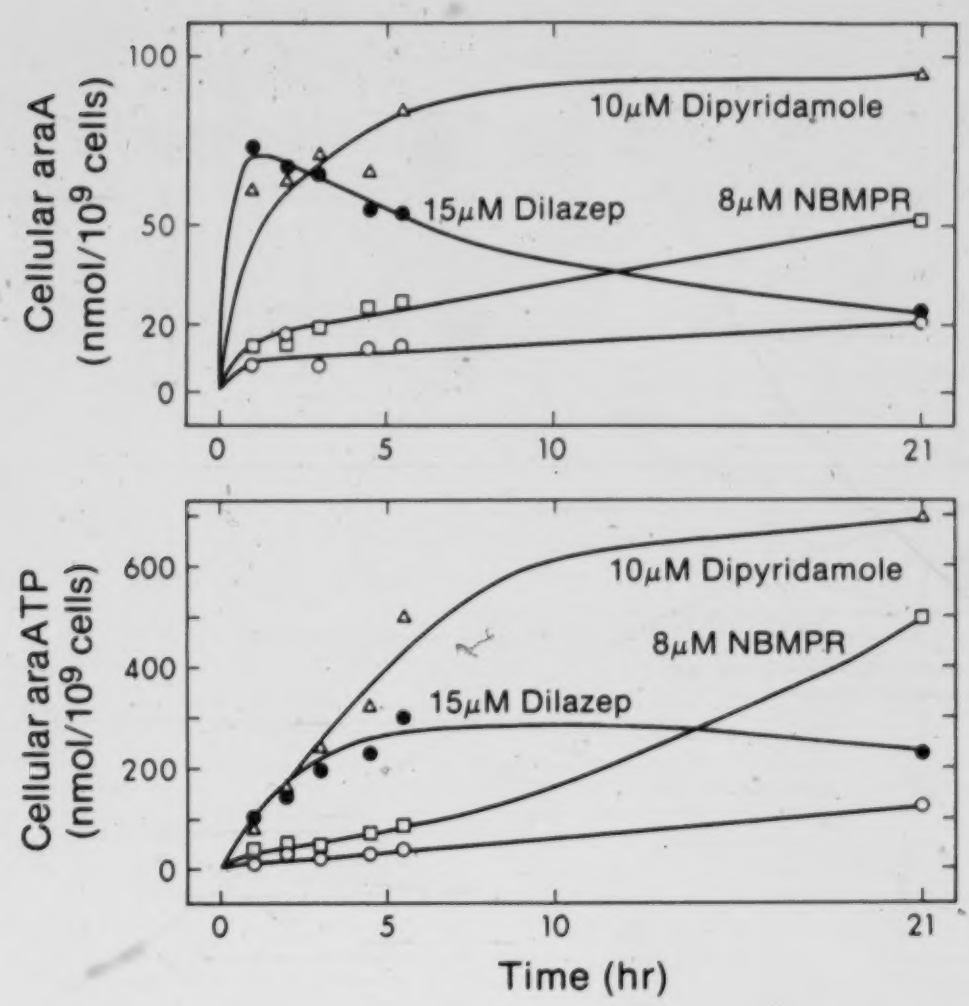

Fig. 7. Accumulation of araA (Panel A) and araATP (Panel B) in L1210/C2 cells. Cell suspensions were incubated with ^{3}H-araA (20 μM, final) as described in Fig. 6, except that EHNA (1.5 μM, final) replaced dCF. Cultures contained araA alone, (○), or araA with: 10 μM dipyridamole (△), 15 μM dilazep (●) or 8 μM NBMPR (□).

The differences in the effects of NT inhibitors on nucleoside accumulation in L1210 cells are discussed in Section II.1.

The experiment of Fig. 6 was interpreted to mean that the induced cellular accumulation of purine nucleosides arose from alterations in NT function.

Assays of nucleoside accumulation were conducted in the presence of 1.1 μM dCF to prevent dAdo or araA catabolism. To test the possibility that dCF was in some way directly involved in the enhancement of cellular araA and araATP levels, experiments similar to those of Fig. 6, but in which 1.5 μM EHNA replaced dCF, were undertaken (Fig. 7). Comparison of Figs. 6 and 7 indicates that, in the presence of dipyridamole, dilazep or NBMPR, cellular levels of free araA were slightly higher when EHNA replaced dCF. Maximum levels of cellular araATP, however, were substantially higher in media containing EHNA, irrespective of the absence or presence of an NT inhibitor. TLC analysis of the cell extracts revealed that less than 5% of the cellular ^{3}H-content was associated with araH in cultures containing either ADA inhibitor (data not shown). Thus, the large differences between the effects of EHNA and dCF are not attributable to variation in the extent of ADA inhibition. The enhancement in cellular araA and araATP levels in EHNA-treated cells relative to those in dCF-treated cells remains unexplained.

The largest increases in cellular levels of araA and araATP occurred in cultures containing dipyridamole and EHNA.

AraA and araATP levels reached 97 nmol/10^9 cells and 700 nmol/10^9 cells, respectively, after 21 h of incubation at 37°C with 20 μM araA (Fig. 7). Peak concentrations of araA in these cultures were equivalent to about 100 μM, since water spaces in L1210/C2 cells incubated with 20 μM araA increased from 0.35 ml/10^9 cells to 0.9 ml/10^9 cells after 21 h of culture with that nucleoside analogue (data not shown). Although the fraction of araA bound to intracellular components such as SAH hydrolase was not measured in these experiments, the cellular level of free (unbound) araA likely exceeded that of the medium (20 μM), implying the presence of concentrative nucleoside uptake mechanisms in L1210/C2 cells (*vide infra*).

The concentrations of araA and araA metabolites achieved in the leukemic cells were apparently the resultant of various processes, including trans-membrane fluxes of the free nucleoside in both inward and outward directions, mediated by more than one NT system, as well as phosphorylation. As discussed in the preceding section, increases in araA and araATP accumulation in these cells may have arisen from a net inhibition of araA efflux.

3. Effect of NT inhibitors on retention of cellular araATP

In the absence of ADA activity, a metabolic scheme similar to that of p. 54 may also be appropriate for araA.

$$AraA_{out} \rightleftarrows araA_{in} \rightleftarrows araAMP \leftrightarrow araADP \leftrightarrow araATP$$

In this scheme, efflux of araA into araA-free medium would likely cause a decrease in cellular araATP levels through phosphorylation-dephosphorylation equilibria. When extracellular levels of araA are low, decay of cellular araATP levels would be expected to correlate with outward movement of araA molecules. To test this idea, L1210/C2 cells were "loaded" with ^{3}H-araATP by incubation with 20 μM ^{3}H-araA at 37°C for 3 h. After a single wash with cold medium, these cells were suspended in araA-free medium and time-dependent changes in ^{3}H-content of the cells and medium were followed. It was found that cellular concentrations of araATP declined with a half-life of 73 min under these conditions (Fig. 8). When cells containing ^{3}H-araATP were suspended in araA-free medium with 10 μM dipyridamole, the half-life of cellular araATP increased 2.6-fold, to 190 min (Fig. 8). The presence of 15 μM dilazep resulted in a 1.7-fold increase in araATP half-life (124 min), whereas 8 μM NBMPR did not significantly alter the cellular retention of araATP relative to inhibitor-free cultures (Fig. 8).

The decline in cellular ^{3}H-araATP pools was accompanied by the appearance in the extracellular medium of corresponding amounts of ^{3}H-labelled material which, as shown by TLC and HPLC analyses, consisted mainly of araA (Fig. 9 and Table 6).

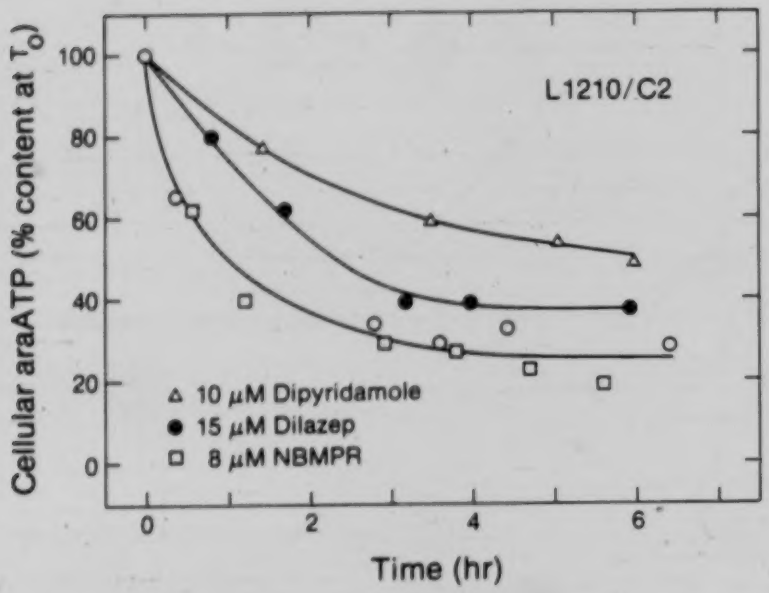

Fig. 8. Decay of cellular levels of araATP in the presence of NT inhibitors. Suspensions of L1210/C2 cells (5 x 10^5 cells/ml) in roller bottles (1.5 rpm) were maintained at 37°C. One hour after addition of dCF (1.1 μM, final), ^{3}H-AraA (20 μM, final) was added and cells were collected 3 h later. Cells were washed once with ice-cold medium and suspended in growth medium without (○), or with NT inhibitors: 10 μM dipyridamole (△), 15 μM dilazep (●), or 8 μM NBMPR (□). The cells were incubated at 37°C for the intervals indicated, and araATP content was quantified by TLC. At time zero, the cell content of ^{3}H-araATP was 85 nmol/10^9 cells.

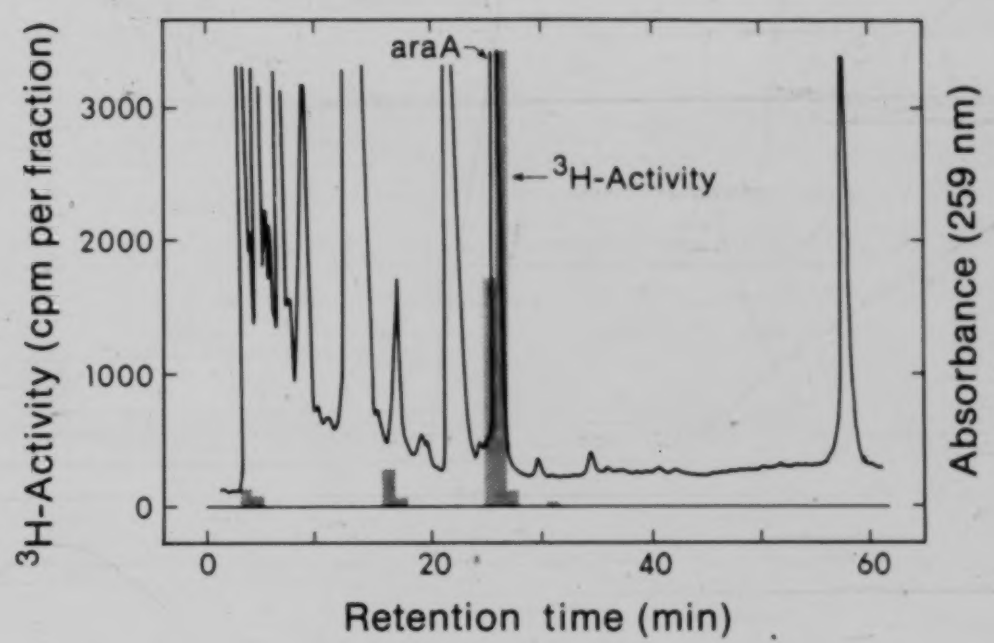

Fig. 9. Decay product of cellular ^{3}H-araATP. L1210/C2 cells containing ^{3}H-araATP, prepared as in Fig. 8, were washed once, suspended in growth medium without additives and incubated at 37°C for 3 h. Medium samples were analyzed as described in Fig. 5. Shaded areas represent ^{3}H-activity above background. The absorbance peak designated as araA (retention time, 26 min) was present only when araA was added as a marker.

Table 6

TLC analysis of medium from suspensions of [^{3}H]araATP-containing cells

Cells containing ^{3}H-araATP, prepared as in Fig. 9, were incubated at 37°C for 3 h, and samples of the incubation medium samples were then analyzed by TLC as described in Table 5. ^{3}H-Activity accompanying added "carrier" araA is expressed as a percentage of total ^{3}H-activity applied to chromatograms.

Stationary phase	Developing solvent	^{3}H-activity accompanying araA
Cellulose	Water	93.5 %
PEI(borate) cellulose	0.1 M H_3BO_3	88.4 %
PEI cellulose	Water	89.4 %
Silica gel	*	85.0 %

* Methanol-chloroform-3% acetic acid 2:3:1 (v/v/v)

The similar relative efficacies of the NT inhibitors in inducing accumulation of araA and araATP, and retention of the latter (10 μM dipyridamole > 15 μM dilazep > 8 μM NBMPR) suggested that NT effects were responsible for both the increased anabolism of araA and the decreased catabolism of araATP.

4. Influence of dipyridamole and araA on cell proliferation rates and viability in cultures of L1210/C2 cells

AraA cytotoxicity towards lymphoid cells has been correlated with cellular formation of araATP and (araA)DNA (114,125). The enhanced cellular accumulation and retention of araATP in dipyridamole-containing L1210/C2 cultures (Figs. 6 and 7) suggested that araA cytotoxicity might be increased in dipyridamole-containing medium.

The antiproliferative activity of araA in cultures with or without 5 μM dipyridamole was measured in the experiment of Fig. 10. The IC_{50} values for inhibition by araA of cell proliferation during 48 h of culture in the presence of 1.1 μM dCF were 8 μM or 2.3 μM, respectively, in the absence or presence of dipyridamole.

The antiproliferative effects of araA in the presence of EHNA were also measured (Fig. 11). Since araATP levels in cells cultured in medium containing dipyridamole and EHNA were ten-fold greater than those in similar experiments with dCF (Figs. 6 and 7), it was expected that the inhibitory

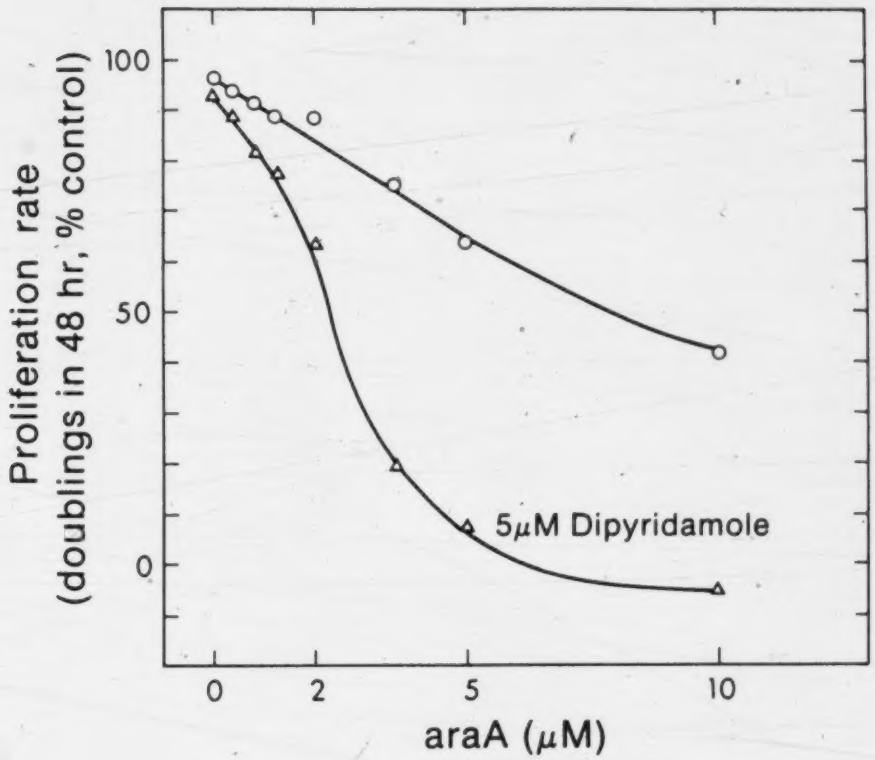

Fig. 10. Proliferation rates of L1210/C2 cells in growth medium containing araA alone (○) or araA plus 5 μM dipyridamole (△). Cells (10^5 cells/ml) were incubated for 1 h with 1.1 μM dCF prior to addition of araA with or without dipyridamole. The cell population doubling time in medium without additives was 14.5 h.

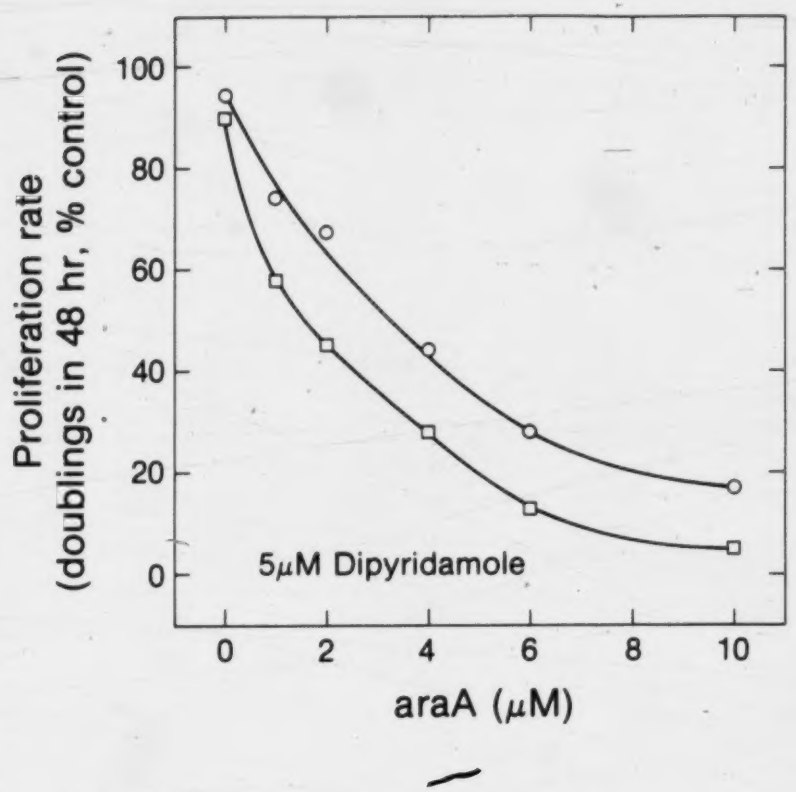

Fig. 11. Effect of araA in the presence (□) or absence (△) of 5 μM dipyridamole on the proliferation of L1210/C2 cells. Culture conditions were as described in Fig. 10, except that 1.5 μM EHNA was used in place of dCF. The cell population doubling time in drug-free cultures was 16 h.

effects of araA on cell proliferation would be substantially larger in EHNA than in dCF-containing cultures. However, the IC_{50} values for araA inhibition of cell proliferation in EHNA-containing cultures were 3.8 μM or 1.9 μM in the presence or absence or dipyridamole, respectively (Fig. 11). This suggested that (i) large increases in araATP levels were not proportional to increases in the antiproliferative activity of araA, or (ii) dipyridamole-induced increases in cellular araATP levels under the experimental conditions of Fig. 11 differed from those observed in experiments measuring araA and araATP accumulation (Fig. 7).

The clonogenic viability of cells cultured with dCF and graded concentrations of araA in the presence or absence of 10 μM dipyridamole for 24 h was also measured. As shown in Table 7, the clonogenic capacity of cells incubated with araA was only slightly decreased by dipyridamole. These results show that culture conditions with major effects on cellular levels of araATP did not induce corresponding changes in araA cytotoxicity. These experiments did not measure repair of araA-induced damage after cells were transferred to drug-free cloning medium.

5. Relationship between cellular formation of araATP and incorporation of araA into DNA

Kufe *et al.* (125) have reported that araA incorporation into the DNA of L1210 cells is accompanied by loss of clonogenic viability. Since, in the present study, the

Table 7

Effect of exposure to araA, dCF and dipyridamole on the clonogenic viability of L1210/C2 cells.

Cells were cultured with graded concentrations of araA in the presence or absence of 10 μM dipyridamole for 24 h at 37°C. Cell so treated were washed, suspended in tubes with soft agar cloning medium and incubated for 10 days before enumerating colonies formed.

Dipyrid-amole (μM)	dCF (μM)	araA (μM)	Cells per tube[1]	Colonies per tube[2]	Rel. cloning efficiency (%)
0	0.0	0.00	200	134	100
0	0.0	1.00	80	41	76
0	0.0	2.00	200	104	78
0	0.0	5.00	200	90	67
0	1.1	0.00	200	129	96
0	1.1	0.25	160	67	62
0	1.1	0.50	160	49	45
0	1.1	1.00	240	49	30
0	1.1	2.00	1000	95	14
0	1.1	5.00	1000	62	9
10	0.0	0.00	200	123	92
10	0.0	1.00	80	35	65
10	0.0	2.00	200	138	103
10	0.0	5.00	200	111	83
10	1.1	0.25	240	67	41
10	1.1	0.50	240	54	33
10	1.1	1.00	240	40	24
10	1.1	2.00	1000	104	15
10	1.1	5.0	1000	34	5

[1] Apparent number of cells per tube; ten tubes per group
[2] Average of ten tubes

induction by dipyridamole of high levels of araATP cells did not coordinately enhance antiproliferative effects of araA, the relationship between araATP concentration and (araA)DNA formation in L1210/C2 cells was investigated. To this end, cells were incubated with 0.5, 1.0, 2.0, 4.0 or 6.0 μM ^{3}H-araA in the presence or absence of 10 uM dipyridamole for 1-24 h.

AraA incorporation into nucleic acids was estimated after isolation of cellular DNA and RNA by phenol extraction and cesium sulphate gradient centrifugation (138-141). In this procedure, RNA and DNA distribute in bands with densities 1.62-1.68 and 1.42-1.48 g/ml, respectively, while proteinaceous material remains at the top of the gradient. In the present study, following incubation of L1210/C2 cells with 2 μM ^{3}H-araA for 3 h, 90% of the ^{3}H-activity associated with polynucleotides was found in DNA (Fig. 12). The data of Fig. 13 show that, in L1210/C2 cells exposed to araA under conditions that introduced graded amounts of araA into DNA, the relationship between (araA)DNA formation and cellular araATP was complex. The increases in cellular araATP were not directly proportional to araA incorporation into DNA, and the presence of dipyridamole appeared not to alter this relationship. The lack of correlation between the extent of cellular araATP accumulation and araA cytotoxicity, evident in the foregoing experiments, may have been due to (i) insufficient araA incorporation into cellular DNA to interfere with DNA replication or expression of genetic information under the

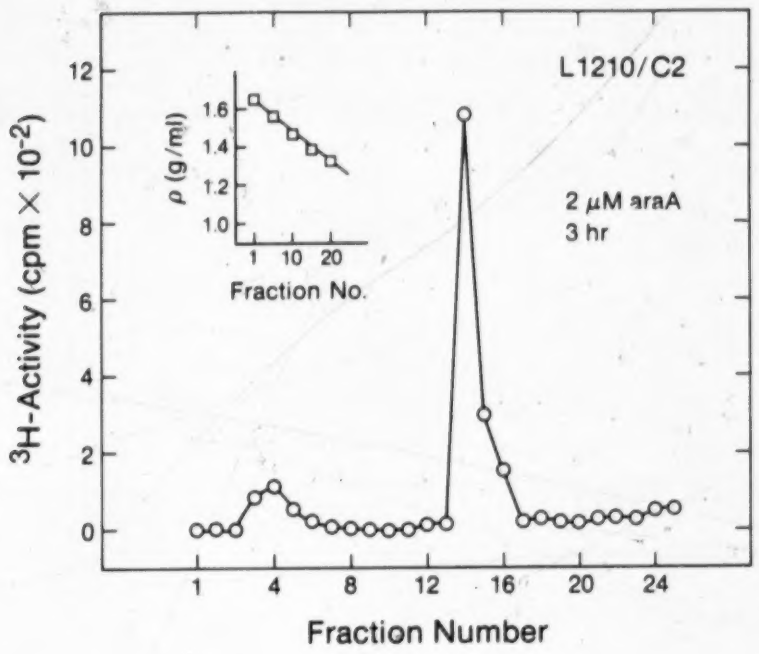

Fig. 12. AraA incorporation into DNA and RNA in L1210/C2 cells. After incubation of 5 x 10^6 cells (5 x 10^5 cells/ml) with 2 μM ^{3}H-araA for 3 h at 37°C (1 μM dCF present), nucleic acids were isolated by phenol extraction and cesium sulphate gradient centrifugation, as described in "Materials and Methods". The density range of the gradient was 1.64-1.31 g/ml. RNA and DNA were located in fractions 3-5 (1.62-1.64 g/ml) and 14-16 (1.40-1.42 g/ml), respectively. ^{3}H-activity above background is shown.

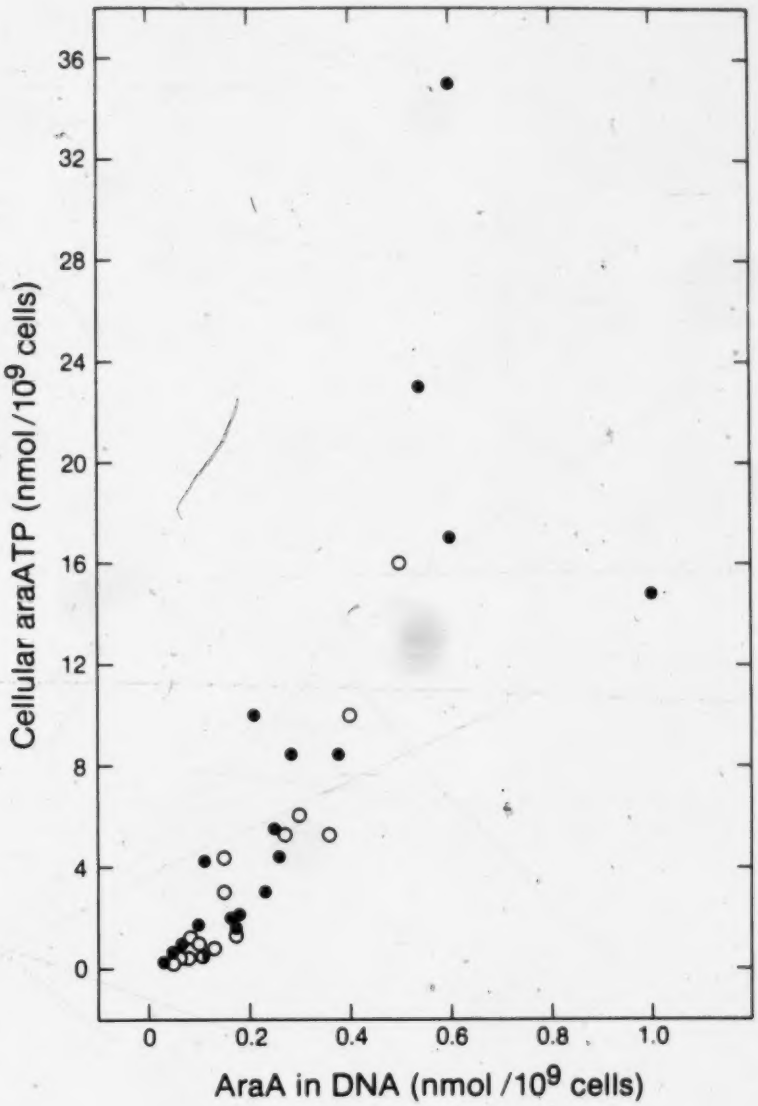

Fig. 13. Relationship between cellular araATP concentrations and araA incorporation into DNA in L1210/C2 cells. Cells were incubated at 37°C in growth medium containing 1.1 μM dCF for 1 h prior to the addition of ^{3}H-araA (0.5, 1.0, 2.0, 4.0 or 6.0 μM) with (●) or without (○) 10 μM dipyridamole. Incubation proceeded at 37°C for 1, 3, 6 or 24 h. AraA incorporation into DNA was measured as described in Fig. 12. Cellular araATP in these cultures was measured by TLC analysis of neutralized TCA extracts.

culture conditions used, or (ii) excision/replacement of araA residues in (araA)DNA.

6. Enhancement by dipyridamole of the antiproliferative activity of purine nucleoside analogues

Since it was likely that dipyridamole would influence the cellular metabolism of nucleosides other than dAdo and araA, the effects of dipyridamole on the antiproliferative activity of 2-halo-nucleosides in cultured L1210/C2 cells were explored. Dipyridamole increased several-fold the antiproliferative effects of dAdo and araA (Figs. 2, 8 and 9), but those nucleosides exhibited low toxicity towards L1210/C2 cells. It was reasoned that nucleoside analogues with relatively greater toxicity towards the leukemic cells might enable exploration of relationships between modulation of analogue anabolism and cytotoxic or therapeutic effects. Against this background, the effect of 10 uM dipyridamole on 2-F-araA inhibition of the proliferation of L1210/C2 cells in culture was investigated. The IC_{50} values obtained in the absence and presence of the NT inhibitor were, respectively, 8.4 µM and 2.7 µM (Fig. 14).

2-F-AraA and araA/dCF combinations were equally toxic to cultured CCRF-CEM cells (118). Comparison of Figs. 10 and 14 indicate that this observation may be extended to include cultured L1210/C2 cells, since IC_{50} values for inhibition of cell proliferation by araA-dCF combinations in L1210/C2 cultures were 8 and 2.3 µM in the absence and presence of

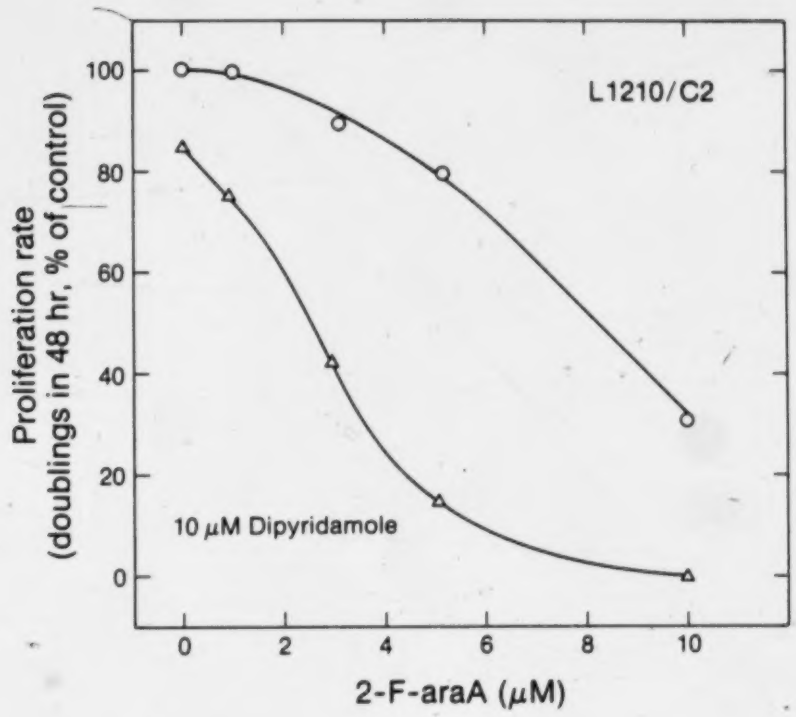

Fig. 14. Enhancement in the antiproliferative effects of 2-F-araA in the presence of dipyridamole. L1210/C2 cells (10^5 cells/ml) were cultured in media containing 2-F-araA with (△) or without (○) 10 μM dipyridamole. The cell population doubling time in medium without additives was 14.5 h.

dipyridamole, respectively (Fig. 10). However, the pharmacologic properties of araA/dCF combinations and 2-F-araA appear to differ: (i) 2-F-araA shows greater anti-neoplastic activity in mice implanted with P388 or L1210 leukemia than similar doses of araA co-administered with dCF (163), and (ii) 2-F-araA exerts host neurotoxicity in humans (164) and mice (*vide infra*).

The presence of 10 μM dipyridamole did not significantly alter the antiproliferative activity of 2-Br-2'-dAdo towards L1210/C2 cells (Fig. 15). IC_{50} values for inhibition of cell proliferation by this agent were 0.58 μM and 0.45 μM, respectively, in cultures without or with dipyridamole. It is not known if dipyridamole modulated cellular anabolism of this agent.

When L1210/C2 cells were cultured in medium containing 2-Cl-2'-dAdo, the inclusion of dipyridamole (10 μM, final) decreased the IC_{50} for inhibition of cell proliferation more than 50-fold, from 0.28 μM to 0.005 μM (Fig. 16). It is not known if the anabolism of 2-Cl-2'-dAdo was enhanced in the presence of dipyridamole.

7. Modulation by dipyridamole of araC cytotoxicity and araCTP retention in L1210/C2 cells

While the antiproliferative activities of several purine 2'-deoxyribonucleosides towards L1210/C2 cells were enhanced in the presence of dipyridamole, that of araC was reduced.

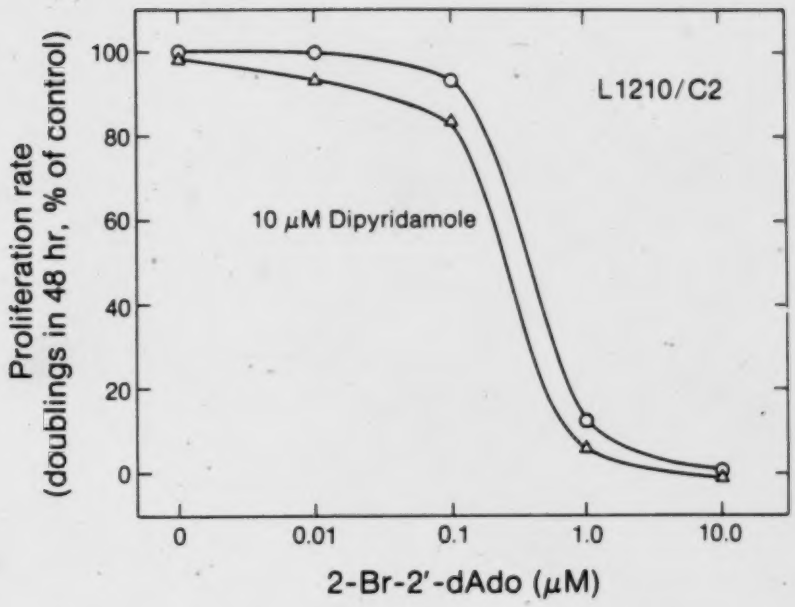

Fig. 15. Effect of 10 μM dipyridamole on the antiproliferative effects of 2-Br-2'-dAdo on L1210/C2 cells. Cells suspended at a density of 10^5 cells/ml were cultured in growth medium containing 2-Br-2'-dAdo with (△) or without (○) 10 μM dipyridamole. The cell population doubling time in medium without additives was 17.1 h.

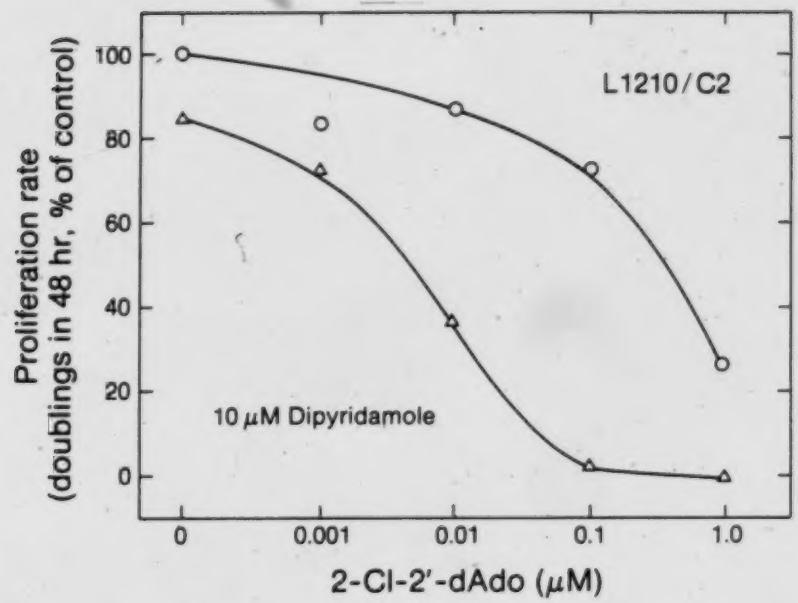

Fig. 16. Dipyridamole enhancement of anti-proliferative activity of 2-Cl-2'-dAdo in L1210/C2 cells. Cells (10^5 cells/ml) were cultured in growth medium containing 2-Cl-2'-dAdo with (△) or without (○) 10 μM dipyridamole. The cell population doubling time in medium without additives was 16 h.

Thus, IC_{50} values for araC inhibition of cell proliferation increased (from 10 nM) to 16 nM or 32 nM, respectively, in the presence of 1 or 10 μM dipyridamole (Fig. 17). Similar results were obtained when cultures were treated with 100 μM dThd for 5 h prior to the addition of araC (data not shown). Protection from the antiproliferative effects of araC by dipyridamole likely derived from inhibition of transporter-mediated influx of araC.

The influence of NBMPR, dipyridamole and dilazep on the retention of araCTP in L1210/C2 cells was next evaluated in the experiment of Fig. 18. After being "loaded" with ^{3}H-araCTP by 8 h of culture in medium containig 5 μM ^{3}H-araC, L1210/C2 cells were washed once with cold medium and suspended in araC-free medium with or without an NT inhibitor. The half-life of araCTP in cells cultured in medium without additives was 33 min, and was increased to 68 min in cells suspended in medium containing 8 μM NBMPR (Fig. 18). Cells in medium containing 10 uM dipyridamole or 15 μM dilazep retained 70% and 56%, respectively, of their initial araCTP content after 120 min of incubation in araC-free medium (Fig. 18). The decrease in cellular ^{3}H-araCTP was accompanied by the appearance of extracellular ^{3}H-activity. The rank order of potency for the enhancement of araCTP retention by NT inhibitors (8 μM NBMPR < 15 μM dilazep < 10 μM dipyridamole) was the same as that for enhancement of araATP retention (Fig. 8). The effects of dipyridamole on the cytotoxicity, accumulation and retention of nucleoside

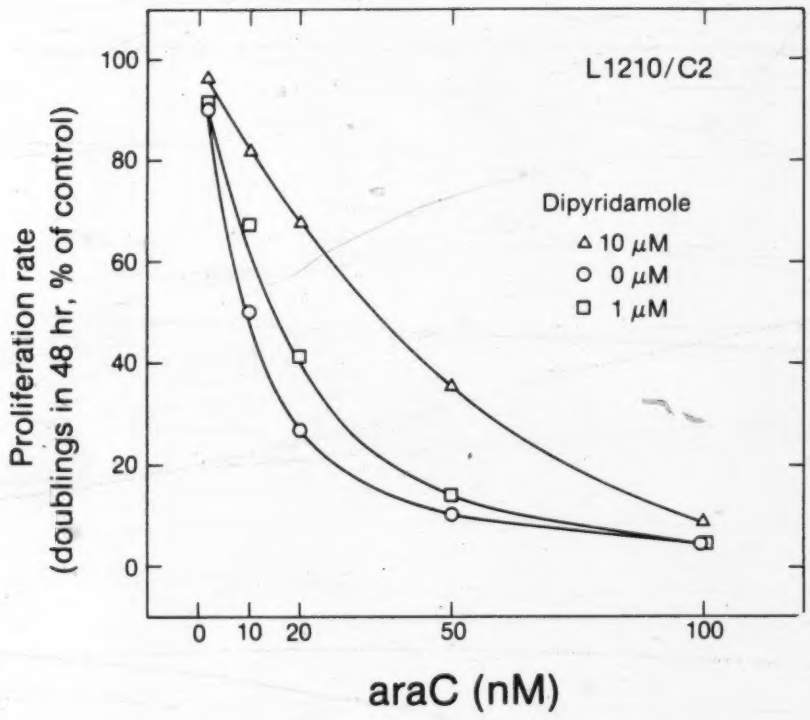

Fig. 17. Dipyridamole protection against the antiproliferative activity of araC in L1210/C2 cells. Culture media contained araC (○), or araC with 1 μM (□) or 10 μM (△) dipyridamole, and suspensions contained 10^5 cells/ml . The cell population doubling time in medium without additives was 13.7 h.

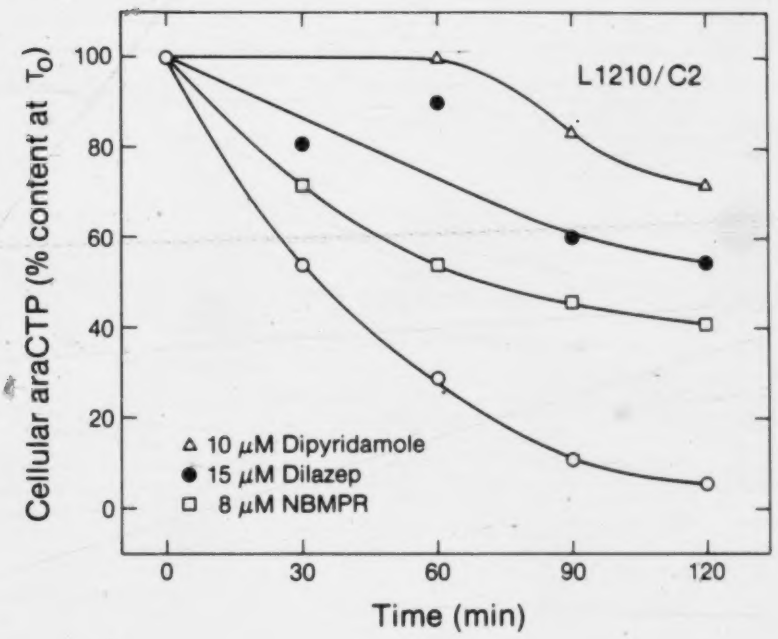

Fig. 18. Enhancement of cellular retention of araCTP by NT inhibitors. L1210/C2 cells (5 x 10^5 cells/ml) were incubated for 8 h in growth medium containing 5 μM ^{3}H-araC, washed once with ice-cold growth medium and suspended in warm, araC-free growth medium in the absence (○) or presence of 10 μM dipyridamole (△), 8 μM NBMPR (□) or 15 μM dilazep (●). TCA extracts were prepared at the indicated intervals and ^{3}H-araCTP was quantified by TLC. At time zero, the cellular araCTP content was 70 nmol/10^9 cells.

analogues are summarized in Table 8.

Because the depletion of cellular pools of dATP, araATP and araCTP correlated with the extracellular appearance of the corresponding nucleosides, and since dipyridamole coordinately reduced both processes, it appeared that a dipyridamole-sensitive nucleoside efflux system was involved. In contrast, the enhancement by dipyridamole of the cellular accumulation and/or antiproliferative activities of some nucleoside analogues suggested participation of an inhibitor-insensitive NT component in the influx of araA, dAdo and certain of their 2-halo-derivatives, but not in that of araC. The discovery and characterization of a dipyridamole-insensitive NT component in L1210 cells is described in the following section.

Table 8

Summary: modulation by dipyridamole of antiproliferative activity and accumulation of nucleoside analogues in L1210/C2 cells

	Dipyridamole modulation[1]		
Analogue	Antiproliferative activity	Accumulation	Retention
araA	++	+++	++
dAdo	++	+++	++
2-Br-dAdo	+	nd	nd
2-Cl-dAdo	+++	nd	nd
2-F-araA	++	nd	nd
araC	--	nd	++

1 +, enhancement
-, reduction
nd, not determined
The multiple signs indicate the extent of the increase (or decrease) of a particular effect relative to the other nucleoside analogues tested.

II. NUCLEOSIDE TRANSPORT IN L1210 CELLS[13]

1. Influx of FB and araA in L1210/C2 cells

The experiments of Figs. 6 and 7 showed that, in the presence of NT inhibitors, L1210/C2 cells acquired internal concentrations of free araA several-fold higher than in the suspending medium, and suggested the operation of a concentrative NT mechanism. This idea was explored with the inosine analogue, FB, which is poorly metabolized in these cells. TLC analyses of extracts of cells incubated with 50 μM ^{3}H-FB for 5 min at 22°C showed that 97% of cellular ^{3}H-activity co-migrated with FB in chromatograms (Table 9).

Early time courses of FB (50 μM) influx in L1210/C2 cells at 22°C were curved and cellular FB levels aproached a steady-state value of about 70 μM within 1 min (Fig. 19). Initial rates of FB influx were significantly reduced in the presence of 10 μM dipyridamole (Fig. 19); however, levels of cellular FB increased progressively and reached about 170 μM after 5 min of uptake in dipyridamole-containing cultures. Thus, a dipyridamole-insensitive NT system mediated uphill influx of FB in L1210/C2 cells.

The data of Fig. 19 provide evidence for the operation of NT systems of two types in L1210/C2 cells: (i) a reversible, facilitated diffusion system sensitive to 10 μM

---

[13] The data reported in Section II are means of triplicate samples and all experiments were repeated two or three times with consistent results.

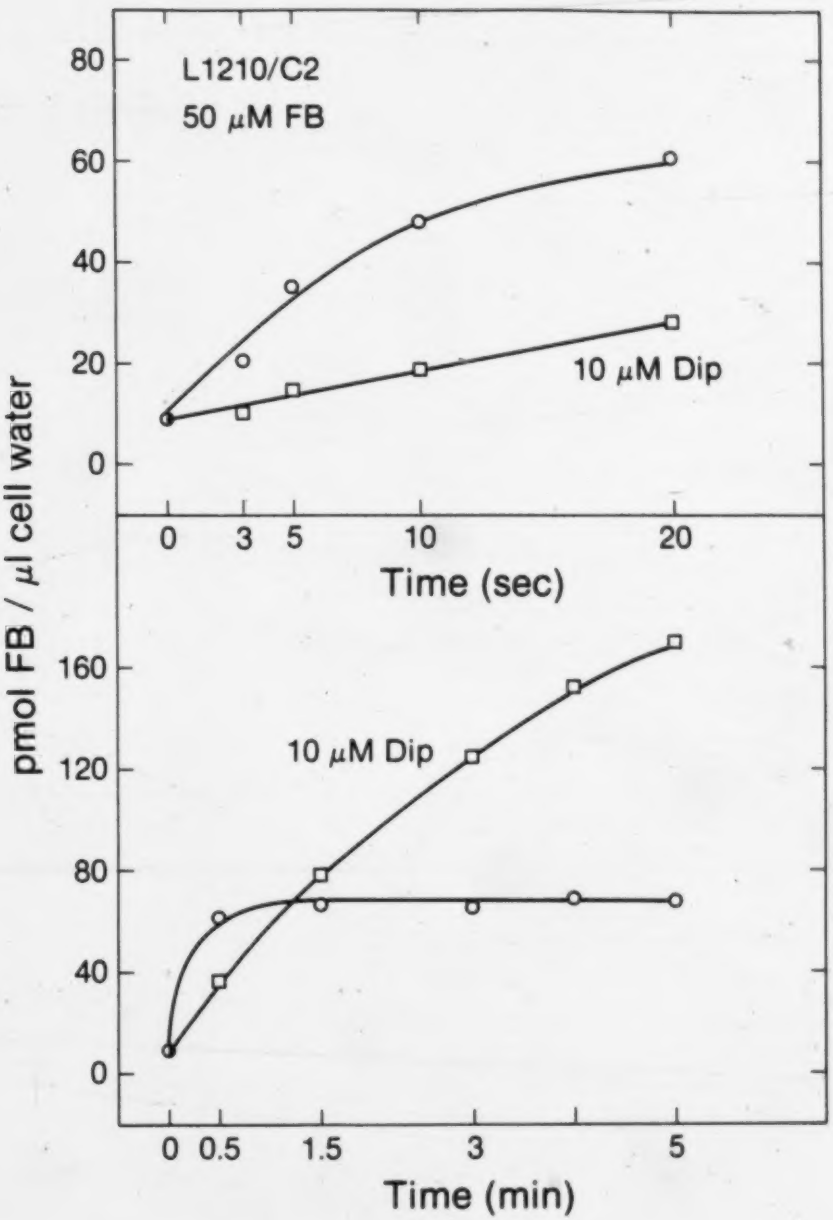

Fig. 19. Dipyridamole-insensitive FB influx in L1210/C2 cells. Time courses of FB (50 μM) influx were obtained with cells suspended in transport medium (HEPES-buffered Fischer's medium without serum) with (□) or without (○) 10 μM dipyridamole at 22°C. Dipyridamole was present in cell suspensions 10-25 min prior to transport measurements.

dipyridamole, and (ii) a concentrative influx system insensitive to dipyridamole. This interpretation attributes FB accumulation to (i) dipyridamole inhibition of outward FB fluxes mediated by facilitated diffusion transporters, and (ii) the dipyridamole-insensitive inward flux of FB mediated by a concentrative NT system. The occurrence of steady-state FB levels (about 70 μM) higher than the extracellular FB concentration (50 μM) may be the resultant of concentrative and non-concentrative inward fluxes, plus a downhill, outward leak.

The concentrative behaviour of the dipyridamole-insensitive FB carrier in L1210/C2 cells suggested that this system might be driven by downhill movement of a co-substrate. The majority of eukaryotic secondary-active transport systems are coupled to downhill translocation of sodium ions or protons (165). Hence, the dipyridamole-insensitive component of FB influx was examined in L1210/C2 cells suspended in media of different ionic composition. Replacement of Na^+ by K^+ (in the presence of 10 μM dipyridamole) resulted in loss of concentrative FB influx (Fig. 20), indicating the operation of a sodium-dependent NT system in these cells in addition to non-concentrative systems previously recognized (50).

In cells with both facilitated diffusion and concentrative transport systems, nucleoside accumulation would result if rates of influx exceeded those of efflux. Nucleoside efflux, which may occur by mediated or non-

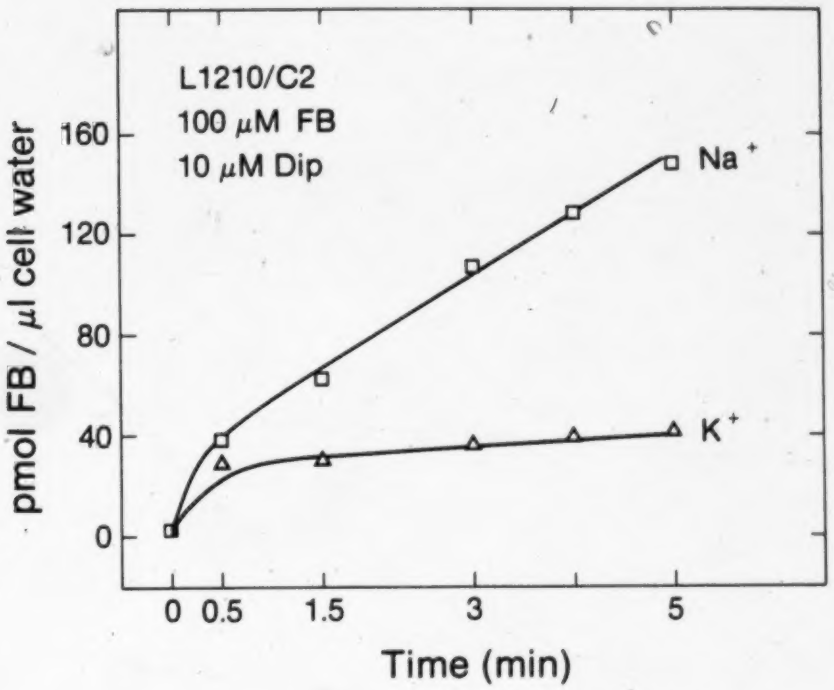

Fig. 20. Sodium-dependence of dipyridamole-insensitive influx of FB (100 μM) in L1210/C2 cells. Cells were suspended in sodium (□), or potassium (△) medium. Influx of FB was measured at 22°C in the presence of 10 μM dipyridamole, as described in "Materials and Methods".

mediated routes, is called "leakage" when not mediated by the concentrative carrier (165). The cellular nucleoside content may be increased by reducing leakage pathways with specific inhibitors (86-89,166). Cellular levels of nucleosides thus achieved should be related to the extent of inhibition of reversible transporters, provided non-mediated nucleoside permeation is minor (166).

AraA and araATP accumulation in L1210/C2 cells cultured with araA differed in suspensions containing 8 μM NBMPR, 10 μM dipyridamole or 15 μM dilazep (Section II.2), suggesting that the three agents did not inhibit facilitated diffusion of araA to the same extent. To test this idea, time courses of FB influx were compared in cells suspended in sodium medium or in NMG medium with or without NT inhibitors. Under the latter conditions, nucleoside influx proceeded without contribution from the sodium-driven carrier. In the experiment of Fig. 21A, in NMG medium, non-concentrative FB transport was maximally inhibited by 10 μM dipyridamole and least affected by 8 μM NBMPR, the effect of 15 μM dilazep being intermediate.

In L1210/C2 cells suspended in sodium medium in the presence of NT inhibitors, FB levels exceeded the steady-state level achieved in inhibitor-free cultures (Fig. 21B). The accumulation of FB induced by each inhibitor was related to the inhibitory effects of that agent on facilitated diffusion (Fig. 21A), that is, FB accumulation and inhibition of non-concentrative systems were greater with 10 μM

Fig. 21. Effect of NT inhibitors on inward fluxes of FB in L1210/C2 cells. Panel A: Influx of ^{3}H-FB (80 μM) was measured in cells suspended in NMG medium without NT inhibitors (○), or containing 10 μM dipyridamole (△),15 μM dilazep (●), or 8 μM NBMPR (□).
Panel B: Influx of ^{3}H-FB (60 μM) was measured in cells suspended in sodium medium containing 10 μM dipyridamole (△), 15 μM dilazep (●), or 8 μM NBMPR (□), or without transport inhibitors (○).

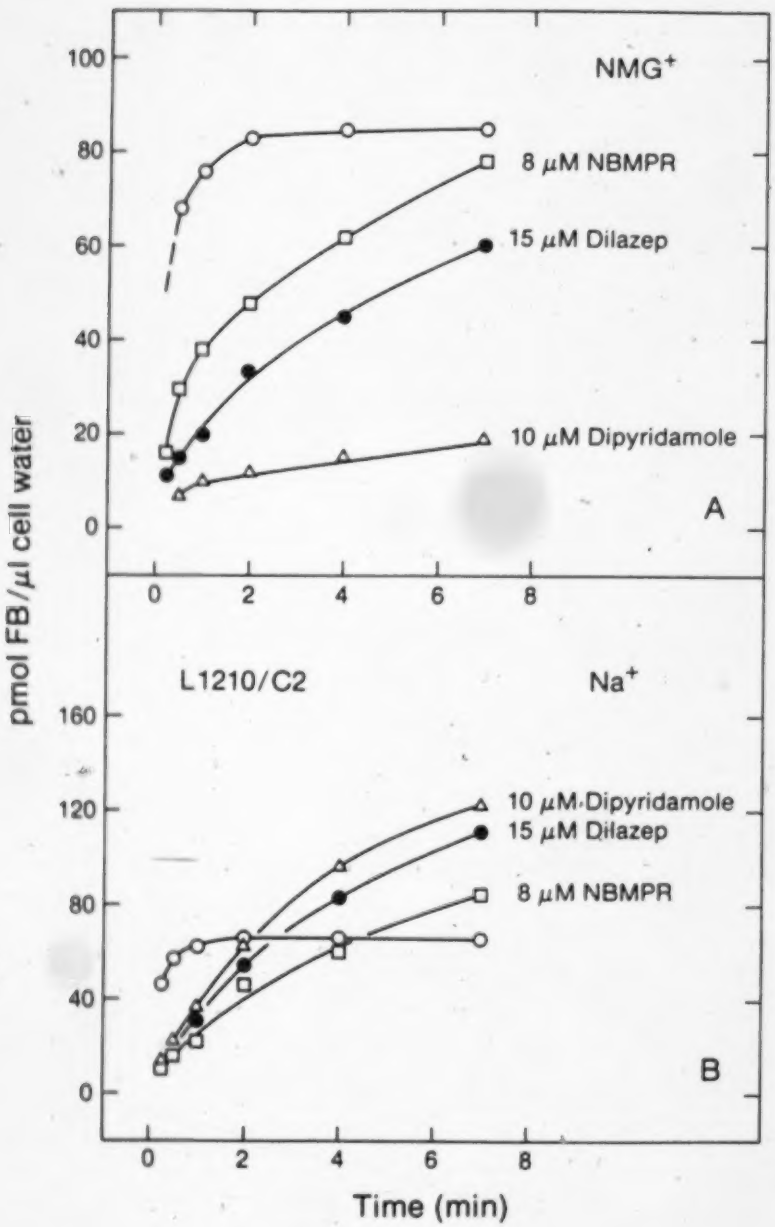
NMG+
8 μM NBMPR
15 μM Dilazep
10 μM Dipyridamole
A
L1210/C2
Na+
10 μM Dipyridamole
15 μM Dilazep
8 μM NBMPR
B
pmol FB/μl cell water
Time (min)
0
20
40
60
80
100
120
160
2
4
6
8

dipyridamole than with 15 μM dilazep or 8 μM NBMPR.

Time courses of araA (20 μM) influx were also measured in L1210/C2 cells suspended in NMG medium with or without an NT inhibitor. As shown in Fig. 22, the rank order of potency for inhibition of the non-concentrative uptake of araA by NT inhibitors was the same as that found for inhibitor induction of araA accumulation in sodium-containing medium (dipyridamole > dilazep > NBMPR, Figs. 6 and 7). Thus, these experiments correlated in L1210/C2 cells the induction of araA accumulation by NT inhibitors (Figs. 6 and 7) and the inhibition of araA fluxes via inhibitor-sensitive, non-concentrative systems (Fig. 22). The extent of nucleoside accumulation following inhibition of non-concentrative NT systems suggested that the latter mediate a substantial proportion of the leakage from nucleoside pools in these cells.

2. Transport of nucleosides in L1210/AM cells

It is evident in the foregoing experiments with L1210/C2 cells and FB that a cell/permeant system in which the permeant is not transformed simplifies demonstrations of concentrative transport. This tactic avoids the need to resolve the tandem processes of transport and permeant "trapping" by phosphorylation. However, not being a physiological nucleoside, FB is not an ideal tool to explore the sodium-linked NT system. An L1210 mutant clone, selected by Bennett *et al.* for nucleoside kinase deficiencies (133),

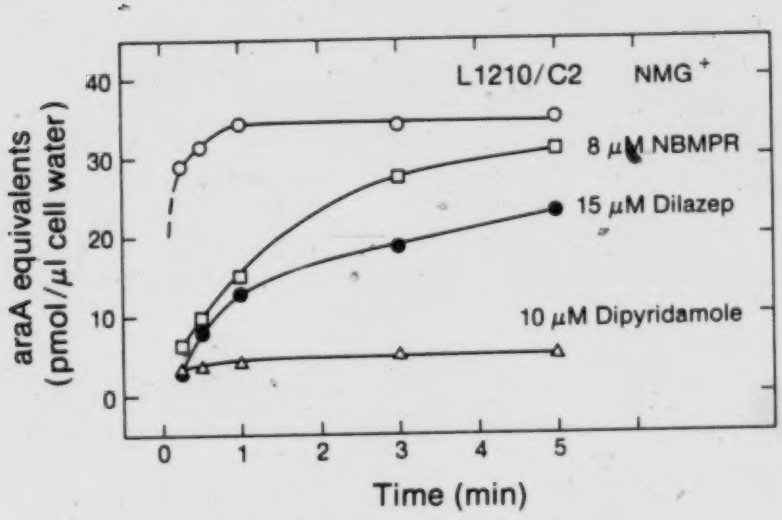

Fig. 22. Inhibition of araA uptake in L1210/C2 cells. Cells were incubated for 1 h with 1.1 μM dCF, washed and suspended in NMG medium containing 20 μM ^{3}H-araA without NT inhibitors (○), or with 10 μM dipyridamole (△), 15 μM dilazep (●), or 8 μM NBMPR (□). Nucleoside fluxes under these conditions are mediated by non-concentrative systems,

provided an opportunity to explore the permeation of adenine nucleosides in the virtual absence of anabolism. Cells of this clone (here designated L1210/AM) lack Ado kinase and dAdo-dCyd kinase activities (133). TLC analysis of cell extracts from L1210/AM cells incubated with ^{3}H-labelled FB, dAdo, Ado, Urd and araA at 22°C for 5 min, showed that only Urd was significantly metabolized (Table 9).

(a) Concentrative NT in L120/AM cells.

Time-courses for influx of 60 μM FB in L1210/AM cells in sodium medium with or without 10 μM dipyridamole were measured in the experiment of Fig. 23. Five-min time courses showed that the cellular FB content reached a steady-state level (80 μM) in the absence of dipyridamole, but progressed beyond this level in dipyridamole-containing medium. The concentration of FB achieved in L1210/AM cells in the presence of dipyridamole after 5 min of influx (Fig. 23) was slightly lower than that reached in L1210/C2 cells (Fig. 19).

Fig. 24 shows the effect of Na^{+} replacement by K^{+} on the influx of 20 μM dAdo in medium containing 1.1 μM dCF and 10 μM dipyridamole. The concentration of free dAdo after 5 min of influx in cells suspended in sodium medium was about 90 μM, that is, four-fold in excess of the dAdo content of cells in potassium medium.

These experiments suggested that the sodium-driven transport of several physiological nucleosides could be studied in L1210/AM cells, and that FB and dAdo were substrates for this NT system.

Table 9

Nucleoside metabolism in L1210 cells.

Cells of the designated lines (10^7 cells/ml in sodium medium containing a ^{3}H-nucleoside at the concentration listed) were incubated at 22°C for 5 min prior to centrifugal pelleting into 0.4 M TCA containing 25% sucrose. The volume of medium that accompanied the cells into the TCA layers was estimated using ^{3}H-PEG. The permeant content of that volume of medium was subtracted from total ^{3}H-content of the cell pellet. The intracellular ^{3}H-labelled material in the TCA extracts was identified and quantitated by TLC analysis.

Cell line	Nucleoside (10 µM)	Rf	Free nucleoside in cells (%)
L1210/C2	FB (50)	0.70	97
L1210/AM	Ado* (20)	0.56	93
"	dAdo* (20)	0.65	92
"	araA* (20)	0.50	94
"	FB (50)	0.70	95
"	Urd (40)	0.73	54

* 1.0 µM dCF present

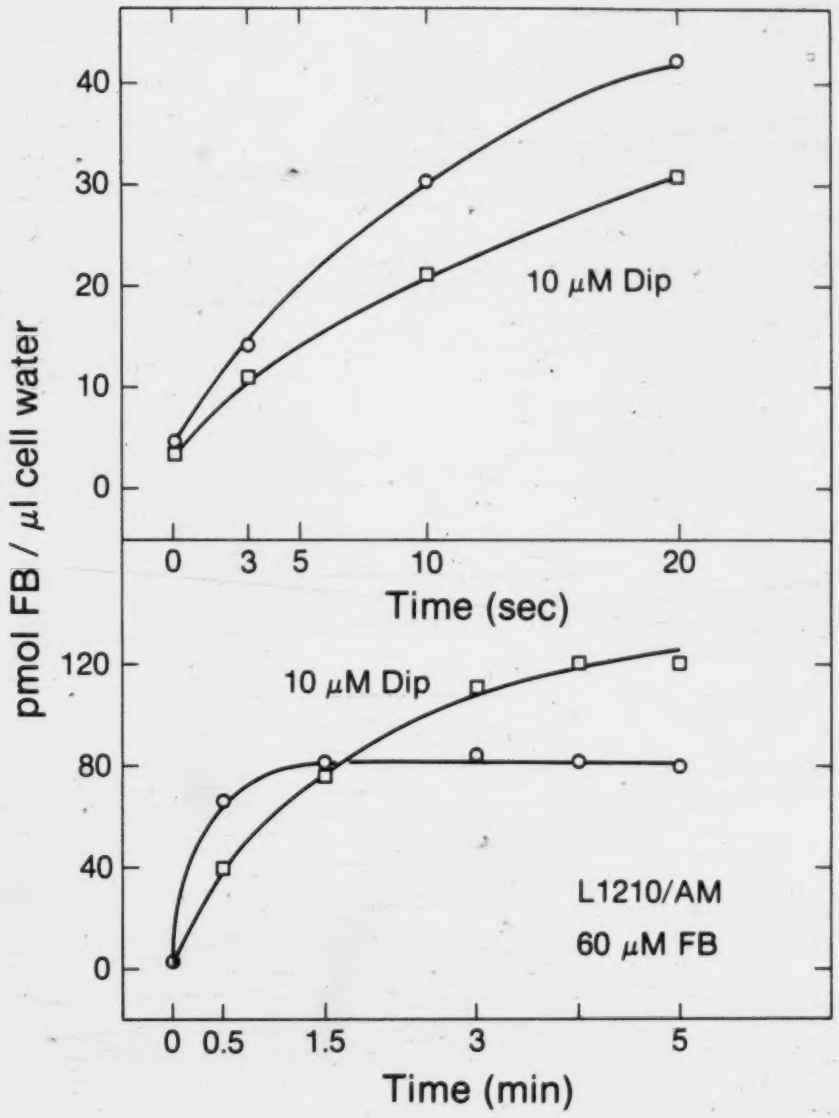

Fig. 23. Concentrative influx of 60 μM FB in L1210/AM cells. Influx of ^{3}H-FB was measured at 22°C in cells suspended in sodium medium without NT inhibitors (○), or with 10 μM dipyridamole (□), as described in "Materials and Methods".

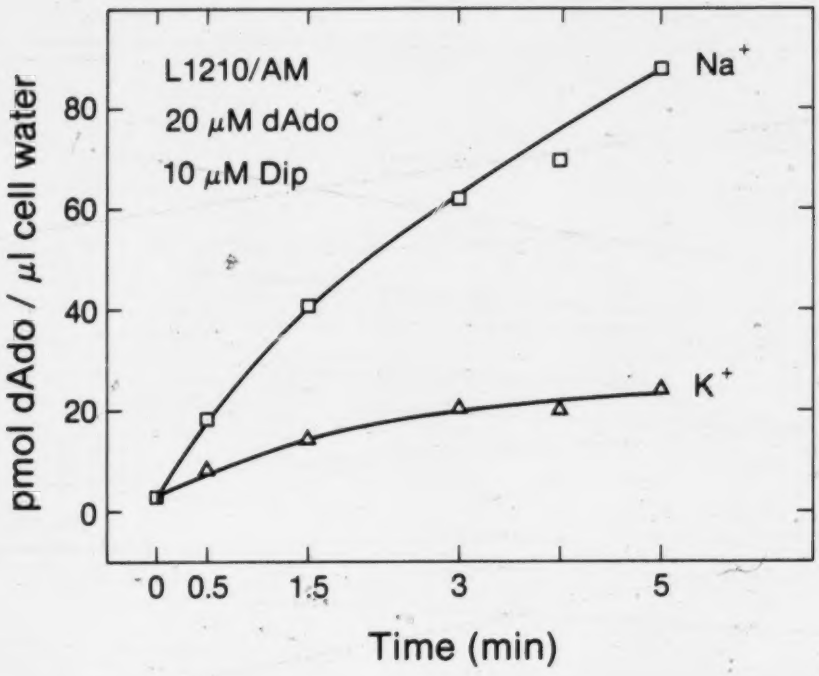

Fig. 24. Sodium-dependence of concentrative dAdo transport in L1210/AM cells. Cells that had been incubated for 1 h with 1.1 μM dCF were suspended in sodium medium (□), or potassium medium (○). Influx of ^{3}H-dAdo (20 μM) was measured in the presence of 10 μM dipyridamole.

(b) Site-specific binding of NBMPR to L1210/AM cells.

NBMPR binding, which has been correlated with inhibition of facilitated diffusion mechanisms of NT in a number of cell types (9,15,27,28), was measured in L1210/AM cells. The time course for the association of 20 nM ^{3}H-NBMPR with L1210/AM cells at 22°C (Fig. 25) showed that site-specific binding of ^{3}H-NBMPR to L1210/AM cells was not progressive beyond 10 min of incubation. The saturability of site-specific binding of NBMPR at equilibrium to L1210/AM cells was demonstrated in the experiment of Fig. 26A. Mass law analysis of the data shown in Fig. 26A yielded the following binding constants: K_D, 0.38 ± 0.04 nM, and B_{max}, (2.49 ± 0.005) x 10^5 sites/cell (Fig. 26B).

An analysis by the same procedure of NBMPR equilibrium binding to L1210/C2 cells at 22°C yielded the following constants: K_D, 0.435 nM; B_{max}, 2.7 x 10^5 sites/cell (data not shown). The NBMPR binding constants for L1210/AM and L1210/C2 cells are similar, and within the range of values reported for high-affinity NBMPR binding to various mammalian cells (3,13). The interpretation of NBMPR binding to L1210 cells is complicated by the presence in these cells of NT elements of low sensitivity to such inhibitor. Since a component of NT in L1210/AM cells is substantially inhibited by NBMPR concentrations similar to the K_D for binding (Fig. 27 and ref. 50), it may be reasonably assumed that the high-affinity NBMPR binding sites are associated with those NT elements. The presence of high-affinity NBMPR binding sites in L1210/AM,

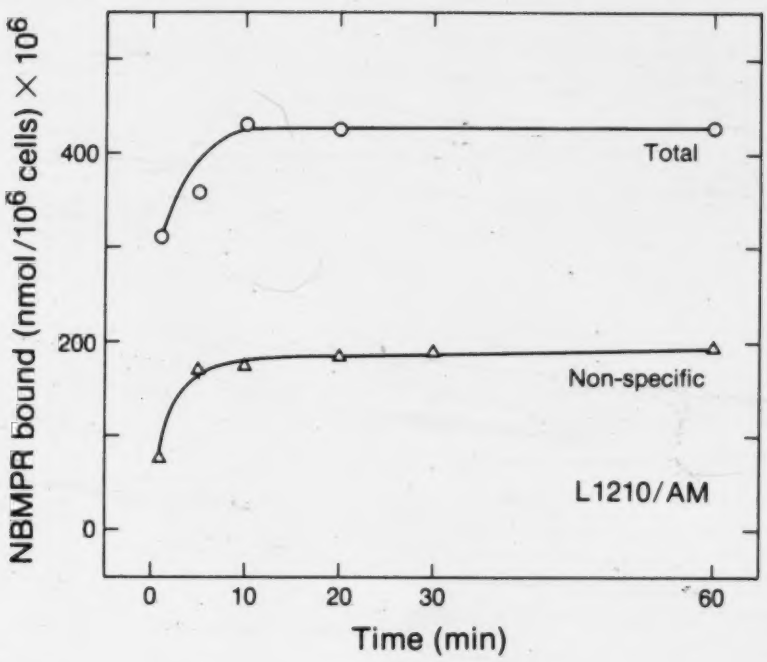

Fig. 25. Time courses of ^{3}H-NBMPR (20 nM, final) binding to L1210/AM cells at 22°C in sodium medium. Non-specific binding of ^{3}H-NBMPR (△) was determined in the presence of 20 μM NBTGR. Data representing total binding (○) were obtained in the absence of NBTGR.

Fig. 26. Site-specific binding of ^{3}H-NBMPR to L1210/AM cells. Panel A. Equilibrium binding of ^{3}H-NBMPR to L1210/AM cells. Cells were incubated at 22°C with graded concentrations of ^{3}H-NBMPR in sodium medium. Cell content of ^{3}H-NBMPR was measured after 30 min of incubation with ^{3}H-NBMPR in the absence (○) or presence (△) of 20 μM NBTGR. Initial ^{3}H-NBMPR concentrations are plotted. Panel B. Scatchard analysis of the NBMPR-binding data shown in Panel A. The fitted line yielded B_{max} and K_D values of (25 ± 0.05) x 10^5 molecules/cell and 0.38 ± 0.04 nM, respectively. In this plot, equilibrium concentrations of free (unbound) NBMPR in the medium were calculated after correcting for depletion of the ligand bound to the cells.

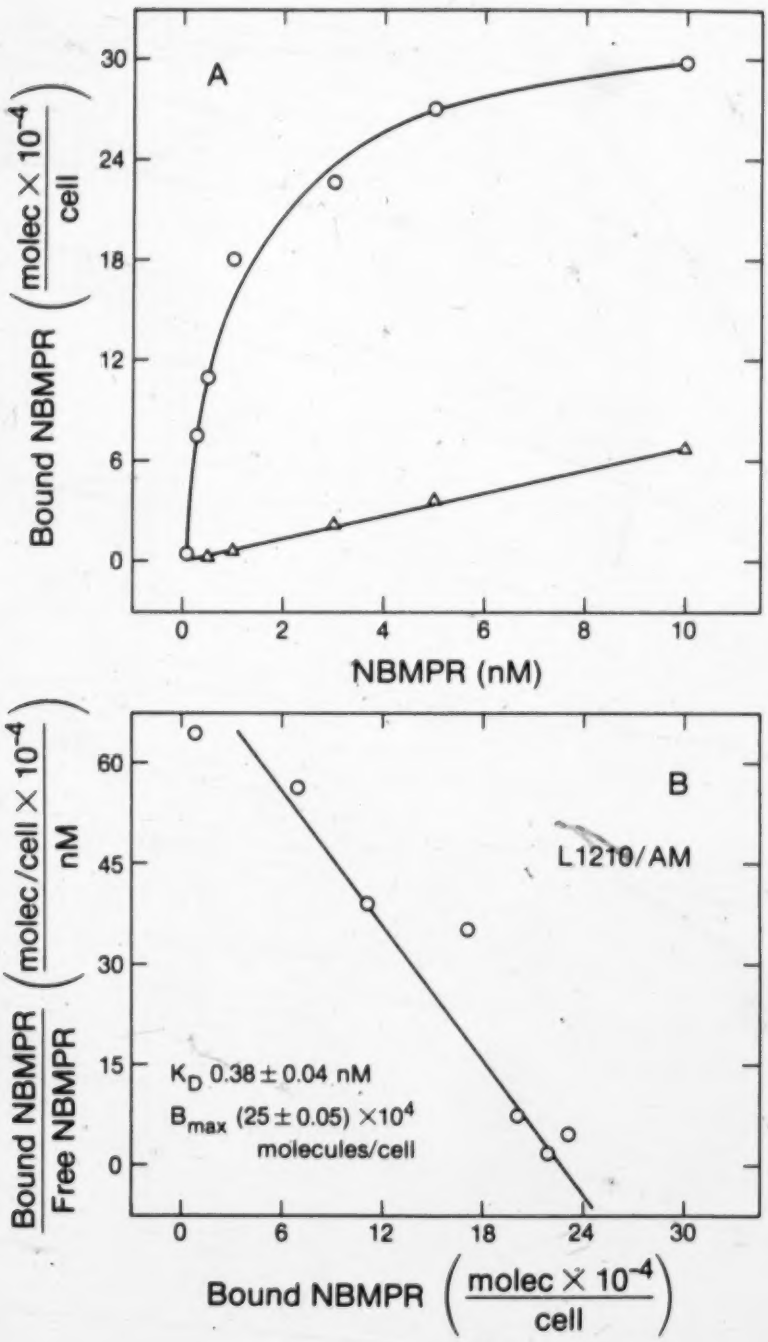
A
Bound NBMPR (molec × 10⁻⁴ / cell)
NBMPR (nM)
B
L1210/AM
K_D 0.38 ± 0.04 nM
B_max (25 ± 0.05) ×10⁴ molecules/cell
Bound NBMPR / Free NBMPR (molec/cell × 10⁻⁴ / nM)
Bound NBMPR (molec × 10⁻⁴ / cell)

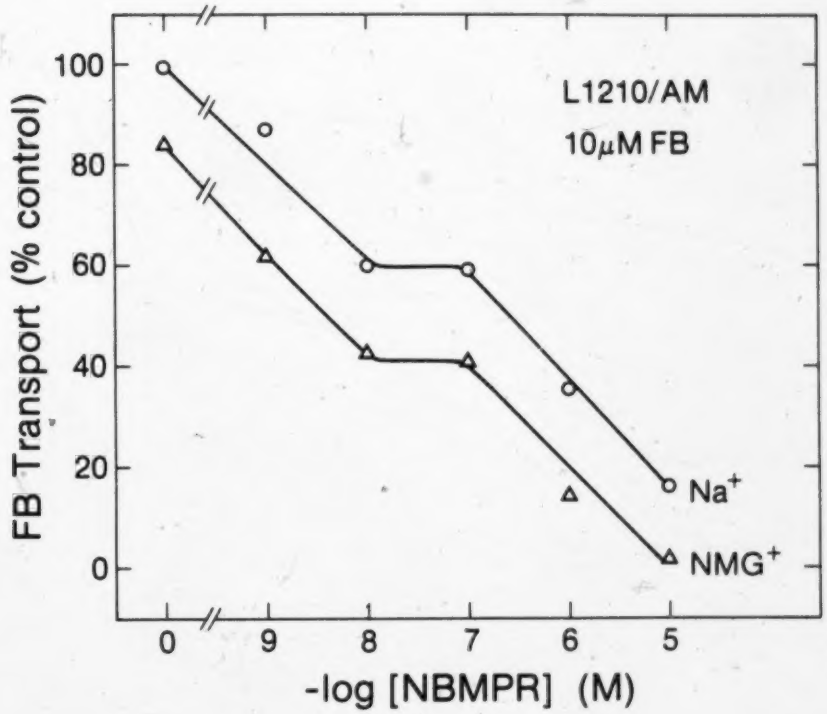

Fig. 27. Concentration-effect plots of inhibition by NBMPR of FB (50 μM) transport in L1210/AM cells. Transport was measured in sodium medium (○) or NMG medium (△). The control value (100%) represents transport rates measured in cells suspended in sodium medium without inhibitors (1.2 pmol/μl cell water.sec). Each point represents the mean of initial rates obtained from three short time courses similar to those of Fig. 30.

L1210/C2 and in other L1210 clones (50) argues for the presence of non-concentrative NT elements in the L1210 clones examined to date.

(c) Sensitivity of NT systems in L1210/AM cells to NBMPR, dipyridamole and dilazep.

Concentration-effect relationships for the inhibition of nucleoside permeation by NBMPR, dipyridamole and dilazep in L1210/AM cells were examined in the experiments of Figs. 27-29. In these assays, rates of inward transport of ^{3}H-FB or ^{3}H-Ado in sodium medium or NMG medium were compared. NT rates were measured with a rapid sampling assay that yielded short time courses of cellular uptake of ^{3}H-permeant, such as those shown in Fig. 30. These time courses provided estimates of initial rates of nucleoside influx which are, by definition, transport rates. Plots of NBMPR inhibition of FB transport (10 μM) revealed two NT components, which were evident in biphasic concentration-effect plots both in sodium medium and NMG medium (Fig. 27). Biphasic concentration-effect plots for the NBMPR inhibition of Urd and Ado transport in L1210 cells have been reported previously (3,50,167), and were also observed in the present study when FB transport in L1210/C2 cells was "titrated" with NBMPR (data not shown). Fig. 27 shows that, in L1210/AM cells, initial rates of FB influx in sodium medium were approximately 20% higher than in NMG medium, irrespective of the concentration of NBMPR present. These data suggest that the sodium-dependent NT component in L1210/AM cells contributed about 20% to the total cellular

influx of FB (when the extracellular concentration of FB was 10 μM) and was little affected by NBMPR at concentrations as high as 10 μM.

The two NT components inhibited by NBMPR do not require extracellular sodium and may be non-concentrative systems (Fig. 27). NBMPR concentrations that inhibited each influx component by 50% were about 1 nM and 1 μM. Examination of Fig. 27 shows that the NT systems of high and low sensitivity to NBMPR each contributed about 40% to the inward flux of FB in this experiment.

Figure 28 shows concentration-effect plots for the inhibition by dipyridamole of Ado transport (10 μM) in L1210/AM cells. Rates of Ado transport in NMG medium were consistently 80% of those measured in sodium medium, indicating that sodium-driven Ado transport systems contributed about 20% of the Ado flux under these conditions. In either medium, the concentration-effect plots showed only one component (compare with Fig. 27), which was 50% inhibited by 0.4 μM dipyridamole. Similar plots for the concentration-dependent inhibition of NT activity by dipyridamole have been reported in a different L1210 line (168). Dipyridamole concentrations greater than 3 μM eliminated non-concentrative Ado transport in L1210/AM cells (data not shown).

Transport of Ado (10 μM) in L1210/AM cells was inhibited by dilazep with an IC_{50} value of 10 nM (Fig. 29). Plagemann and Kraupp (169) have reported that dilazep inhibited Urd transport in L1210 cells with an IC_{50} value of about 30 nM.

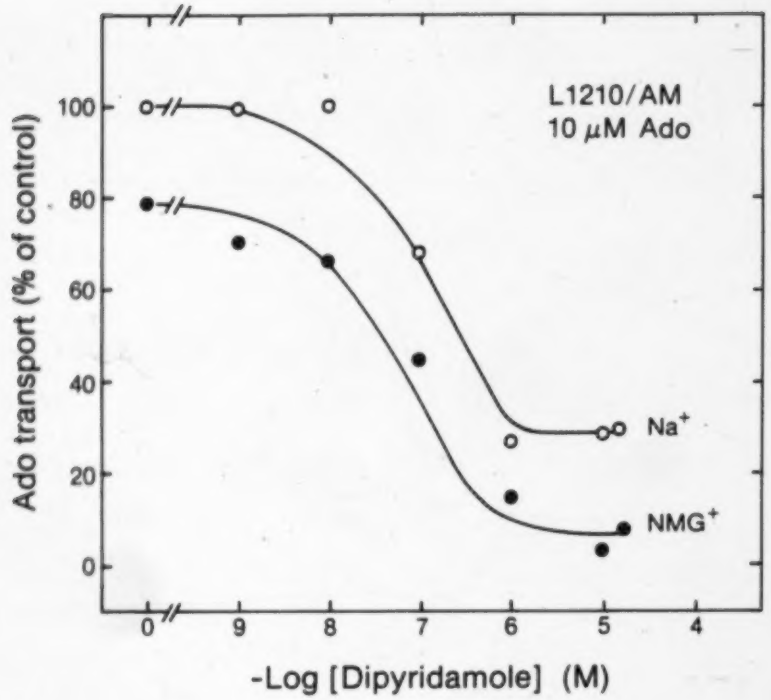

Fig. 28. Concentration-effect plots for the inhibition by dipyridamole of Ado (10 μM) transport in L1210/AM cells. Rates of Ado transport were measured as described in Fig. 27. Media contained 1 μM dCF and cells were suspended in such media 1 h before the measurement of ^{3}H-Ado permeation. Relative transport rates in sodium or NMG medium are plotted, respectively, with the symbols ○ and ●. The control value represents transport rates measured in cells suspended in sodium medium without inhibitors (6.5 pmol/μl cell water.sec, 100%)

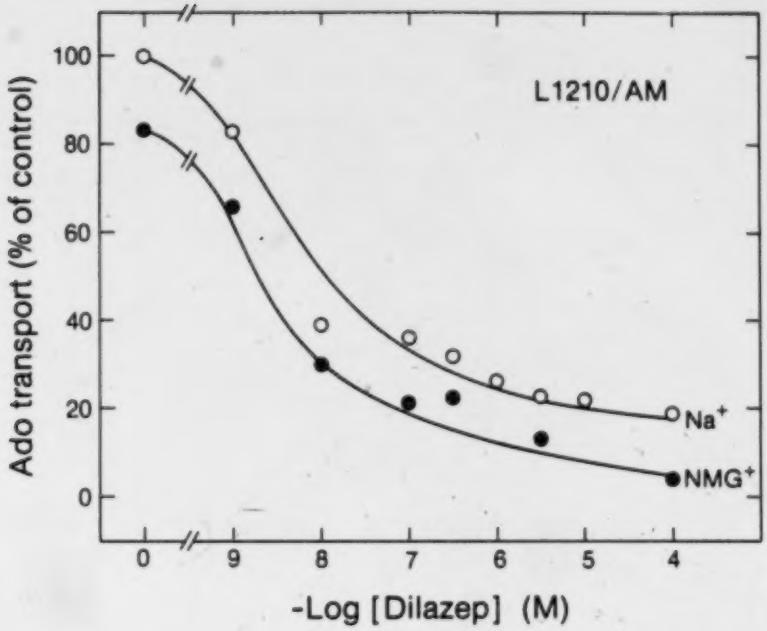

Fig. 29. Concentration-effect plots of inhibition by dilazep of Ado (10 µM) transport in L1210/AM cells. Media contained 1 µM dCF and cells were suspended in such media 1 h before assays of ^{3}H-Ado transport. The control rate (100%), that of Ado transport in sodium medium without additives, was 8.0 pmol/µl cell water.sec. Relative transport rates in sodium or NMG medium are plotted, respectively, with the symbols ○ and ● .

In the present study, plots of dilazep inhibition of Ado transport showed the presence of one transport component that did not require sodium; influx rates in sodium medium again were approximately 20% higher than in NMG medium. Dilazep concentrations near 100 μM were necessary for total inhibition of non-concentrative Ado transport (Fig. 29).

These results show that (i) concentrations of NBMPR, dipyridamole and dilazep as high as 10, 20 and 100 μM, respectively, had little effect on sodium-dependent NT in L1210/AM cells, and (ii) facilitated diffusion systems in L1210/AM cells are similar to those present in other L1210 lines. The relative contributions of concentrative and non-concentrative systems to the total NT activity may vary depending on the identity of the permeant and its concentration. In the present studies, in which the transport of 10 μM FB or 10 μM Ado was measured, the sodium-driven NT contributed about 20% to total nucleoside transport.

3. Dependence of the concentrative NT system in L1210/AM cells on sodium electrochemical gradients

The experiments described here for characterization of the sodium-driven NT system in L1210/AM cells employed solutions containing 10-20 μM dipyridamole to eliminate NT contributions from non-concentrative systems.

The dependence on extracellular Na^+ of the concentrative NT system in L1210/AM cells was further explored by replacing Na^+ by Li^+, Cs^+ or NMG^+ ions in cell suspension media

Fig. 30). When time courses of Ado influx (20 μM) were obtained in dipyridamole-free sodium medium, the steady-state level of cellular Ado was about 30 μM. During 5 min of incubation, the Ado level in cells suspended in sodium medium with dipyridamole reached 86 μM. Substitution of Na^+ by Li^+, Cs^+ or NMG^+ ions in dipyridamole-containing media essentially abolished cellular uptake of Ado during the 20-sec assay intervals, and concentrative uptake of Ado was not evident even after 5 min of exposure to the permeant. Thus, a strong Na^+ requirement by the concentrative NT system in L1210/AM cells was indicated. Residual influx in the presence of Li^+ or K^+ suggests that those ions may serve as poor substrates of the sodium-driven NT system.

The sodium-coupled transport of organic solutes is driven by gradients of that ion across the cell membrane. Transmembrane sodium gradients may be dissipated by treatment of cells with appropriate ionophores, such as nystatin and gramicidin (170,171). Incubation of L1210/AM cells for 15 min in the presence of 50 μg/ml nystatin[14] elevated the cellular concentration of sodium from 18 mM to 64.4 mM (Table 10). Sodium-linked Ado influx was significantly reduced in nystatin-treated cells (Fig. 31). The results of Figs. 30 and 31 suggest that a transmembrane sodium gradient is required for concentrative Ado uptake.

---

[14] 20 mM sucrose was added to prevent cell swelling caused by water entry following nystatin-induced ion movements (170)

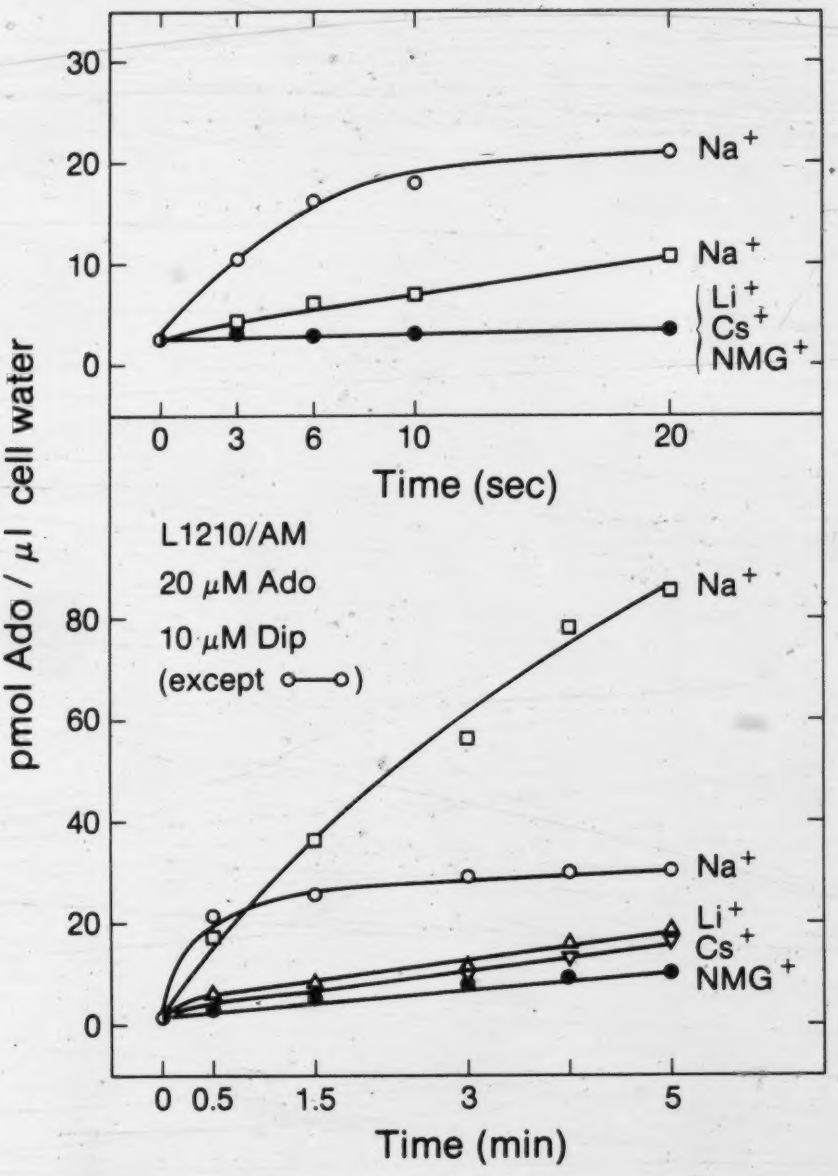

Fig. 30. Sodium dependence of Ado permeation in L1210/AM cells in medium containing dipyridamole. Time courses of ^{3}H-Ado uptake by L1210/AM cells that had been treated with 1.1 µM dCF for 1 h prior to transport assays, were measured in sodium medium without dipyridamole (○), or in medium containing 10 µM dipyridamole with Na^+ (□), Li^+ (△), Cs^+, (▽), or NMG^+ ions (●).

Table 10

Intracellular sodium concentrations

Cells were treated as specified and the sodium content of TCA extracts of the cells was measured by atomic emission spectrophotometry.

Treatment	Time (min)	Na^+ (mM)
None	--	18.2
5°C	15	65.0
Nystatin (50 µg/ml)	15	64.4
Ouabain (2 mM)	40	40.7

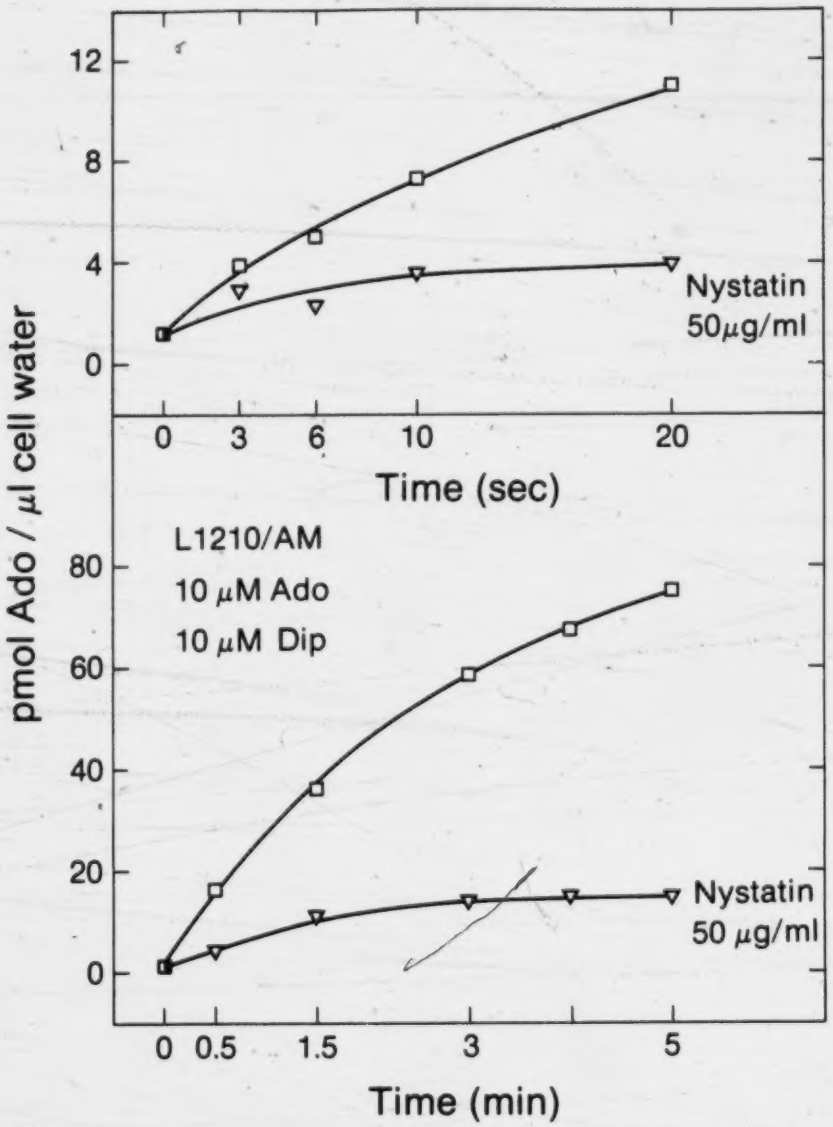

Fig. 31. Effect of nystatin on Ado permeation in L1210/AM cells in dipyridamole-containing medium. Cells were incubated with (▽) or without (□)50 μg/ml nystatin at 22°C in the dark for 15 min in sodium medium supplemented with 20 mM sucrose. Cells were washed four times with nystatin-free sodium medium and suspended in sodium medium with 10 μM dipyridamole. Cells were exposed to 1.1 μM dCF for 1 h prior to assays of Ado uptake.

The energy requirement of the sodium-linked NT system was next examined to determine if this system was a secondary-active carrier. Secondary-active systems do not exhibit ATPase activity and mediate uphill permeant translocation through coupling to downhill ion movements. Secondary-active systems are indirectly dependent on cellular energy status, since ATP is required to maintain ionic electrochemical gradients across the plasma membrane. However, secondary-active carriers can function in ATP-depleted cells in which the membrane potential has been clamped. This may be achieved by incubating cells in sodium-free media containing a metabolic inhibitor, K^+ and valinomycin (a potassium ionophore, ref. 171). When cells prepared in that way are suspended with Na^+-containing media, an inward gradient for that ion is established and Na^+ enters the cells. In valinomycin-treated cells, one K^+ ion will exit for each Na^+ ion that enters, thus maintaining electrical neutrality. This process will sustain the function of a sodium-dependent system until the K^+ content of the cell is exhausted or the Na^+ gradient is dissipated.

Following (i) depletion of ATP (Table 4) by incubation with 25 μM rotenone (to block mitochondrial ATP production), and (ii) treatment with 1 μg/ml valinomycin, L1210/AM cells exhibited sodium-driven NT activity, as indicated by the progress curve for cellular uptake of Ado shown in Fig. 32. Ado was not concentrated in ATP-depleted cells likely because transmembrane Na^+ gradients were rapidly dissipated in the

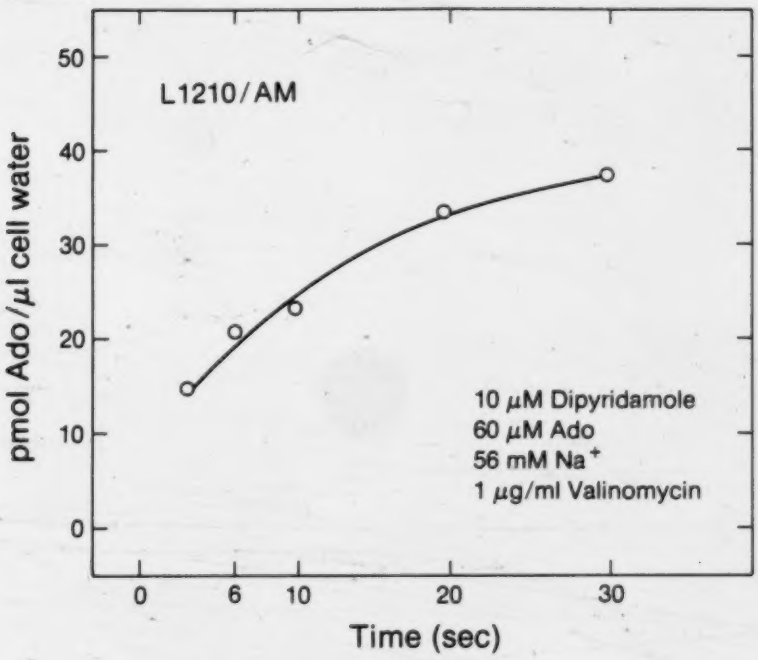

Fig. 32. Dipyridamole-insensitive transport of 60 µM Ado in energy-depleted L1210/AM cells. Cells were incubated, first in growth medium with dCF (1.1 µM, final) for 1 h, and then for 15 min at 37° in Tris medium containing 1 µg/ml valinomycin and 25 µM rotenone. Suspensions were allowed to cool to 22°C and dipyridamole (20 µM, final) was added. The permeant was dissolved in Tris/NaCl medium and mixed with the cell suspension at time zero to complete the assay mixtures (56 mM Na^+, final) and to initiate uptake assays.

absence of cellular energy sources. These results suggested that dipyridamole-insensitive NT in L1210/AM cells may be coupled to downhill movements of Na^+ ions.

4. Anion requirements of sodium-driven Ado transport

Maintenance of electrical neutrality is a requirement for Na^+-solute coupled movements across the plasma membrane. Electrical neutrality can be achieved by outward movement of a cation (electrogenic transport), or by simultaneous entry of an anion (electroneutral transport). To determine whether co-transport of an anion was required for sodium-dependent NT, Ado influx was measured in L1210/AM cells suspended in medium containing Cl^-, SCN^- or SO_4^{-2}. Thiocyanate ions penetrate biological membranes more readily than Cl^-, whereas SO_4^{-2} ions are largely impermeant (172-174). Accordingly, sodium-linked Ado transport would be expected to increase in the presence of SCN^- and to decrease with SO_4^{-2}, if anion movements were necessary for operation of the concentrative carrier. As shown in Fig. 33, dipyridamole-insensitive Ado influx in L1210/AM cells was not affected by substitution of Cl^- by SCN^- or SO_4^{-2} in the suspension medium, indicating the lack of a specific anion requirement in sodium-dependent Ado transport.

5. Temperature dependence of sodium-driven NT activity in L1210/AM cells

Time courses of Ado influx (20 μM) in L1210/AM cells in

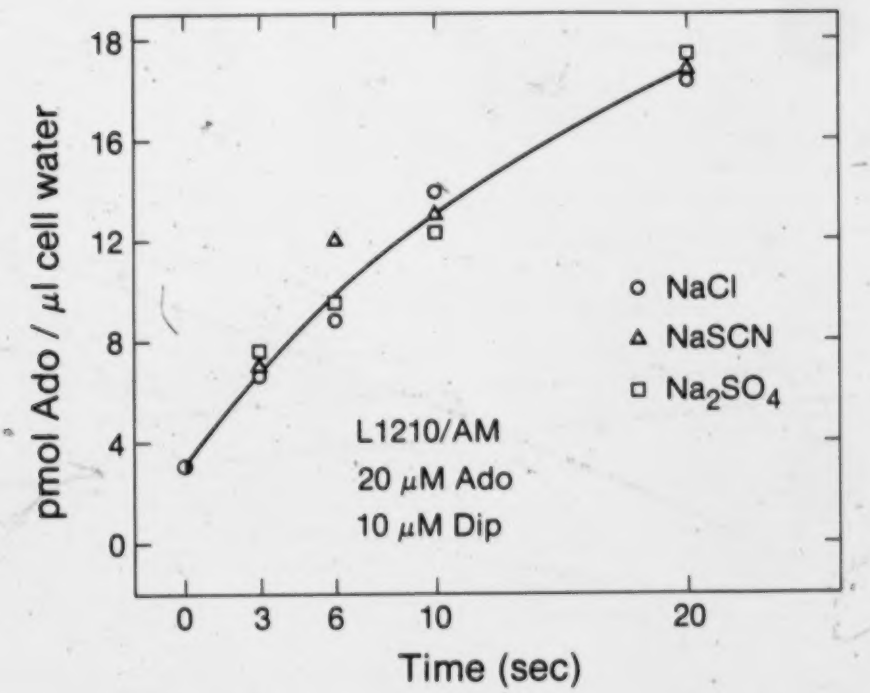

Fig. 33. Effect of chloride ion replacement on the sodium-linked transport of Ado (1 μM dCF, 10 μM dipyridamole) in L1210/AM cells. Time courses of ^{3}H-Ado (20 μM) uptake were measured in cells suspended in media containing 20 mM Tris, 5 mM glucose, 75 mM mannitol and 100 mM NaX, where X=Cl^- (○) or SCN^- (△), or 70 mM Na_2SO_4 (□), yielding solutions 300 ± 20 mOsm.

sodium medium with 10 μM dipyridamole were obtained at 5°C, 22°C or 37°C, and yielded, respectively, the following initial rates of Ado influx (calculated from 30-sec time courses of Ado influx similar to those of Fig. 30, data not shown): 0.03, 1.2 and 3.4 pmol/μl cell water.sec (Fig. 34). At 22°C, cellular levels of Ado approached a steady-state level of about 53 μM after 30 sec of Ado influx in dipyridamole-free medium. Concentrative Ado fluxes measured in the presence of 10 μM dipyridamole resulted in cellular Ado levels of 53 μM and 120 μM, respectively, in 0.5 and 4 min of incubation. Steady-state Ado levels at 37°C were approximately 86 μM (Fig. 34). The difference between steady-state cellular concentrations of Ado at 22°C and 37°C suggests that, at the higher temperature, the concentrative NT system in L1210/AM cells may contribute a larger fraction to total Ado transport than at lower temperatures.

Adenosine influx in the presence of dipyridamole was virtually abolished at 5°C (Fig. 34). The apparent lack of sodium-dependent Ado transport at 5°C was possibly due to temperature-induced dissipation of transmembrane Na^+ gradients (*vide infra*) and to direct effects of temperature on transport activity. Atomic emission spectrophotometric analysis of extracts prepared from cells incubated at 5°C in sodium medium for 15 min showed that intracellular Na^+ levels increased from 18 to 65 mM (Table 10). This change in cellular Na^+ levels, similar to that found in nystatin-treated cells (Table 10), would decrease the Na^+ gradient

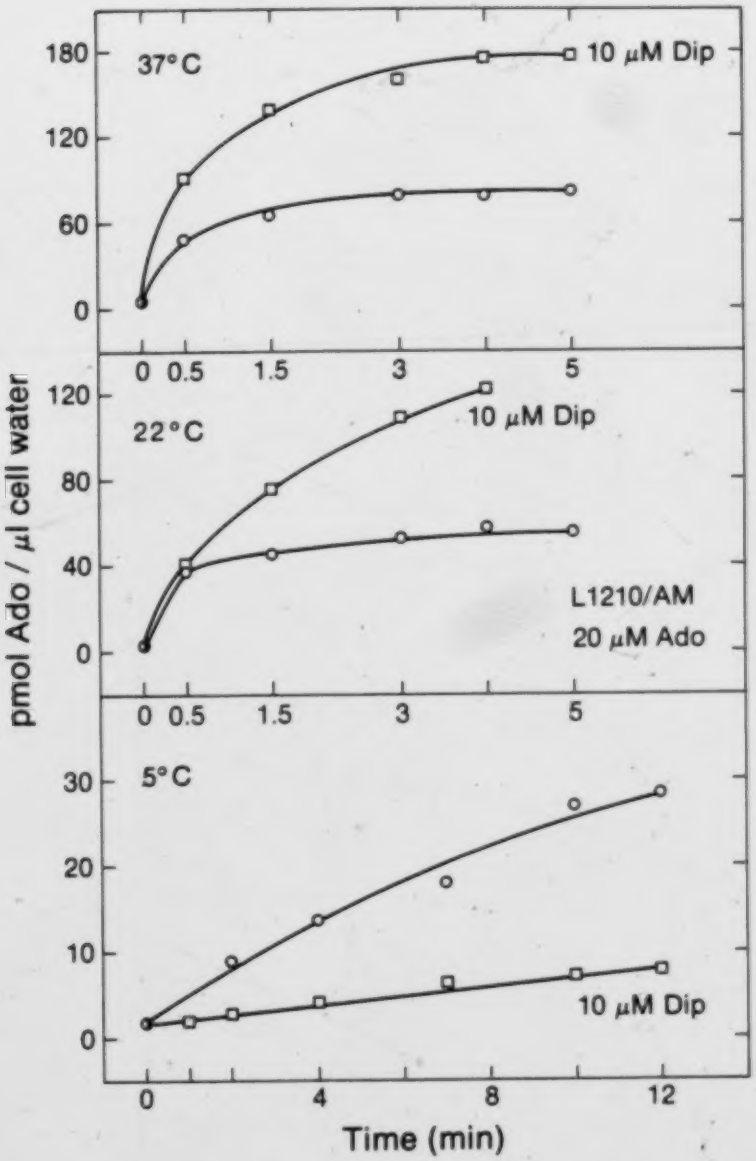

Fig. 34. Effects of temperature on sodium-linked transport of 20 μM Ado. The cells were incubated for 1 h with 1.1 μM dCF and then incubated at the temperature indicated for 15 min in sodium medium with (□) or without (○) 10 μM dipyridamole prior to influx measurements.

across the cell membrane, and, thereby, reduce rates of sodium-dependent Ado transport.

To investigate the direct effect of low temperature on concentrative Ado transport, cells were first incubated in NMG medium at 5°C for 15 min, and then time courses of ^{3}H-Ado influx were followed after initiating influx by addition of a ^{3}H-Ado solution in sodium medium (60 μM Ado and 56 mM sodium, final). This procedure provided a Na^+ gradient at 5°C in the cell suspension that would sustain sodium-dependent Ado influx. The Na^+ content of cells treated in this manner reached extracellular levels after approximately 30 sec (data not shown). Rates of Ado influx were low under these conditions (Fig. 35), suggesting that transporter function was directly impaired at low temperature.

6. Substrate specificity

The substrate specificity of the sodium-driven nucleoside transporter of L1210/AM cells was explored by (i) comparing time courses for the influx of several ^{3}H-labelled permeants, and (ii) measuring inhibition of ^{3}H-Ado influx (10 μM) by competing nucleosides. The latter tactic assumes competition between non-labelled test nucleosides and ^{3}H-Ado at a transporter site.

Time courses of araA (20 μM) influx in L1210/AM cells in the presence or absence of 10 μM dipyridamole are illustrated in Fig. 36. In this experiment, the level of araA in cells suspended in dipyridamole-containing medium was about 40 μM

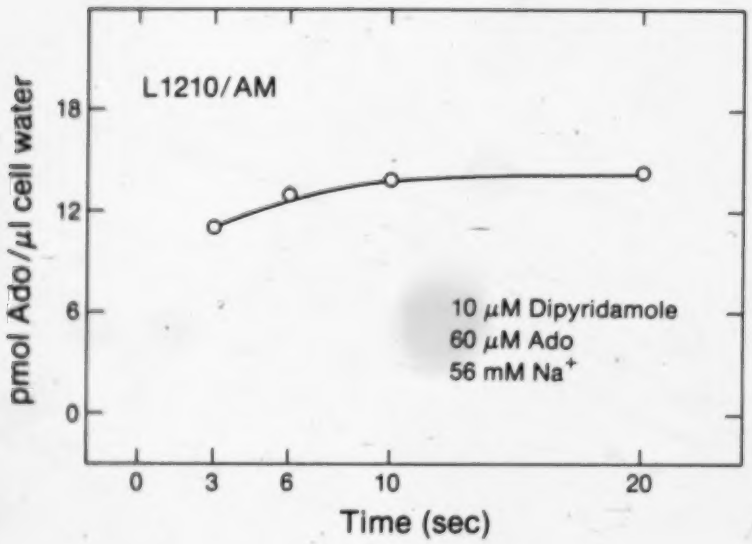

Fig. 35. Low rates of sodium-linked Ado influx in L1210/AM cells at 5°C. After incubation at 37°C in growth medium with dCF (1.1 μM, final), cells were incubated in NMG medium for 15 min at 5°C. The permeant (^{3}H-Ado) solution contained dipyridamole and 112 mM Na^+, so that the mixing of that solution with cell suspensions to begin intervals of cellular uptake of Ado also provided a Na^+ gradient for operation of the sodium-linked NT system. Concentrations in assay mixtures were: ^{3}H-Ado, 60 μM; dipyridamole, 10 μM; Na^+, 56 mM.

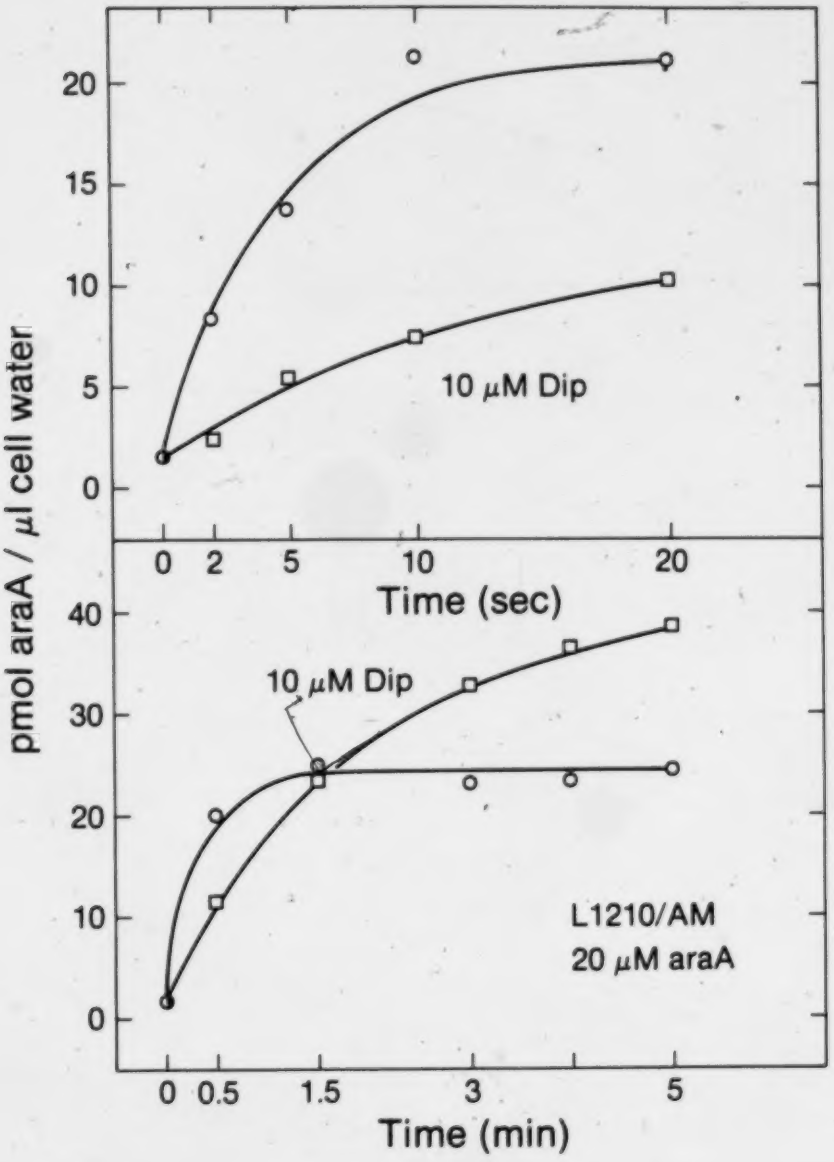

Fig. 36. Concentrative influx of araA in dCF-treated L1210/AM cells. Influx of 20 μM ^{3}H-araA was measured at 22°C in cells suspended in sodium medium with (□), or without (○) 10 μM dipyridamole, as described in Fig. 19.

after 5 min of influx, a 0.6-fold excess relative to the steady-state levels of araA found in the absence of dipyridamole. AraA is evidently a substrate for the sodium-linked NT system present in L1210/AM cells (Fig. 36) and in L1210/C2 cells (Fig. 19).

Dipyridamole-insensitive nucleoside fluxes were also observed in L1210/AM cell suspensions containing 40 μM Urd (Fig. 37A) or 10 μM ddAdo (Fig. 37A and 37B). However, dThd (15 μM) did not enter cells in dipyridamole-containing medium (Figs 37D), indicating that (i) dThd is not a substrate (or is a poor one) for the sodium-linked NT system, and (ii) dThd enters L1210/AM cells primarily by a dipyridamole-sensitive, likely a facilitated diffusion, system.

The inhibition of Ado transport by other nucleosides was explored by comparing initial rates of Ado influx (a measure of transport) by L1210/AM cells in the absence or presence of graded concentrations of competing nucleosides. IC_{50} values for inhibition of 10 μM Ado transport by several physiological pyrimidine nucleosides were greater than 400 μM; these values were several-fold higher than those for most purine nucleosides tested (Table 11).

Substitution of hydrogen by halogens at the C-2 position of purine nucleosides produced increases in IC_{50} values for inhibition of Ado (10 μM) transport: from 25 μM for 2'-dAdo, to 90 and 183 μM for 2-Cl-2'-dAdo and 2-Br-2'-dAdo, respectively, and from 140 μM for araA to >400 μM for 2-F-araA (Table 11). Because the Van der Waal's radii of H, F, Cl

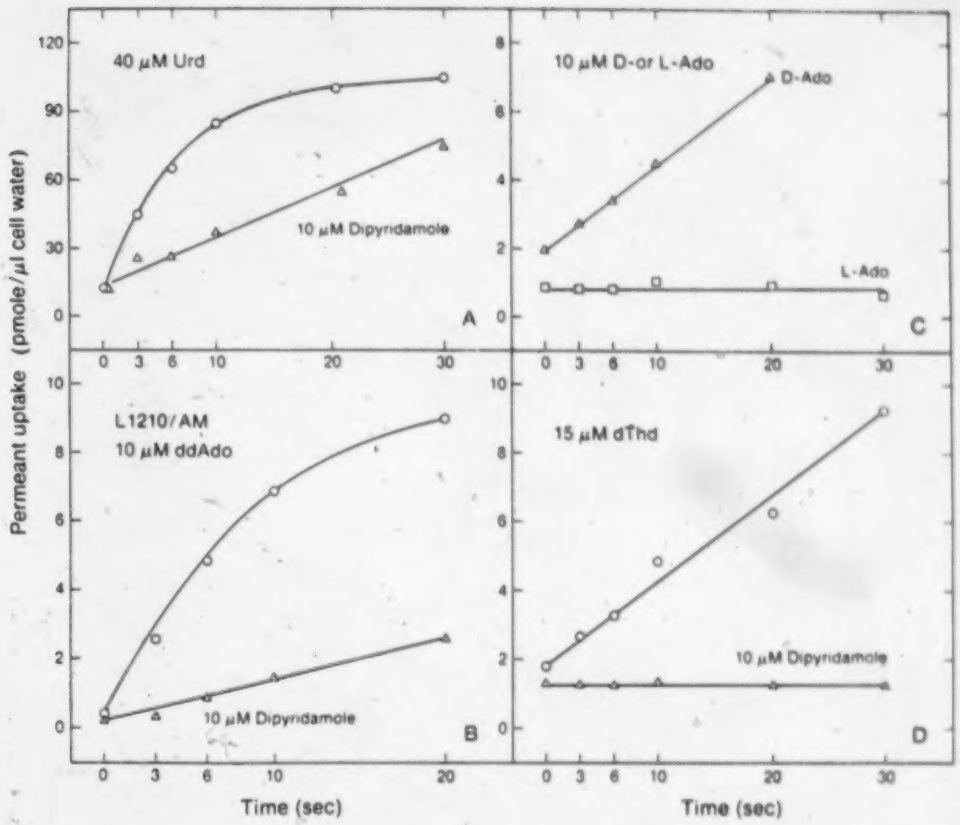

Fig. 37. Permeant specificity of the sodium-linked NT system in L1210/AM cells. Time courses for the cellular uptake of the following ^{3}H-nucleosides were measured in sodium medium with (△ , □) or without (○) 10 μM dipyridamole: 40 μM Urd (Panel A), 10 μM ddAdo (Panel B), 10 μM D-Ado and 10 μM L-Ado (Panel C), and 15 μM dThd (Panel D).

Table 11

Inhibition of sodium-linked transport of Ado in L1210/AM cells by purine and pyrimidine nucleosides.

Assays yielded time courses for uptake of 10 μM ^{3}H-Ado by cells in media containing 10 μM dipyridamole with and without graded concentrations of competing nucleosides. Initial rates of Ado uptake (i.e. rates of inward transport) were estimated from the time courses and were expressed as a percentage of Ado transport rates measured in the absence of other nucleosides. IC_{50} values were determined from plots of Ado transport rates *versus* concentration of competing nucleoside. Initial rates of Ado influx in the absence of nucleosides were 0.71-0.95 pmol/μl cell water.sec.

Nucleoside	Percentage inhibition with 400 μM nucleoside	IC_{50} (μM)
dAdo	90	25
2-Cl-dAdo	75	90
2-Br-dAdo	60	183
araA	45	140
2-F-araA	10	>400
Ino	85	35
L-Ado	0	--
Urd	40	>400
dCyd	22	>400
araC	20	>400
dThd	20[1]	>1000

[1] 1 mM dThd

and Br atoms are, respectively, 1.20, 1.35, 1.80 and 1.95 Å (175), these findings indicate that increases in the size of the C-2 substituents decreased the ability of substrates to interact with the transporter. Negative inductive effects of the halogens might also play a role in the distinctions between these putative substrates.

The hydroxyl groups at the nucleoside 2'- and 3'-positions appear not to be essential features in substrates for the sodium-linked nucleoside transporter, since ddAdo was active as a substrate (Fig. 37A). However, IC_{50} values for the inhibition of Ado transport by dAdo and araA were, respectively, 25 μM and 140 μM (Table 11), suggesting that 2'-hydroxyl groups do participate in the permeant-transporter interaction.

Figure 37C shows that, in medium with dipyridamole, ^{3}H-D-Ado (9-beta-D-ribofuranosyladenine, "physiological" Ado) entered L1210/AM cells, whereas ^{3}H-L-Ado (9-beta-L-ribofuranosyladenine) did not enter these cells, or did so at a rate below the sensitivity of the assay. In addition, concentrations of L-Ado as high as 400 μM had no apparent effect of the sodium-dependent entry of D-Ado (Table 11). Enantioselectivity in the interaction between permeant and carrier was expected, since this is a feature of enzymatic reactions and transport processes (176,177). The three-dimensional structures of D-Ado and L-Ado are mirror images of each other. Although the chemical properties of these isomers in solution are identical in the absence of chiral

reagents, the interactions of D-Ado (the physiological enantiomer) with three-dimensional, enantioselective[15] sites in membrane NT systems may not be possible with L-Ado. In this instance, the biological properties of the two enantiomers will differ substantially. Marked differences in the enzymatic reactivity of D-Ado and L-Ado have been reported (176), and the enantiomeric selectivity of Na^+-linked glucose transport systems, such as that found in rat kidney brush-border membrane vesicles (177), has been demonstrated.

The possibility that L-Ado might have interacted with the permeation site in the sodium-linked NT system to form a complex incapable of translocation across the plasma membrane is unlikely, since concentrations of L-Ado as high as 400 μM had no effect on sodium-linked transport of D-Ado (Table 11).

The discrimination by the sodium-driven NT system in L1210/AM cells between Ado and Urd (as substrates), and dThd (as a non-substrate) contrasts with the broad specificity of non-concentrative NT systems (1,13,16,42-50). A sodium-linked NT system present in murine splenocytes also transports purine nucleosides and Urd, but does not accept dThd and

---

[15] Site enantioselectivity is intended to imply "handedness" (hand-glove analogy) in permeant or substrate binding sites that will distinguish between enantiomenrs such as D-Ado and L-Ado

several other pyrimidine nucleosides (90).

Substrate selectivity of the sodium-linked NT system of L1210/AM cells, indicated from measurements of inhibition of ^{3}H-D-Ado influx by putative permeants, needs to be confirmed by direct assays of permeant transport and kinetic studies.

7. Kinetic studies of sodium-linked Ado transport in L1210/AM cells

The kinetics of ion-linked solute movements may be complex because the two permeating species act as co-substrates. Binding of the ion may modify interaction of the organic substrate with the permeation site and variation in the extracellular concentration of the driving ion may also alter substrate translocation rates (178,179).

Zero-*trans* inward fluxes of Ado in L1210/AM cells, when measured in the presence of 100 mM Na^{+}, were a hyperbolic function of the extracellular Ado concentration (Fig. 38A). Similarly, Ado influx rates, when the extracellular concentration of Ado was 100 μM, were a saturable function of the extracellular Na^{+} concentration, which was increased from 5 mM to 100 mM in the experiment of Fig. 38B.

A more extensive kinetic analysis, summarized in Tables 12A and 12B, involved measurement of Ado fluxes (initial rates derived from time courses of Ado uptake) as functions of:

a) Extracellular Ado concentration, when the concentration of extracellular Na^{+} was 5, 10, 20, 40 or

Fig. 38. Dependence of sodium-driven Ado transport on extracellular concentrations of Ado (Panel A) and Na^+ (Panel B). L1210/AM cells were incubated with 1.1 μM dCF for 1 h prior to transport assays. Osmolality was adjusted to 300 ± 10 mOsm with mannitol. All measurements were made in the presence of 10 μM dipyridamole. Initial rates of Ado influx were calculated from triplicate time courses of Ado uptake, as described in Fig. 24.

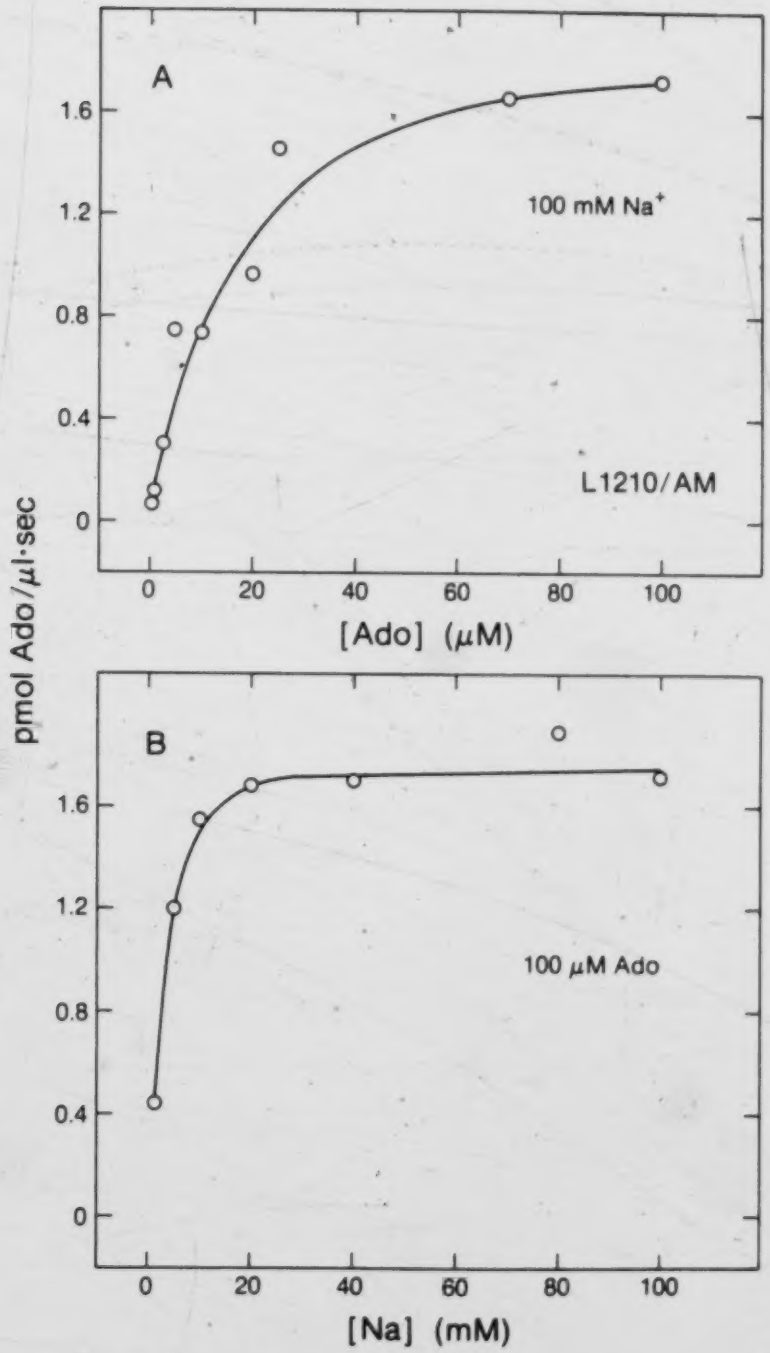
A
100 mM Na+
L1210/AM
1.6
1.2
0.8
0.4
0
0
20
40
60
80
100
[Ado] (μM)
pmol Ado/μl·sec
B
100 μM Ado
1.6
1.2
0.8
0.4
0
0
20
40
60
80
100
[Na] (mM)

Table 12A

The sodium-linked NT system of L1210/AM cells: dependence of Ado transport characteristics (K_m, V_{max}) on the extracellular concentration of Na^+.

Rates of inward transport of ^{3}H-Ado were measured at 22°C in in cells that had been treated for 1 h with 1.1 μM dCF. Initial rates of Ado uptake by the cells were estimated as described in Table 11, in experiments similar to that of Fig. 38A. Na^+ concentrations in the media were graded as noted and medium osmolality was maintained at 300 ± 10 mOsm by addition of mannitol.

	Kinetic constants for Ado transport	
$[Na_o]$ (mM)	K_m (μM)	V_{max} (pmol/μl cell water.sec)
5	31.0 ± 12.1[1]	1.15 ± 0.2
10	23.1 ± 6.8	1.43 ± 0.2
20	16.8 ± 3.2	1.40 ± 0.1
40	12.4 ± 3.7	1.47 ± 0.2
80	14.6 ± 4.3	1.65 ± 0.2
100	9.4 ± 2.6	1.67 ± 0.2

[1] S.D.

Table 12B

The sodium-linked NT system of L1210/AM cells: dependence of "Na^+/Ado" transport characteristics ($K_{0.5}$) on the extracellular concentration of Ado.

Rates of inward transport of ^{3}H-Ado were measured at 22°C in cells that had been treated for 1 h with 1.1 μM dCF. Initial rates of Ado uptake (expressed as "Na^+/Ado" fluxes) by the cells were estimated as described in Table 11, in experiments similar to that of Fig. 38B.

[Ado] (μM)	$K_{0.5}$ (mM)
0.5	11.8 ± 0.4
5.0	9.3 ± 0.9
10.0	5.9 ± 2.7
20.0	4.6 ± 0.5
70.0	5.1 ± 2.4
100.0	3.1 ± 0.1

[1] S.D.

80 mM. Each of these experiments was similar to that of Fig. 38A, except for the Na^+ content of the medium.

b) Extracellular Na^+, when initial Ado concentrations were 0.5, 5, 10, 20 or 70 μM (similar to the experiment of Fig. 38B). This part of the study was intended to evaluate the dependence of inward sodium fluxes on extracellular concentrations of Ado. Because the Ado-dependent fraction of Na^+ fluxes occurring in these cells were not measurable, Ado fluxes were measured in place of Na^+ fluxes, and for this particular purpose are designated as "Na^+/Ado fluxes" (see Table 12B). It is shown subsequently in this study that the sodium-linked NT system of L1210/AM cells appears to mediate the inward passage of Ado and Na^+ molecules in a 1:1 stoichiometry. In all cases, rate-concentration relationships of the fluxes of Ado were saturable and similar to those shown in Figs. 38A and 38B. The hyperbolic nature of the rate-concentration relationships, evident at all Na^+ concentrations tested, was confirmed by the linearity of double reciprocal plots (data not shown).

K_m and V_{max} values for Ado fluxes measured at different levels of extracellular Na^+ were calculated using Woolf-Agustinsson-Hofstee plots. Apparent $K_{0.5}$[16] values for

---

[16] The $K_{0.5}$ parameter denotes the concentration of Na^+ ions at which "Na^+/Ado" fluxes, assayed at particular extracellular concentrations of Ado, were one-half maximal

"Na^+/Ado" fluxes were calculated from similar plots, considering that initial rates of Ado influx were representative of Na^+ fluxes; such rates were plotted as a function of the extracellular Na^+ concentrations. K_m values for Ado influx decreased from about 30 μM to 10 μM when the extracellular Na^+ levels were increased from 5 mM to 100 mM (Table 12A). Similarly, $K_{0.5}$ values for "Na^+/Ado" fluxes decreased from 12 mM to 3 mM as extracellular Ado concentrations were increased from 0.5 to 100 μM (Table 12B). Although these experiments were conducted at 22°C, they suggest that, under physiological conditions (about 120 mM Na^+ and 0.1-0.5 μM Ado), the Na^+-binding site of the concentrative transporter would be saturated, thus maximizing the efficiency of uphill transport. The increase in transporter affinity for Ado that is apparent as Na^+ levels are increased may reflect Na^+-induced shifts in equilibria between different carrier conformations. For instance, Na^+ interaction with the transporter might enhance the accessibility of the permeant binding site to Ado, without necessarily facilitating Ado binding *per se*. As another possibility, the ternary complex (Ado-Na^+-carrier) may be more stable than a binary complex with Na^+ or Ado only. Ado fluxes also increased from 1.15 pmol/μl cell water.sec to 1.67 pmol/μl cell water.sec as extracellular Na^+ concentrations were increased from 5 to 100 mM. Other sodium-driven systems in which transporter affinity for a permeant and transport rates increase with increasing levels of

extracellular Na^+ include (i) a gamma-aminobutyric acid transporter in Ehlrich ascites cells (180), (ii) a glycine transporter from rate renal brush border vesicles (181), and (iii) a system involved in serotonin transport in platelets (182).

Double reciprocal plots of (i) Ado fluxes *versus* Ado concentration, or (ii) "Na^+/Ado" fluxes *versus* Na^+ concentration, yielded groups of lines that intersected in the second quadrant (data not shown). That characteristic is considered to be indicative of random order of the binding of Na^+ and the organic substrate in sodium-linked transport systems (165) and, in this instance, implies the existence of independent binding sites for Na^+ and Ado in the transporter (179).

8. Stoichiometry of sodium-linked Ado transport in L1210/AM cells

The coupling stoichiometry of the co-transport of an organic solute and an activator ion can provide information about (i) the mechanism of substrate translocation, (ii) the concentrative capacity of the system, and (iii) the energetic cost of the process.

The concentrative capacity of a co-transport system is directly related to the coupling stoichiometry of the solute and the activator (183,184), as shown below.

$$S_i/S_o \leq [A_o/A_i \exp (F\Delta\psi/RT)]^n \qquad (1)$$

where R, T and F have their usual thermodynamic interpretation. The subscripts i and o represent intracellular and extracellular; S and A are substrate and activator activities; $\Delta\psi$ is the transmembrane potential, and *n* is the ratio of activator ions to solute molecules co-transported (transport stoichiometry).

Equation 1 shows that a large coupling stoichiometry will increase the capacity of the system to concentrate a substrate. Thus, under conditions in which an ion:solute coupling ratio of 1 resulted in a 10-fold concentration of S inside the cell, a 2:1 coupling ratio would result in concentration of substrate 100-fold above medium levels, provided other variables remain unchanged.

The energetic cost of ion-coupled transport will be determined by the work necessary to extrude activator ions against their electrochemical gradient (183,185). Hence, the operation of a system with an activator:substrate coupling ratio of 2:1 will require twice as much energy as a system with a 1:1 stoichiometry.

The coupling stoichiometries of solute molecules and activator ions in various co-transport processes have been estimated by various methods, including (i) direct measurement of activator and solute coupled fluxes, or (ii) analysis of the dependence of substrate fluxes on activator concentration (186).

Direct determination of the Na^+:Ado stoichiometry was attempted in experiments using ^{3}H-Ado (60 μM) and $^{22}Na^+$

(56 mM). Cells were incubated with 25 μM rotenone at 37°C for 15 min in Tris medium, a procedure that reduced cellular ATP levels by 90% (Table 4). Depletion of cellular energy stores was considered necessary to preclude active extrusion of Na^+ during transport assay intervals, which would lead to underestimation of Na^+ fluxes. Prior incubation of cells in sodium-free, Tris medium established conditions in which an inwardly-directed Na^+ gradient could be established at the start of Ado uptake intervals, as in the experiment of Fig. 35. After clamping the transmembrane potential with valinomycin in potassium-rich medium, time courses of ^{3}H-Ado and $^{22}Na^+$ influx were obtained. After 30 sec of incubation under these conditions, the cellular concentrations of Ado and Na^+ were, respectively, 38 μM and 43 mM (Fig. 39). Assuming that one Na^+ ion accompanied each Ado molecule transported (*vide infra*), the Ado-coupled influx of Na^+ would have contributed only 0.1% of the total Na^+ entry. Thus, large background Na^+ fluxes precluded the possibility of directly measuring the Na^+:Ado coupling stoichiometry.

Some animal cells, including lymphocytes, possess furosemide- and amiloride-sensitive Na^+ fluxes (187,188). Although treatment of L1210/AM cells with furosemide and amiloride resulted in a 30% reduction in $^{22}Na^+$ entry, basal fluxes of that ion were still too high to allow measurement of Na^+ movements associated with Ado transport (data not shown).

A different approach to determine the Na^+:Ado coupling

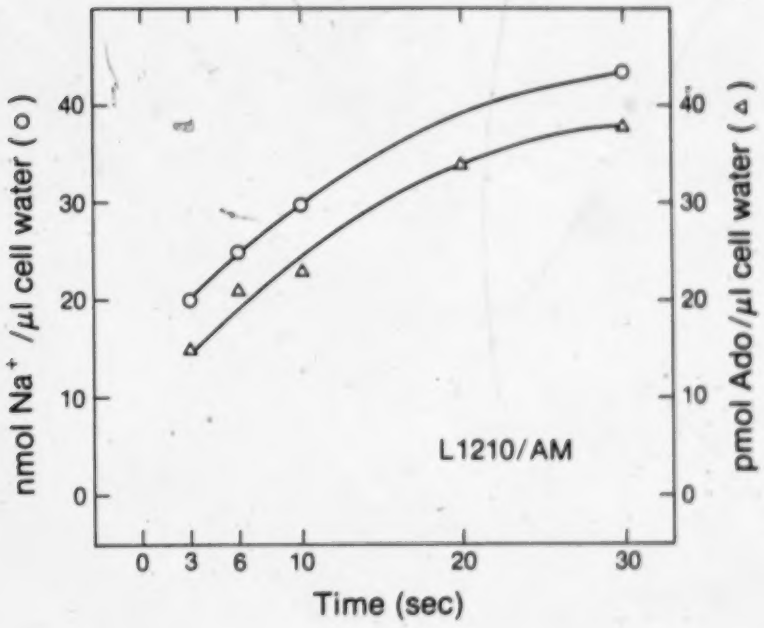

Fig. 39. Ado and $^{22}Na^{+}$ influx in sodium-depleted and ATP-depleted L1210/AM cells. Cells were incubated with 1.1 µM dCF in growth medium for 1 h, washed and suspended in Tris medium containing rotenone (25 µM, final) and valinomycin (1 µg/ml, final), and incubation proceeded for a further 15 min at 37°C. Cellular contents of ^{22}Na and ^{3}H-Ado were measured after cells were exposed for the indicated intervals to medium containing 10 µM dipyridamole, 56 mM $^{22}Na^{+}$ (○), and 60 µM ^{3}H-Ado (△). Thus, upon mixing cell suspensions with that medium to begin intervals of uptake, a Na^{+} gradient was also established for operation of the sodium-linked NT system.

stoichiometry used the kinetic data described earlier (Fig. 38 and Table 12B). In the application of multi-site enzyme kinetics to transporter models, conformity with simple Michaelis-Menten kinetics, that is, the existence of hyperbolic relationships between transport rate and permeant concentration (i) signifies the absence of cooperativity in the interactions between transporter, substrate, and activator molecules (189), and (ii) constitutes evidence for a 1:1 coupling stoichiometry between substrate and activator (183,190). The dependence of substrate fluxes on activator concentration may be analyzed by means of the Hill equation (183,190):

$$\log [v/(V_{max}-v)] = n \log [A] - \log K \qquad (2)$$

A plot of log $[v/(V_{max}-v)]$ *versus* log [A] is a straight line with slope n, where n is the coupling stoichiometry of the substrates.

Hill analysis of Ado fluxes in L1210/AM cells measured at graded Na^+ concentrations (data from Fig. 38B) yielded data which were fitted by a line with slope 1.067 (Fig. 40), indicating that the Na^+:Ado ratio is 1. Hill analyses of three experiments yielded a mean Na^+:Ado ratio of 1.06 $\pm$ 0.07 ($\pm$ S.D.). As well, a 1:1 Na^+:Ado coupling stoichiometry was indicated by the hyperbolic relationship between Ado fluxes and extracellular Na^+ concentrations apparent in Fig. 38B. Evaluations of stoichiometry by Hill analysis do not distinguish between (i) co-transport of the activator ion

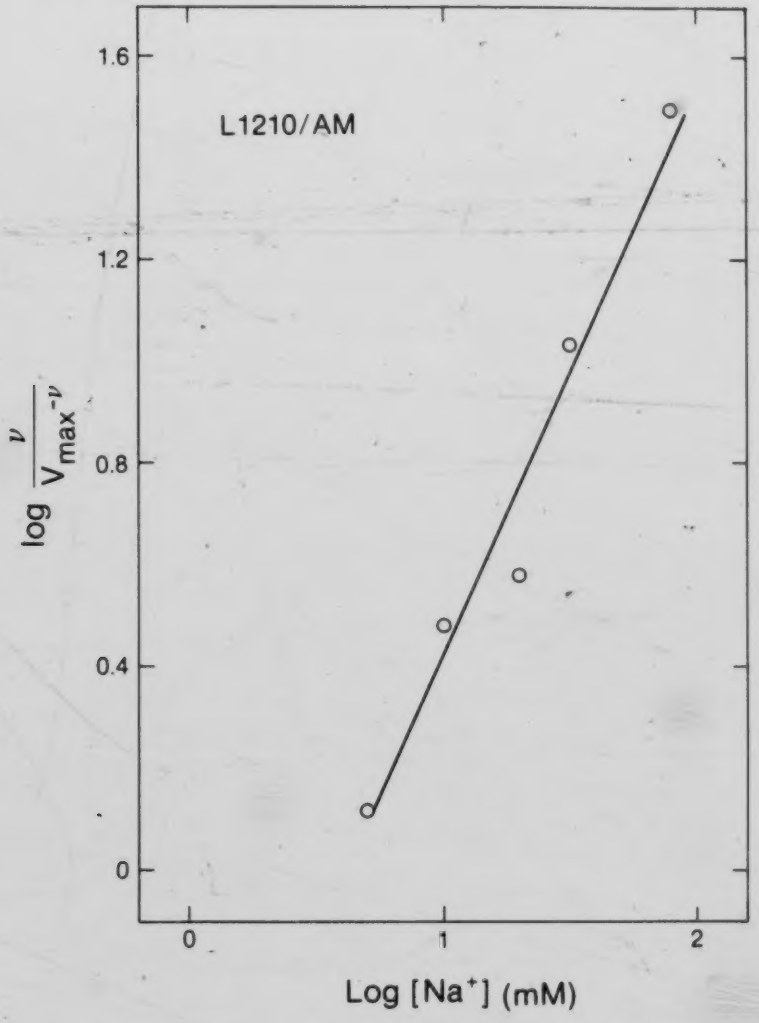

Fig. 40. Hill analysis of the dependence of Ado transport rates on the extracellular concentrations of Na^+ and Ado. Initial rates of Ado (100 μM) influx in L1210/AM cells were measured in medium that contained graded concentrations of Na^+, as in the experiment of Fig. 38B. The slope of the line (obtained by linear regression) is 1.067, indicating that the Na^+:Ado coupling stoichiometry is 1:1.

with the substrate, or (ii) binding of the activator ion to the transport mechanism without translocation (183).

9. Drug effects on sodium-dependent Ado transport

Secondary-active transport systems may be affected directly or indirectly by drugs. Since these systems require a transmembrane gradient of activator ion, interference with ion movements may indirectly alter transport of the organic substrate, by altering the transmembrane potential, or the gradient for the activator ion. Some pathways for Na^+ permeation in cultured cells, erythrocytes and lymphocytes are sensitive to inhibition by agents such as furosemide, amiloride, and ouabain (187,188,191,192).

Furosemide and ouabain inhibit, respectively, concerted (electroneutral) movement of Na^+, K^+ and Cl^- ions (173), and the Na^+/K^+ ATPase (191,192). Fig. 41A illustrates the reduction of Ado (10 μM) influx by 2 mM furosemide in the presence or absence of 2 mM ouabain in L1210/AM cells that had been incubated in sodium medium with those drugs at 22°C for 40 min. Shorter incubation times or lower drug concentrations had little effect on sodium-linked Ado transport (data not shown). Incubation of cells with 2 mM ouabain for 40 min increased cellular concentrations of Na^+, from 18 mM to 41 mM (Table 10).

The experiment of Fig. 41B was undertaken to distinguish between (i) the possibility of direct inhibitory effects of furosemide and ouabain on sodium-driven NT and (ii) the

Fig. 41. Effect of agents that influence ion movements on inward Ado fluxes mediated by the sodium-linked NT system in L1210/AM cells. Ado fluxes were measured at 22°C in media containing 10 μM dipyridamole. Cells were incubated in growth media containing 1.1 μM dCF for 1 h at 37°C prior to assays of ^{3}H-Ado (10 μM) influx. Data from control cultures (without additives other than dipyridamole) are plotted as (○) in all panels of this Figure.

Panel A. Time courses of Ado influx were measured in L1210/AM cells after incubation with 2 mM furosemide (□) or 2 mM furosemide plus 2 mM ouabain (△) for 40 min at 22°C in sodium solution.

Panel B. Cells were subjected to treatment analogous to that described in Panel A, except that NMG medium was employed. (□), 2 mM furosemide; (△), 2 mM ouabain.

Panel C. Time courses of Ado influx were measured in the presence of 1 mM amiloride (▽), or 500 μM phloridzin (▼) in cells that had been exposed to those agents for 40 min.

Panel D. Time courses of Ado influx were measured in cells depleted of ATP (■) by incubation with 250 μM DNP for 15 min at 37°C in NMG medium without glucose. The permeant was dissolved in solutions containing 112 mM Na^{+} (final Na^{+} concentration was 56 mM) and mixed with the cell suspension.

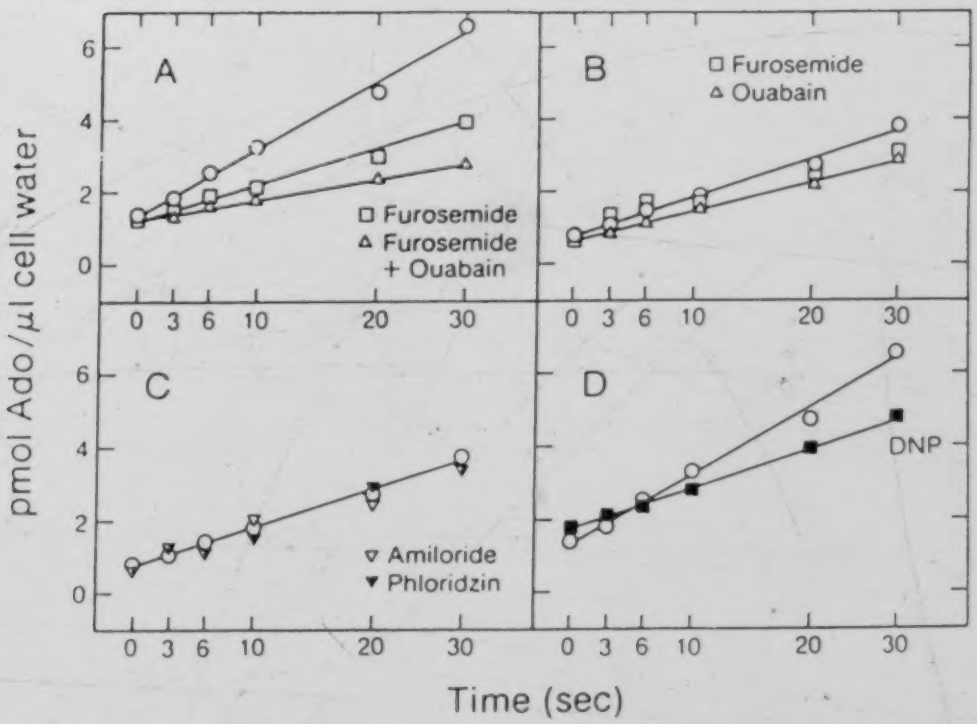
A
B
C
D
□ Furosemide
△ Furosemide + Ouabain
□ Furosemide
△ Ouabain
▽ Amiloride
▼ Phloridzin
DNP
pmol Ado/μl cell water
Time (sec)
0 3 6 10 20 30
0 2 4 6

possibility that inhibition of Ado fluxes by these agents were a consequence of alteration in cell ionic content. In this experiment, cells were first incubated in NMG medium with 2 mM furosemide or with 2 mM ouabain, as in Fig. 41A. The permeant, ^{3}H-Ado, was dissolved in sodium medium, and, upon initiation of uptake intervals, concentrations of Ado and Na^{+} were, respectively, 10 μM and 56 mM. The effects of this treatment on Ado transport, shown in Fig. 41B, indicated little effect of ouabain and furosemide on sodium-dependent Ado transport under incubation conditions that precluded increases in cellular Na^{+} during treatment of the cells with the two agents.

Phloridzin has been reported to inhibit facilitated diffusion NT systems (59) and sodium-coupled glucose transport (191) in various cell types, while amiloride interferes with the Na^{+}/H^{+} antiporter (176) and other ion-driven systems, including a sodium-linked NT system in rat renal brush-border vesicles (193,194). Incubation of L1210/AM cells at 22°C for 40 min in NMG medium with concentrations of phloridzin or amiloride as high as 500 μM or 1 mM, respectively, had no effect on the sodium-linked influx of 10 uM Ado in these cells (Fig. 41C).

The effect of ATP depletion by DNP on sodium-linked Ado fluxes in L1210/AM cells was measured in the experiments of Fig. 41D. As with rotenone, DNP treatment reduced cellular ATP concentrations by about 90% (Table 4). Following incubation of L1210/AM cells with 250 μM DNP in NMG medium

for 15 min at 37°C, a 44% reduction in Ado transport relative to that in untreated cells was observed (10 μM Ado and 56 mM Na^+ Fig. 41D), confirming the influence of cellular energy status on secondary-active transport.

10. Effect of thiol-modifying reagents

Chemical modification of proteins may provide information about structure and function. Most amino acids can be derivatized (195), but modification of cysteine residues in polypeptides is especially useful because the highly reactive thiol groups may be modified under non-denaturing conditions (195,196). Chemical modification of thiol groups is known to alter the function of receptor and transporter proteins (196).

The hydrogen atom in sulfhydryl groups is acidic and, consequently, protein thiol groups are ionized even at slightly alkaline pH values. The $R\text{-}S^-$ moiety is a good nucleophile that reacts with alkyl halides and maleimide derivatives, and forms stable complexes with Hg^{+2} and other metal ions.

Modification of -SH groups in erythrocytes and some nucleated cells, including L1210 cells (50) has been shown to inhibit NT function. The two components of facilitated diffusion present in L1210 cells (Fig. 28) appear to differ in their relative sensitivities to *p*CMBS and NEM (50).

The effects of the sulfhydryl-reactive agents, *p*CMBS, NEM and showdomycin (maleimide riboside) on sodium-linked Ado

transport in L1210/AM cells were investigated in the concentration-effect experiments summarized in Figs. 42-44. Because initial reagent concentrations are reported here and reagent depletion has not been taken into account, the IC_{50} values for inhibition of Ado transport presented in this study may be overestimated. In these experiments, cell suspensions were incubated for 10 min at 22°C (unless otherwise stated) with graded concentrations of a thiol-reactive agent. The cells were washed once, suspended in medium with 10 μM dipyridamole and incubated at 22°C for at least 10 min prior to assays of Ado influx. Incubation for more than 20 min with NEM or *p*CMBS at concentrations greater than 100 μM (NEM) or 60 μM (*p*CMBS) damaged cells, as shown by increased cellular volumes and trypan blue intake.

Concentration-dependent inhibition by NEM of Ado (10 μM) transport is shown in Fig. 42. The IC_{50} value for NEM inhibition of Ado transport (40 μM) did not change significantly when L1210/AM cells were incubated with the alkylating agent in the presence of 40 μM or 100 μM Ado. Failure of the permeant to protect sodium-dependent NT against NEM inhibition suggested that the reactive groups do not participate in substrate recognition. Concentrations of NEM greater than 60 μM abolished sodium-linked Ado transport. NEM is known to react with the imidazole ring of histidine and with free amino groups (195,196). However, modification of those groups under the mild conditions employed in these experiments may have been minimal (195,196).

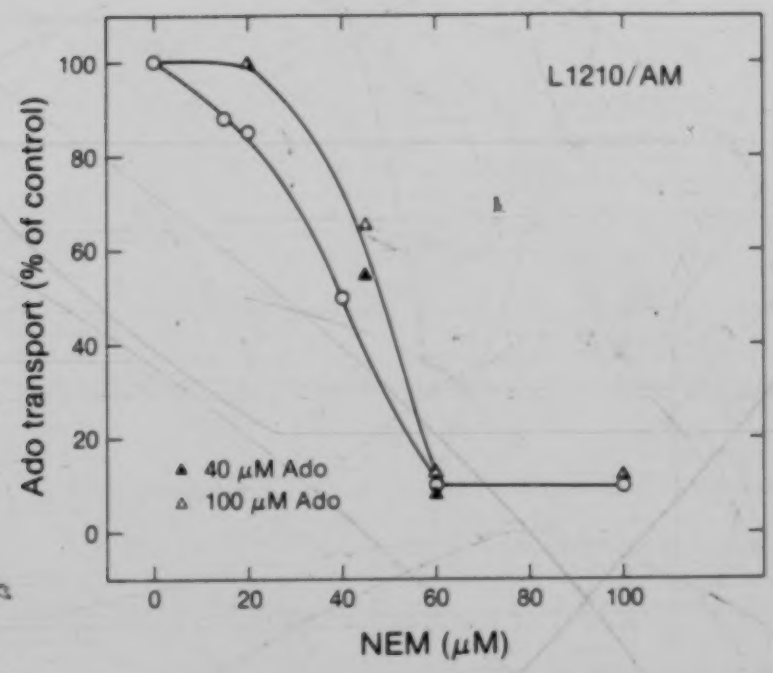

Fig. 42. Effect of NEM on the sodium-dependent transport of 10 μM Ado in L1210/AM cells. Cultures were incubated with NEM at 22°C in the dark for 10 min in the presence of 0 (○), 40 (▲) or 100 (△) μM Ado. Cells were washed once and resuspended in medium with 10 μM dipyridamole prior to assay of Ado transport rates. The latter were determined as initial rates measured from short time courses of Ado uptake by the cells, as in Fig. 27. Transport rates were expressed as a percentage of control rates (0.7 pmol/μl cell water.sec), measured in cells without prior treatment and suspended in medium containing 10 μM dipyridamole.

Protection by NT inhibitors against the anti-proliferative effects of showdomycin in cultures of RPMI 6410 and L1210 cells (6,197) suggested that the uptake of showdomycin by these cells is transporter-mediated. In the present study, exposure of L1210/AM cells to showdomycin reduced sodium-linked Ado (10 uM) transport in a concentration-dependent manner (IC_{50}, 10 μM), as shown in Fig. 43. Although the IC_{50} value for showdomycin inhibition of sodium-linked Ado transport was four-fold lower than that for NEM (Figs. 42 and 43), showdomycin concentrations of approximately 300 μM were necessary to eliminate Ado transport. The difference between the IC_{50} values for NEM and showdomycin inhibition of Ado transport may be related to recognition of showdomycin by the permeation site.

Treatment of L1210/AM cells with *p*CMBS at 22°C strongly inhibited sodium-dependent Ado transport (IC_{50} = 2.0 μM), as shown in Fig. 44. The presence of Ado in incubation mixtures containing *p*CMBS afforded concentration-related protection against inhibition of NT activity by the organomercurial agent. Co-incubation with 40 μM Ado shifted the IC_{50} for *p*CMBS inhibition to 6 μM, while in 100 μM Ado, the IC_{50} was 18 μM (Fig. 44).

Inhibition of Ado transport by *p*CMBS was partially reversed by treatment with 100 μM 2-mercaptoethanol, confirming that thiol groups are involved in the Ado permeation process (Fig. 44). Treatment of L1210/AM cells with 100 μM 2-mercaptoethanol alone did not significantly

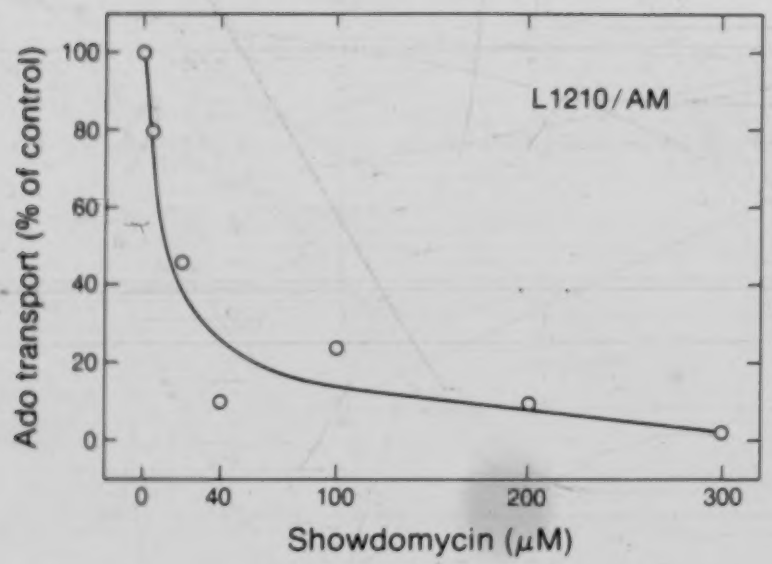

Fig. 43. Effect of prior incubation of L1210/AM cells with showdomycin on sodium-linked Ado (10 μM) transport. Cultures were incubated with showdomycin and effects of this treatment on Ado transport were measured as in Fig. 42. The initial rate of Ado influx in untreated cells was 0.67 pmol/μl cell water.sec.

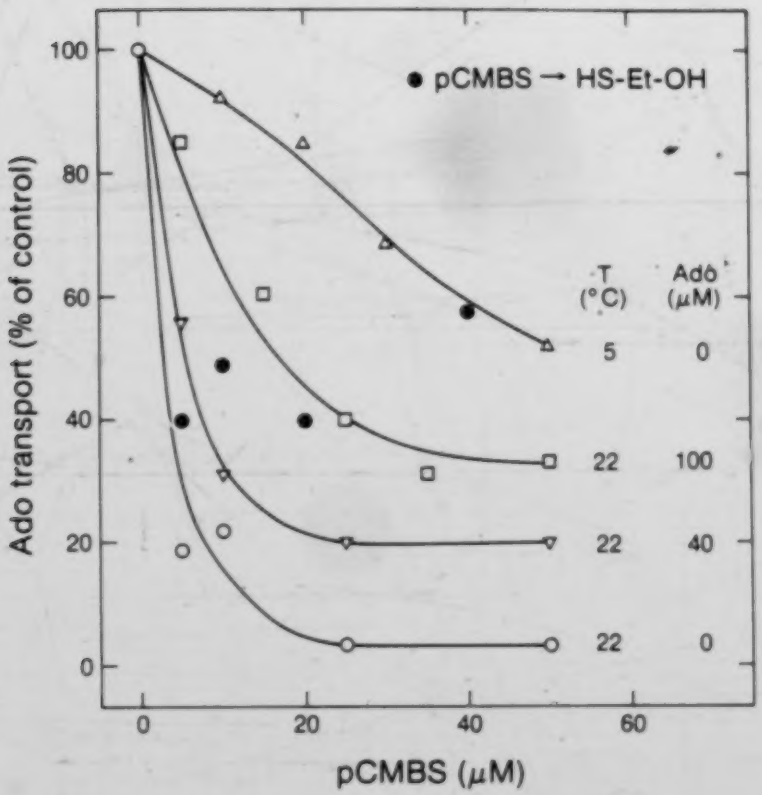

Fig. 44. Effect of *p*CMBS on sodium-linked Ado transport in L1210/AM cells. Cells were incubated in sodium medium containing graded concentrations of *p*CMBS for 10 min in the dark at 5°C (△), or at 22°C in the presence of 0 (○), 40 (▽) or 100 μM Ado (□). After these procedures, the cells were washed once and resuspended in dipyridamole-containing medium prior to transport assays. Rates of Ado transport (10 μM) were obtained as described in Fig. 24. A number of assay mixtures (●) were treated first with *p*CMBS, washed once, then treated with 100 μM 2-mercaptoethanol for 15 min, and washed once again prior to suspension in dipyridamole-containing medium, as described above. Rates of Ado influx in untreated cells were 0.8 ± 0.06 pmol/μl cell water.sec (mean ± S.D. of 3 experiments).

alter rates of Ado transport (data not shown), suggesting that disulfide linkages in the sodium-dependent NT system were inaccessible or not involved in transporter function.

When L1210/AM cells were incubated in medium with *p*CMBS at 5°C, the IC_{50} value for inhibition of sodium-linked Ado transport by the organomercurial increased to about 50 μM (Fig. 44). This increase may stem from several factors, including (i) limited diffusion of *p*CMBS to reach susceptible groups, possibly located within the plasma membrane or in its cytoplasmic face, (ii) reduction in the reactivity of *p*CMBS and/or thiol groups at low temperature, and (iii) temperature-induced modification of carrier conformation, which could shield thiol groups from *p*CMBS.

In L1210 cells, concentrative nucleoside influx was evident only in the presence of inhibitors of facilitated diffusion sytems. Features of the sodium-dependent nucleoside transporter in L1210/AM cells demonstrated in this study are summarized in Table 13.

Table 13

Characteristics of the sodium-dependent NT system in L1210/AM cells

Characteristic		Fig.	Table
Co-substrate cation	Na^+	24,31	
Electrochemical gradient	required	32	
Transmembrane potential	not required	33	
ATP requirement (direct)	none	33,40	
Anion requirement	none	34	
Temperature effects	inactive at 5°C	35	
Inhibitors:			
NBMPR	insensitive	28	
Dipyridamole	insensitive	29	
Dilazep	insensitive	30	
Phloridzin	insensitive	42	
Amiloride	insensitive	42	
Substrate specificity	purine nucleosides and Urd	23,24 37,38	11
Kinetic behaviour	Hyperbolic	39	12
Permeant binding sites	independent	39	
Permeant binding order	random		
Coupling stoichiometry	1:1	41	
Fraction of total NT[1]	20%	28-30	
Free -SH groups	essential	42-44	

[1] 10 µM Ado or 10 µM FB as permeant

III. SELECTION OF A CLONE OF L1210 CELLS DEFICIENT IN SODIUM-LINKED NUCLEOSIDE TRANSPORT.

A number of cultured cell clones with aberrant NT characteristics have been isolated, including those derived from S49 mouse lymphoma (198-200), an NT-deficient variant of the HCT-8 human colorectal carcinoma (148), and an NT variant designated as L1210/MC5-1[5].

The study of NT in L1210 clones deficient in sodium-driven NT activity should help to understand the role of this system in the cellular accumulation of nucleosides and their metabolites. Described below is the selection and characterization of a clone of L1210 cells, L1210/B23.1, apparently devoid of sodium-dependent NT activity.

L1210/B23.1 cells originated from L1210/MC5-1 cells. The latter clone was selected from a mutagenized population of wild-type L1210/B2 cells for resistance to the combination, 0.1 μM tubercidin, 1.0 μM araC and 5.0 μM NBMPR. L1210/MC5-1 cells differ from wild-type cells in the absence of a facilitated diffusion NT mechanism of low sensitivity to NBMPR[17]. In the present study, L1210/MC5-1 cells were chosen

---

[17] The author wishes to acknowledge the kind provision by Dr. J.A. Belt of L1210/MC5-1 cells, the wild-type parent line (L1210/B2) and a manuscript concerning the selection and characterization of L1210/MC5-1 cells in advance of publication.

as the parental line in a mutagenesis/selection experiment because their NT characteristics are simpler than those of L1210/C2 cells.

Concentration-effect relationships in the inhibition of FB transport by NBMPR were explored in L1210/MC5-1 cells in the presence or absence of extracellular Na^+ (Fig. 45). This relationship was monophasic, in contrast to the biphasic nature of the inhibition of FB transport by NBMPR, obtained from similar experiments with L1210/AM cells (Fig. 27). In cells suspended in sodium medium, rates of FB transport were reduced by 75-80% in the presence of 10 nM NBMPR. The reduction of FB fluxes in NMG medium, irrespective of the concentration of NBMPR present, signified the presence of a sodium-dependent nucleoside transporter, as in earlier experiments with L1210/AM cells (Fig. 27).

It was expected that accumulation of nucleosides above extracellular levels in L1210/MC5-1 cells would occur in the presence of NT inhibitors, such as NBMPR. These cells express non-concentrative and sodium-driven NT components, and permeant efflux (leakage) may take place *via* the former route. Time courses of FB (20 μM) influx in L1210/MC5-1 cells suspended in sodium medium or in NMG medium, with or without 10 μM NBMPR, are shown in Fig. 46. In the presence of NBMPR, cells in sodium medium achieved an FB concentration of 250 μM in 5 min. When the suspending medium contained NMG^+ in place of Na^+, little FB influx occurred during the same interval.

The effectiveness of 10 uM NBMPR in enhancing FB

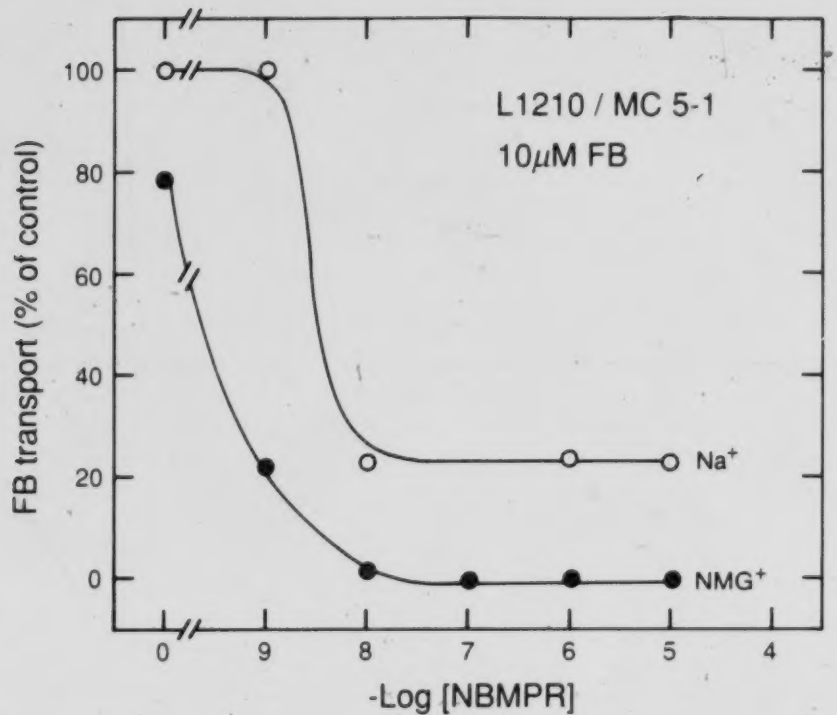

Fig. 45. Concentration-effect relationships for the inhibition by NBMPR of FB transport in L1210/MC5-1 cells. Cells were suspended in sodium medium (○), or NMG medium (●) at 22°C. Initial rates of ^{3}H-FB (10 μM) uptake were derived from time courses, as in Fig. 27, and were expressed as a percentage of FB uptake rates in cells suspended in sodium medium without additives (1.7 pmol/μl cell water.sec).

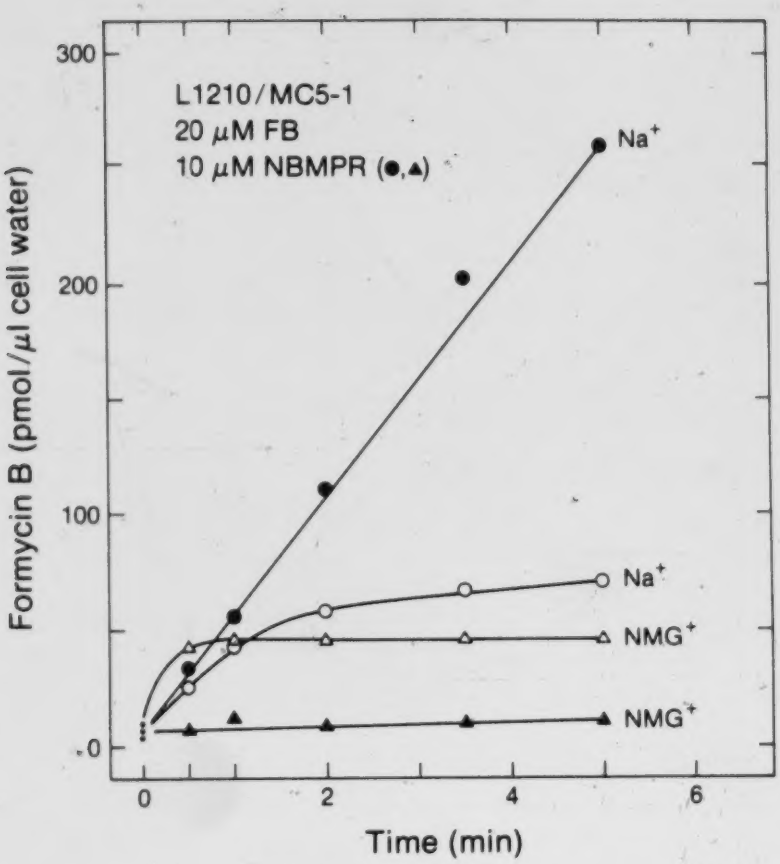

Fig. 46. Effect of NBMPR on the influx of FB in L1210/MC5-1 cells. The influx of 20 μM ^{3}H-FB was measured in cells suspended in sodium medium with (●) or without (○) 10 μM NBMPR, or NMG medium with (▲), or without 10 μM NBMPR (△) (data obtained by M. Selner).

accumulation in L1210/MC5-1 cells (Fig. 46) contrasted with that of 8 μM NBMPR in similar experiments with L1210/C2 cells (Fig. 21B). The concentration of NBMPR (10 μM) utilized in experiments with L1210/MC5-1 cells abolished the movement of FB by facilitated diffusion (Fig. 45). However, in the experiment of Fig. 21, the concentration of NBMPR employed (8 μM) did not completely block FB permeation by the non-concentrative route (Fig. 21A). These observations are consistent with the concept that the accumulation of a nucleoside in L1210 cells is related to the extent of inhibition of nucleoside fluxes via non-concentrative systems in those cells.

The effect of NT inhibition by dipyridamole on the antiproliferative activity of araA towards L1210/MC5-1 cells was examined in the experiment of Fig. 47. Cells were cultured for 48 h with graded concentrations of araA, with or without 5 μM dipyridamole (1.1 μM dCF was present). The presence of dipyridamole decreased the IC_{50} value for araA inhibition of cell proliferation from 3.0 to 1.0 μM (Fig. 47); dipyridamole may have induced cellular accumulation of araA and araA metabolites. In a similar experiment, dipyridamole enhanced the antiproliferative activity of araA towards L1210/C2 cells (Fig. 8).

The foregoing results indicated that L1210/MC5-1 cells possess both sodium-linked and non-concentrative NT systems. Because the NT properties of these cells were less complex than those of wild-type cells, an attempt was made to select

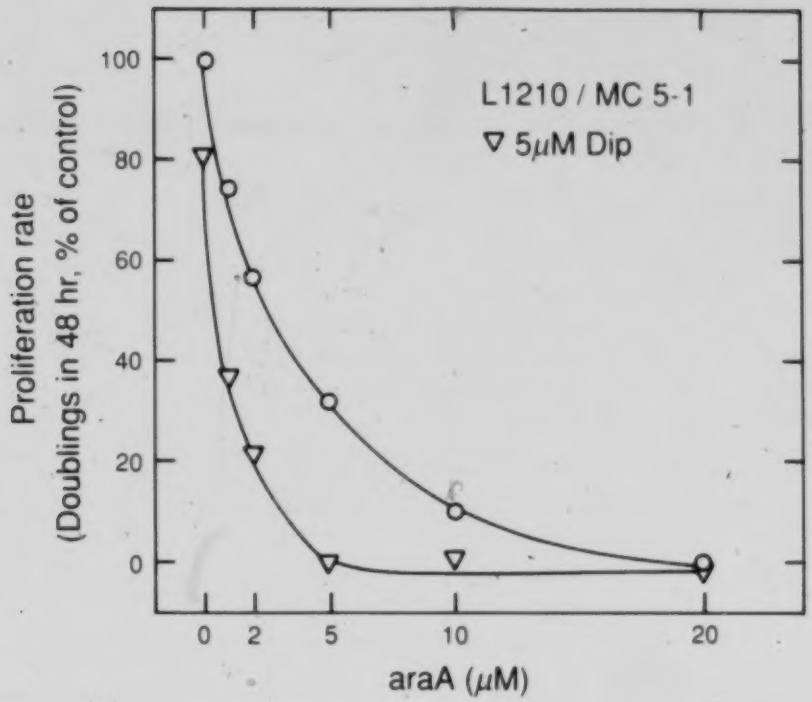

Fig. 47. Enhancement by dipyridamole of the antiproliferative effects of araA towards L1210/MC5-1 cells. Cells were cultured as described in Fig. 10. Cell population doublings in 48 h in cultures without dipyridamole (○), and with 5 μM dipyridamole (▽) were expressed as a percentage of population doublings in control cultures that lacked additives (3.1 doublings).

clones deficient in sodium-linked NT activity from a mutagenized population of L1210/MC5-1 cells. A culture containing 4.4×10^8 L1210/MC5-1 cells was treated with MNNG[17] (3 µg/ml) for 1 h at 37°C and the surviving cells (20-30%) were transferred to fresh medium and cultured for about 10 cell generations under non-selective conditions.

The L1210/B23 clone was isolated by positive selection conditions, which attempted to eliminate undesired phenotypes from the cell population. In the selection conditions of this study, the mutagen-treated cells were cultured in soft-agar medium containing 7 µM araA, 5 µM EHNA, and 5 µM dipyridamole or 10 µM NBMPR.

AraA was chosen as the toxic agent in the selection medium because (i) it is a substrate for the sodium-dependent nucleoside transporter, and (ii) as a substrate of both Ado kinase and dCyd kinase (151-153), the probability of isolating kinase-deficient mutants was reduced. It was reasoned that inclusion of NT inhibitors in the cloning medium would increase the toxicity of araA towards cells that expressed sodium-driven NT, as shown with cells of the parent line (Fig. 47).

---

[17] Mutagens such as MNNG enhance the frequency of mutations in a cell population by 10- to 100-fold (209) and produce point mutations, rather than chromosomal breaks or rearrangements (201).

Because dipyridamole was somewhat toxic to L1210/MC5-1 cells (10 μM dipyridamole alone decreased cellular proliferation rates by 40%, data not shown), NBMPR was utilized as NT inhibitor in some of the selection cultures.

Following culture of the mutagen-treated cells for 14 days in soft-agar selection medium, 34 clones were isolated from about 35 x 10^7 cells (see "Materials and Methods"), which represented a surviving fraction of about 10^7 for a cell population subjected to those selection conditions. These 34 clones were expanded and tested for (i) growth in a secondary selection medium containing 7 μM araA, 1 μM dCF and 5 μM dipyridamole, and (ii) absence of sodium-dependent NT activity. Clone B23, which arose in primary selection medium containing NBMPR, was selected in this manner. After re-cloning by limiting dilution, this clone was designated B23.1. The clonal expansion and some of the NT assays reported in this study were carried out by Mrs. M. Selner under the supervision of Dr. A.R.P. Paterson and Dr. C.E. Cass.

NBMPR-sensitive uptake of FB in L1210/B23.1 cells in NMG^+ medium resulted in a steady-state level of FB, suggesting the operation of a non-concentrative NT system (Fig. 48). The steady-state levels of cellular FB achieved in sodium medium were similar to those in NMG medium.

The contribution of a concentrative NT system to FB uptake in L1210/MC5-1 cells in sodium medium became evident only in the presence of NBMPR (Fig. 46). Under that

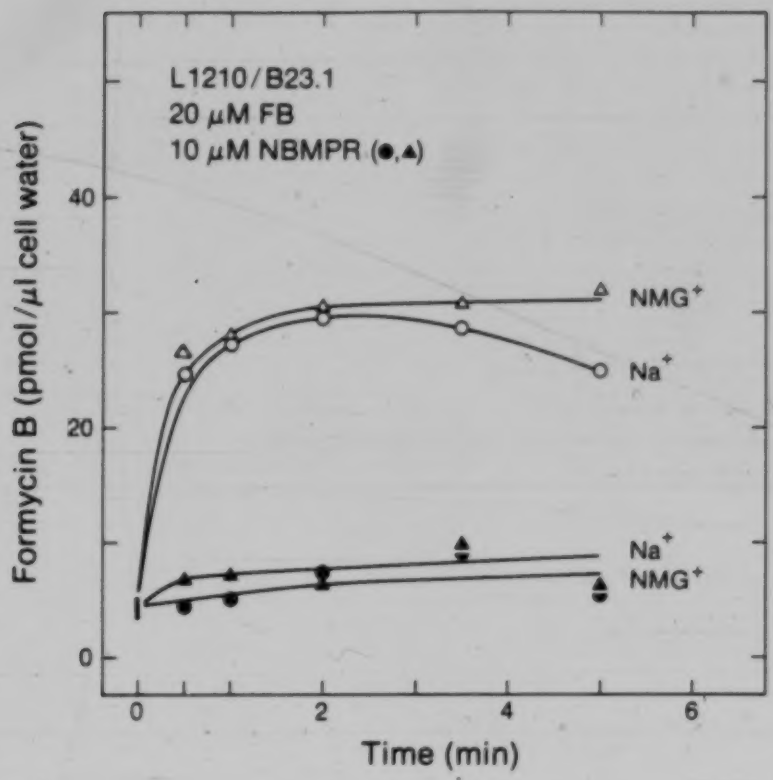

Fig. 48. Effect of NBMPR on the influx of FB in L1210/B23.1 cells. Cells were suspended in sodium medium (○, ●) or NMG medium (△, ▲) in the presence (filled symbols) or absence (empty symbols) of 10 μM NBMPR. After exposure to 20 μM FB at 22°C under these conditions for the intervals specified, the content of FB in these cells was measured (data obtained by M. Selner).

condition, FB leakage was substantially reduced and the concentrative capacity of the sodium-dependent system was manifested. The almost total abolition of FB flux by substitution of NMG^+ in place of Na^+ (in the presence of NBMPR) proved the presence of the sodium-linked transporter in those cells.

The absence of FB accumulation in L1210/B23.1 cells suspended in NBMPR-containing sodium medium, indicated that (i) the sodium-linked nucleoside transporter was absent from that clone, or (ii) a sodium-linked NT component susceptible to inhibition by NBMPR was present in those cells.

Concentration-effect relationships for NBMPR inhibition of FB transport in L1210/B23.1 cells in sodium or NMG medium were explored in the experiment of Fig. 49. The inhibitory effect of NBMPR on FB transport in these cells was not significantly different in the two media, supporting the above evidence that L1210/B23.1 cells lack sodium-dependent NT activity.

NT inhibitors might reasonably be expected to enhance the antiproliferative activity of nucleoside analogues towards L1210 cells in culture if the presence of the inhibitor enhances the cellular content of the analogue and its metabolites. Enhancement by dipyridamole of the antiproliferative activity of araA towards L1210/B23.1 cells would not be expected. Fig. 50 illustrates the results of an experiment in which proliferation rates of L1210/B23.1 cells were measured in the presence of graded concentrations of

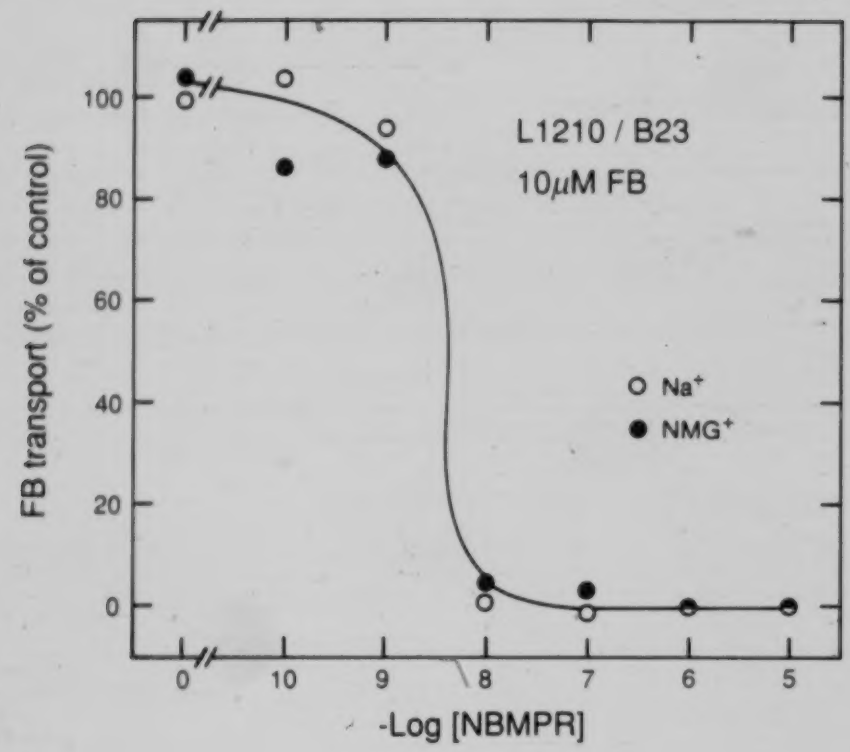

Fig. 49. Concentration-effect relationships for NBMPR inhibition of FB (50 μM) transport in L1210/B23.1 cells. The cells were suspended in sodium (○), or NMG (●) medium and, after incubation of the cells at 22°C with NBMPR for 20 min, initial rates of ^{3}H-FB influx were measured as described in Fig. 27. Initial rates of FB influx are expressed as percentages of the rate (6.9 pmol/μl cell water.sec) in cells in sodium medium without additives.

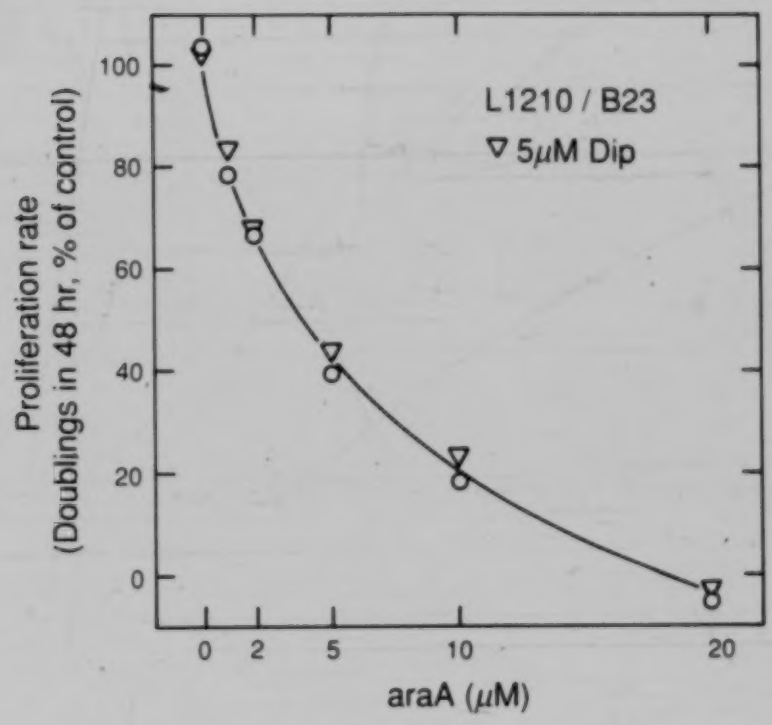

Fig. 50. Effect of dipyridamole on antiproliferative activity of araA towards L1210/B23.1 cells. Cells were cultured as described in Fig. 10 without dipyridamole (○), or with 5 μM dipyridamole (△). Cell population doublings in 48 h are expressed as percentages of the population doublings (3.2) in cultures without additives.

araA (1.1 μM dCF present) with or without 5 μM dipyridamole. The inclusion of dipyridamole in the suspension medium of L1210/B23.1 cultures did not enhance the antiproliferative activity of araA.

Since the concentration of dipyridamole used in the experiment of Fig. 50 abolished NT in L1210/B23.1 cells[18], the absence of a dipyridamole protective effect was noteworthy, and suggested that non-mediated permeation (simple diffusion) of araA was sufficient to inhibit proliferation of L1210/B23.1 cells.

---

[18] M. Selner, C.E. Cass and A.R.P. Paterson, unpublished observations.

IV. CHEMOTHERAPY OF L1210 MOUSE LEUKEMIA WITH ARA-AMP OR FAMP AND INHIBITORS OF NUCLEOSIDE TRANSPORT.

Enhancement by NT inhibitors of the anti-proliferative activity of nucleoside analogues towards L1210 cells in culture (Sections II and IV) suggested that the therapeutic activity of some nucleoside drugs against L1210 cells *in vivo* might be increased by co-administration of an NT inhibitor. Since araA served as a substrate for the sodium-linked NT system in L1210/C2 cells, experiments were undertaken in which mice implanted with L1210/C2 cells were treated with combinations of araAMP[19], dCF and dipyridamole. Fifteen min prior to araAMP administration, mice were treated with 0.25 mg/kg dCF by the i.p. route, a dosage shown to inhibit ADA activity in host tissues and L1210 cells for several hours (206). AraAMP doses of 50, 100 or 150 mg/kg, with or without 3-50 mg/kg dipyridamole, were administered once daily for 9 consecutive days (Q1D x 9) to normal and leukemic mice. These treatment regimens, which were not toxic to normal mice (data not shown), had poor antineoplastic activity, irrespective of the presence or absence of dipyridamole (Table 14).

2-F-araA (administered as the pro-drug, FAMP[20]) has

---

[19] AraAMP is a pro-drug form of araA with high aqueous solubility (202). AraAMP and FAMP are rapidly dephosphorylated *in vivo* by ecto-5'-nucleotidase activity (203-205)

[20] FAMP is the 5'-monophosphate ester of 2-F-araA

Table 14

Treatment of mice implanted with leukemia L1210/C2 cells with combinations of araAMP, dCF and dipyridamole.

$B6D2F_1$ female mice were implanted i.p. with 10^6 cells and treatment (Q1D x 9 by i.p. injection) began 24 h later.

Treatment				
AraAMP (mg/kg)	dCF (mg/kg)	Dipyrid-amole (mg/kg)	ILS[1] (%)	Mice alive on Day 60
0	0.25	0	8	0/6
50	0.25	0	18	0/6
100	0.25	0	48	0/6
150	0.25	0	91	0/6
50	0.25	50	18	0/6
100	0.25	50	39	0/6
150	0.25	50	56	0/6

[1] ILS (increase in life-span): The difference between median survival times of treated and untreated (control) animals that died, expressed as a percentage of the control group survival time. Median survival times in control groups (6 mice) were 7-8 days.

been shown to be more effective than araA/dCF combinations against L1210 leukemia *in vivo* when the analogues were administered at similar molar dosages (118). The difference in the therapeutic activities of the two nucleoside analogues may stem from araA catabolism, which occurs in animals even after administration of high doses of dCF (202,206,207). FAMP, currently undergoing Phase I and II clinical trials, appears to be useful in the therapy of acute leukemias, chronic lymphocytic leukemia and malignant lymphoma (208-211). Intravenous administration of FAMP causes acute, dose-dependent toxicity deriving mainly from bone marrow suppression. This problem has been managed in the clinic by reducing dosage and duration of therapy (208). FAMP, like certain other antimetabolites, may cause dose-related neurological toxicity (208,212-214). The neurotoxic effects of FAMP are characterized by delayed onset and by neuronal injury that is unique in nature and in the region of the central nervous system that is affected (Table 15). Substantial variation has been found in the neuropathology of FAMP (213). The extent of neuronal damage appears to be related to the interval between onset of the symptoms and death, and the most extensive damage occurred in brain areas with high metabolic activity (e.g. the visual system).

The mechanism of FAMP neurotoxicity is unclear. 2-F-araA is incorporated into RNA in some cells (126), a fate that may impair protein synthesis. A cytotoxic metabolite of FAMP,

Table 15

Neurological toxicity of antimetabolites[1]

Agent	Onset	Clinical manifestations	Neuropathological features
MTX	Acute	Headache, nausea fever, meningismus	CSF pleiocytosis
MTX	Late	Confusion, tremors somnolence, dementia	Demyelination, coagulative necrosis in periventricular matter gray matter spared
5-FU	Acute	Ataxia, nystagmus, dysmetria	Loss of Purkinje cells and neurons in olivary and dentate nuclei
araC	Acute	Ataxia, nystagmus, dysmetria	Loss of Purkinje cells
2-FAMP	Late	Blindness, incontinence, dementia, quadraparesis	Occipital white matter mainly; extensive demyelination with axonal damage

[1] Modified from ref. 208

2-F-adenine, has been found in mice, dogs and monkeys receiving 2-F-araA (119,215), and in some cells, 2-F-adenine appears to give rise to 2-F-ATP (216).

The present study assessed the therapeutic effectiveness of FAMP administered Q1D x 5 with or without NT inhibitors against leukemia L1210/C2 *in vivo*[21]. The LD_{10} for FAMP alone in this regimen is 275 mg/kg (164). Normal mice that received 75 mg/kg or 150 mg/kg FAMP Q1D x 5, with or without 3-20 mg/kg dipyridamole, did not lose weight or show other signs of drug toxicity during a 60-day post-treatment interval.

Treatment of leukemic mice with FAMP alone administered Q1D x 5 at dosages of 75-175 mg/kg/day, achieved dose-dependent increases in life-span (ILS) ranging from 60 to 94%, but yielded only one long-term survivor in 101 treated mice (Table 16). Treatment with (i) 100 or 150 mg/kg FAMP for 5 days, or (ii) 100 or 150 mg/kg araAMP (with dCF) for 9 days, yielded similar increases in the life-span of leukemic mice, suggesting that FAMP is more effective than the araAMP/dCF combinations against leukemia L1210.

In evaluating the therapeutic activity of FAMP/dipyridamole combinations, the two agents were co-administered in the Q1D x 5 regimen, starting 24 h after

---

[21] Some of the experiments with FAMP described in this section, and summarized in Table 16, were conducted in collaboration with Dr. A.A. Adjei.

leukemic cell implantation. Leukemic mice treated in this way with FAMP and dipyridamole at the respective dosages of 75 and 3 mg/kg/day achieved life span increases of about 55% (Table 14) which were similar to those in animals treated with FAMP alone at the same dosage. Treatment with FAMP and dipyridamole at 150 and 3 mg/kg/day increased the median life span of leukemic mice by 160% (Table 16). Dipyridamole is bound extensively to plasma proteins (217), and perhaps concentrations of free dipyridamole achieved *in vivo* were too low to influence the toxicity of 2-F-araA towards the L1210/C2 cells.

Therapeutic regimens that combined NBdAMP at 25 mg/kg/day with FAMP dosages of 100, 125 or 150 mg/kg/day were slightly more effective than those with FAMP alone (Table 16). In contrast, the co-administration of NBMPR-P (a soluble pro-drug form of NBMPR) at 25 mg/kg/day and FAMP at the above dosages was substantially more effective than that of FAMP alone (Table 16). In mice that received NBMPR-P and FAMP, increases in life span for mice that died leukemic deaths were approximately two-fold greater than in animals treated with FAMP alone, and long-term survivorship was achieved by these treatments. Survivorship was related to FAMP dosage; the optimal combination in this limited series, FAMP and NBMPR-P at 125 and 25 mg/kg/day, respectively, yielded about 62% long-term survivors.

While concentrations of 2-F-araA and its anabolites achieved in leukemic cells after co-administration with

TABLE 16

Treatment of mice implanted with leukemia L1210/C2 cells with FAMP and NT inhibitors.

$B6D2F_1$ female mice were implanted i.p. with 10^6 cells and treatment (Q1D x 5 by i.p. injection) began 24 h later.

Treatment				
FAMP (mg/k)g	NT inhibitor[1] (mg/kg)	ILS[2] (%)	Mice alive on Day 60	Toxic deaths[3]
75	0	60	0/6	0/6
100	0	63	0/20	4/20[4]
125	0	75	0/30	5/30[4]
150	0	88	1/35	26/41
175	0	94	0/10	5/10
75	3[a]	55	0/6	0/6
150	3[a]	160	0/6	5/6
100	25[b]	94	0/10	3/10
125	25[b]	76	1/10	2/10
150	25[b]	135	1/10	3/10
100	25[c]	136	5/20	3/20(1)[5]
125	25[c]	150	25/40	4/40
150	25[c]	217	18/35	12/35(2)[5]
175	25[c]	150	6/10	2/10

1 The NT inhibitors used were: (a) dipyridamole, (b) NBdAMP, (c) NBMPR-P

2 ILS (Increase in life span): The difference between median survival times of treated and untreated (control) animals that died, espressed as a percentage of the control group survival time. The median survival times of the control groups were 7-9 days.

3 Neurological toxicity, evident initially (Days 15-30) as hind-limb paralysis, was progressive and fatal.

4 Leukemic deaths may have obscured neurological toxicity.

5 Early treatment-related deaths, not due to neurotoxicity.

NBMPR-P have not yet been measured, it is reasonable to speculate that NBMPR-induced increases in the cellular accumulation and retention of the nucleoside drug may be the basis of the enhancement by NBMPR-P of the therapeutic effect just noted. NBMPR may also have limited the influx of 2-F-araA into host tissues.

Treatment of leukemic mice with FAMP produced a fatal, delayed toxicity in some animals that was judged to be neurological because the first symptom was paralysis of the hind limbs. Such paralysis became evident 15-30 days following tumour implantation (9-24 days after cessation of therapy). The nature of the neurological damage in those animals remains to be established.

NBMPR-P and, to a lesser extent, NBdAMP afforded some protection against the FAMP-induced neurotoxicity. The protective effects of the NT inhibitors were difficult to quantify because of the complexity of the system studied. Neurotoxicity symptoms were evident only in tumour-bearing mice treated with FAMP. Untreated mice implanted with 10^6 L1210/C2 cells lived approximately 8 days after implantation. When FAMP was administered Q1D x 5, neurotoxicity symptoms appeared, at the earliest, 15 days after inoculation. Thus, for the neurotoxicity to be apparent, the treatment had to increase life span by at least 88%. In some treatment groups, many animals died from leukemia before day 15, that is, before onset of neurotoxicity symptoms.

The larger dosages of FAMP used (250 mg/kg/day)

increased the life span of leukemic animals sufficiently that the neurotoxicity became evident. For example, about 63% of mice treated with FAMP alone at 150 mg/kg/day exhibited fatal neurotoxicity, whereas the incidence was 34% in groups also receiving NBMPR-P (Table 16). These data suggest that NBMPR-P may protect against the neurotoxicity of FAMP in this mouse model. Experiments attempting to optimize dosages in the FAMP and NBMPR-P combination regimen against the L1210/C2 leukemia are in progress. To the author's knowledge, neurological toxicity induced by FAMP has not hitherto been reported in animals, and leukemic mice may represent a model system that would allow exploration of protection by NT inhibitors against FAMP neurotoxicity.

Protection against FAMP neurotoxicity in animals treated with NBMPR-P, which is evident in Table 16, may have originated from inhibition of 2-F-araA uptake by neurons and/or blockade of 2-F-araA passage across the blood-brain barrier. Nucleosides appear to be transported across the blood-brain-barrier by a carrier-mediated process (218). Studies with rat brain and bovine cortex capillaries have shown the presence of non-concentrative, dipyridamole-sensitive NT systems (219,220). Dipyridamole and NBMPR have been shown to inhibit Ado uptake in synaptosomes from rat and guinea-pig cerebral and cerebellar cortex (221), cultured glial cells and primary neurons (222-224).

The failure of dipyridamole to protect against FAMP neurotoxicity may be due to low dipyridamole concentrations

in the vicinity of susceptible cells. Dipyridamole would not cross the blood-brain-barrier while bound to plasma proteins.

Mice implanted with L1210/C2 leukemia cells represent a test system in which potentiation of nucleoside analogue toxicity towards neoplastic cells and selective protection of the host have been demonstrated. Thus, selective modulation of the toxic effects of nucleoside drugs with NT inhibitors would appear to be achievable *in vivo*. This approach to chemotherapy with nucleoside drugs may also be applicable in the treatment with dideoxynucleosides of viral diseases, such as hepatitis B and acquired immune deficiency syndrome. Although 2',3'-dideoxynucleosides appear to permeate some cells by simple diffusion (2,225), some of these derivatives may enter other cells by mediated processes, as shown in this study for the influx of ddAdo in L1210/AM cells (Fig. 37B). Dose-related toxicity of ddAdo has been reported in dogs and rats (226), and inclusion of NT inhibitors in therapy regimens using dideoxynucleosides may protect dose-limiting tissues in clinically relevant circumstances.

The results presented in this section indicate that selective enhancement of nucleoside analogue toxicity towards neoplasms with concomitant protection of host tissues may be possible with appropriate combinations of drugs and NT inhibitors.

SUMMARY AND FUTURE DIRECTIONS

Three NT components are apparent in L1210 cells: two non-concentrative systems (distinguishable by their relative sensitivities to inhibition by NBMPR, ref. 50 and Fig. 27), plus a system driven by extracellular Na^+. Operation of the sodium-dependent NT system in the L1210 clones, L1210/C2, L1210/AM, and L1210/MC5-1 was demonstrated in the present study. This system was examined in L1210/AM cells, which, lacking Ado, dAdo and dCyd kinase activities, allowed study of the permeation of the physiological nucleosides, Ado and dAdo, and of several nucleoside analogues, in the absence of permeant metabolism.

In contrast to the non-concentrative systems present in L1210 cells, the sodium-driven transporter (i) is resistant to inhibition by NBMPR, dipyridamole and dilazep, (ii) requires a transmembrane Na^+ gradient to operate, and (iii) does not appear to translocate several pyrimidine nucleosides, including dCyd or dThd, although Urd is a substrate.

When the influx of 10 μM FB or 10 μM Ado was measured in L1210/AM cells at 22°C in the presence of graded concentrations of NBMPR, dipyridamole or dilazep, the contribution of the sodium-driven system (given by the difference between the influx rates in sodium medium and in NMG medium) to total nucleoside transport was approximately 20%, irrespective of the concentration of transport inhibitor present (Figs. 27-29). In the presence of dipyridamole at

concentrations $\geq$ 3 μM, the non-concentrative systems did not contribute significantly to the transport of nucleosides. For this reason, characterization of the sodium-driven NT system of L1210/AM cells was undertaken in the presence of 10-20 μM dipyridamole. Rates of dipyridamole-insensitive Ado (10 μM) influx decreased substantially when extracellular Na^+ was replaced by other alkali metal ions or NMG^+. Low levels of residual Ado influx were observed in the presence of Li^+ or K^+ ions. These ions may serve as poor substrates for the sodium-driven NT system.

The presence of a transmembrane Na^+ gradient was essential for the operation of this system, as demonstrated by (i) loss of dipyridamole-insensitive transport activity in cells treated with nystatin (a sodium ionophone), and (ii) the presence of dipyridamole-insensitive Ado influx in energy-depleted cells in which the membrane potential had been clamped with valinomycin. Ado influx in these cells proceeded while a Na^+ gradient was present (Fig. 39). Uphill Ado transport did not appear to require the presence of a particular extracellular anion. Together, these results suggest that the sodium-driven NT mechanism in L1210/AM cells is electrogenic.

The interaction between the sodium-driven nucleoside transporter of L1210/AM cells and nucleosides was found to be enantioselective. L-Ado, the non-physiological enantiomer of Ado (or "D-Ado"), did not appear to enter L1210/AM

cells *via* the sodium-linked NT system when present at the extracellular concentration of 10 μM, and concentrations of that nucleoside as high as 400 μM did not inhibit the transport of D-Ado (10 μM, Fig. 37 and Table 11). The sodium-dependent NT system of L1210/AM cells mediated the entry of Urd and of the purine nucleosides Ado, dAdo, araA and their 2-halo derivatives.

Sodium-dependent Ado transport was virtually abolished at 5°C. In the absence of dipyridamole and under saturating, or nearly saturating, conditions for the sodium-dependent carrier (138 mM Na^+ and 20 μM Ado), ratios of intracellular to extracellular Ado levels achieved in steady-state conditions were about 2:1 and 3:1, at 22°C and 37°C, respectively.

Kinetic studies of sodium-dependent NT in L1210/AM cells revealed that the affinity of the transporter for Ado increased with increasing extracellular Na^+. Thus, K_m values for Ado transport decreased from about 30 μM to 10 μM when the extracellular Na^+ was increased from 5 mM to 100 mM (Table 12A). In a similar manner, $K_{0.5}$ values for "Na^+/Ado" fluxes (considered to be a measure of Na^+ fluxes, p. 133) decreased from 30 mM to 3 mM, when extracellular Ado was increased from 0.5 μM to 100 μM (Table 12B). Hill analysis of the dependence of Ado fluxes on the extracelluar Na^+ concentration indicated that the Na^+/Ado coupling stoichiometry was about 1.

Agents known to interfere with ion movements or ion-coupled permeation of organic solutes (e.g. furosemide, amiloride, ouabain, phloridzin) did not affect sodium-driven Ado transport in L1210/AM cells. In contrast, the thiol reactive agents, NEM, showdomycin, and *p*CMBS inhibited the sodium-driven transport of Ado (10 μM) with IC_{50} values of 40 μM, 10 μM, and 2 μM, respectively. The presence of Ado in incubation medium containing *p*CMBS afforded concentration-dependent protection of NT function against *p*CMBS (Fig. 44).

The physiological significance of the sodium-dependent NT system in L1210 cells has yet to be established. The expression of this transport activity may have arisen as a result of the neoplastic transformation process that gave rise to L1210 cells, or may have been present in the normal cell that was the L1210 progenitor. L1210 cells were isolated from the spleen and lymph nodes of a leukemic mouse (131), and it is known that a sodium-driven NT system similar to that present in L1210 cells is present in normal mouse splenocytes (91). The sodium-dependent NT system of mouse splenocytes is also resistant to inhibition by NBMPR and dipyridamole, and mediates the translocation of purine nucleosides and uridine, but does not transport dThd or dCyd (91), properties seen in L1210 cells in the present study.

The substrate specificity of the sodium-driven nucleoside transporter of L1210 cells suggests that this system probably fulfills a specific function. Ado is a good per-

meant for this system and, under physiological conditions, Ado from the circulation likely enters L1210 cells to some extent by way of the concentrative transporter. Physiological advantages that would be attributable to the joint presence of the three distinct NT systems in L1210 cells are not apparent. The operation of a concentrative transporter, however, requires the expenditure of cellular energy and may only be justified if that system mediates a significant fraction of substrate permeation under physiological conditions. The experimental evidence obtained in the present study is insufficient to establish the role of the sodium-driven NT system of L1210 cells.

An L1210 clone deficient in sodium-depdendent NT activity, designated L1210/B23.1, was isolated after treatment of L1210/MC5-1 cells with MNNG. Cells of the latter clone appear to be devoid of the non-concentrative NT system of low sensitivity to NBMPR[5]. Following the mutagenic treatment, variants were selected in medium containing 7 μM araA, 5 μM EHNA and 10 μM NBMPR. Features of NT in L1210/B23.1 cells that indicate the absence of sodium-dependent NT activity, are (i) loss of FB influx in the presence of 10 μM NBMPR or 7.5 μM dipyridamole, irrespective of the presence or absence of extracellular Na^+, (ii) similarity of initial rates of FB influx in sodium medium and in NMG medium in the presence of 0-10 μM NBMPR, and (iii) lack of enhancement by dipyridamole of the antiproliferative activity of araA.

Specific inhibitors or ligands for the sodium-driven nucleoside transporter of L1210 cells have not been identified. The pharmacological characterization of this system has provided information about the mechanism of permeant translocation. However, purification of the transporter polypeptide(s) will be necessary to examine the molecular events involved in permeant translocation. Thus, future studies should include (i) an extended pharmacological characterization of the sodium-linked NT system, including a search for selective ligands, (ii) purification of the sodium-dependent transporter, and (iii) molecular studies.

Showdomycin was a more potent inhibitor of sodium-dependent Ado transport than NEM, suggesting that the reactive nucleoside might serve as a prototype molecule for the development of selective probes for the concentrative transporter. Treatment of cells with dipyridamole or NBMPR during exposure to showdomycin might reduce interaction of showdomycin with non-concentrative NT system components in L1210 cells. Since ion-substrate cotransporters constitute a minor fraction of the proteins present in the plasma membrane, detection, purification and reconstitution of elements of the sodium-linked NT system into phospholipid vesicles will be difficult. Specific ligands may play a key role in study of the sodium-driven NT system, as NBMPR and congeners have done in molecular studies of the erythrocytic nucleoside transporter.

In purification and reconstitution of the sodium-dependent NT system, additional problems may be encountered because the transporter polypeptide(s) must be solubilized with detergents, which may affect function. The use of organic solvents in the solubilization step may facilitate removal of lipids and crystallization. An approach to isolation of the sodium-dependent NT system of L1210 cells could include:

(a) DNA-mediated transfer (transfection) of genetic material from L1210 cells with the gene coding for sodium-dependent NT activity into a cell type that does not express that activity. This gene could be retrieved from the transformant if a marker gene, previously cloned as a recombinant DNA molecule (e.g. a plasmid), is also expressed in the transformant. Markers that have been used for this purpose include an engineered neomycin-resistance gene that confers drug resistance to any mammalian cell (228), and the herpes virus dThd kinase gene (229). The use of selection conditions that permit survival of only those cells that express both sodium-dependent NT activity and the protein coded by the marker gene would be necessary.

(b) Following selection of a transfected clone that expressed both the desired gene and the marker gene (primary transformant), the isolation of a secondary transformant should be attempted. This could be done by transfection of the wild-type cells that gave rise to the primary transformant with genetic material from the latter. A selection

process identical to that used to isolate the primary transformant would be implemented, and the gene of interest could probably be found by screening a genomic library from the second transformant for sequences from the marker gene.

(c) Molecular cloning using a viral vector could then be undertaken. This step should lead to the identification and sequence determination of the mRNA coding for the transporter. Analysis of the mRNA would give the amino acid sequence of the polypeptide.

The approach just described does not require knowledge about the structure of the protein, or availability of purified polypeptide (230). In addition, once the gene coding for the protein is isolated, a cell system capable of expressing the transporter in large amounts, and more suitable to purification of the NT system, might be found. With the availability of pure protein, antibodies could then be raised for the study of NT systems of other cell types.

Although amino acid sequences can be used to predict the folding of polypeptide chains in the lipid bilayer of the plasma membrane, they cannot provide a picture of the transporter in operation. Crystallographic studies have a similar limitation, although useful information could likely be derived from the crystal structures of loaded and unloaded carriers.

Like other ion-substrate transporters, the sodium-dependent NT system of L1210 cells must have remarkable properties. Conformational changes likely cause binding

sites for Na^+ and nucleosides to become accessible at alternative sides of the plasma membrane. These movements must involve considerable spatial reorganization of some part of the transport polypeptide. On the other hand, the structure of the transporter must preclude diffusion of other small solutes across the membrane through the protein domain. The application of physical, biochemical and genetic techniques will likely help formulate dynamic and static models, leading to an understanding of the co-transport process.

The initial objectives of the present study, outlined in the introductory chapter, were as follows: (i) to determine if cellular retention and toxicity of nucleoside analogues could be modulated by NT inhibitors, (ii) to investigate the effects of NT inhibitors on nucleoside efflux, and (iii) to evaluate the antineoplastic activity of combinations of nucleoside drugs and NT inhibitors. This study showed that, in L1210/C2 cells, (i) NT inhibitors, especially dipyridamole, enhanced the cellular retention of araATP, araCTP and dATP, probably by preventing efflux of nucleosides *via* non-concentrative NT systems present in those cells, and (ii) NT inhibitors enhanced the accumulation and/or cytotoxicity of nucleoside analogues such as araA, dAdo and some of their 2-halo derivatives. Those nucleosides are substrates for the sodium-dependent, concentrative NT system present in L1210 cells.

The co-existence in L1210/C2 cells of three NT systems with different properties allowed manipulation of nucleoside effects with NT inhibitors. The enhancement by NT inhibitors

of cellular accumulation of nucleosides that were substrates for the sodium-linked transporter likely resulted from blockade of bi-directional nucleoside movement *via* non-concentrative transport activity, while the inwardly-directed concentrative transport activity remained unaffected. Thus, modulation of the cytotoxicity of some nucleoside analogues by NT inhibitors was indeed possible in L1210 cells. However, the possibility of such modulation does not appear to be a general property of cells, but would appear to be confined to cells of an appropriate transporter phenotype and to particular nucleosides. These observations were extended to the treatment with FAMP of leukemia L1210/C2 in mice. The results indicated that NBMPR, but not dipyridamole, enhanced the therapeutic activity of FAMP against the leukemia cells, while protecting the host animals from neurological toxicity caused by the nucleoside drug. These effects possibly resulted from (i) appropriate pharmacokinetics and distribution of the drugs, and (ii) presence of NT systems in tumour cells and host cells with different susceptibilites to inhibition by NBMPR in tumour and host cells.

Host protection by NBMPR against FAMP-induced neurotoxicity may be of some general significance in chemotherapy with nucleoside drugs, because of the implication that therapeutic indices of nucleosides with potential or established clinical value might be improved by co-administration with inhibitors of NT.

Some time ago, it was stated that the "characterization of nucleoside transport is as yet only rudimentary...[and] it is not certain whether one or several types of nucleoside transporter exist" (16). Although it is clear now that systems mediating nucleoside translocation across plasma membranes differ in various cell types (and even within individual cells, as shown in this study), the understanding of those systems is still very limited. An appropriate way to summarize the progress made in the NT field in recent years may be found in a quotation that W. Thorpe described as his favourite (231): "I have yet to see a problem, however complicated, which, when you looked at it the right way, did not become still more complicated."

REFERENCES

1. Paterson, A.R.P., Harley, E.R. and Cass, C.E. Measurement and inhibition of membrane transport of adenosine. Meth. Pharmacol. 8:165-180,1985.
2. Zimmerman, T.P., Mahony, W.B., and Prus, K.L. 3'-azido-3'-deoxythymidine. An unusual nucleoside analogue that permeates the membrane of human erythrocytes and lymphocytes by nonfacilitated diffusion. J. Biol. Chem. 262:5748-5754,1987.
3. Paterson. A.R.P., Jakobs, E.S., Ng, C.Y.C., Odegard, R., and Adjei, A.A. Nucleoside transport inhibition in vitro and in vivo. In: Gerlach, E. and Becker, B.F. (eds) Topics and Perspectives in Adenosine Research, Springer-Verlag, Berlin, pp. 89-101,1987.
4. Domin, B.A, Mahony, W.B. and Zimmerman, T.P. 2',3'-dideoxythymidine permeation of the human erythrocyte membrane by non-facilitated diffusion. Proc. Amer. Assoc. Cancer Res. 29:12,1988.
5. Adjei, A.A. and Paterson, A.R.P. Non-mediated permeation of adenosine in a human ovarian carcinoma cell line. Proc. Amer. Assoc. Cancer Res. 29:14,1988.
6. Paterson, A.R.P., Yang. S., Lau, E.Y. and Cass, C.E. Low specificity of the nucleoside transport mechanism of RPMI 6410 cells. Mol. Pharmacol. 16:900-908,1979.

7. Warnick, C.T., Muzik, H. and Paterson, A.R.P. Interference with nucleoside transport in mouse lymphoma cells proliferating in culture. Cancer Res. 32:2017-2022,1972.

8. King, M.E., Naporn, A., Young, B. and Howell, S.B. Modulation of cytarabine uptake and toxicity by dipyridamole. Cancer Treat. Rep. 68:361-366,1984.

9. Cass, C.E., Kolassa, N., Uehara, Y., Dahling-Harley, E., Harley, E.R. and Paterson, A.R.P. Absence of binding sites for the transport inhibitor nitrobenzylthioinosine on nucleoside transport-deficient mouse lymphoma cells. Biochim. Biophys. Acta 649:769-777,1981.

10. Aronow, B. and Ullman, B. Thymidine incorporation in nucleoside-transport deficient lymphoma cells. J. Biol. Chem. 260:16274-16278,1985.

11. Sobrero, A.F., Moir, R.D., Bertino, J.R. and Handschumacher, R.E. Defective facilitated diffusion of nucleosides, a primary mechanism of resistance to 5-fluoro-2'-deoxyuridine in the HCT-8 human carcinoma. Cancer Res. 45:3155-3160, 1985.

12. Cass, C.E., Belt, J.A. and Paterson, A.R.P. Adenosine transport in cultured cells and erythrocytes. Prog. Clin. Biol. Res. 230:13-40,1987.

13. Paterson, A.R.P., Jakobs, E.S., Harley, E.R., Fu, N.-W., Robins, M.J. and Cass, C.E. Inhibition of

nucleoside transport. In: Berne, R.M., Rall, T.W. and Rubio, R. (eds) Regulatory function of adenosine. Martinus Nijhoff, The Hague, pp. 203-220,1983.

14. Plagemann, P.G.W. and Wohlhueter, R.M. Permeation of nucleosides, nucleic acid bases, and nucleotides in animal cells. Curr. Top. Memb. Transp. 14:225-330,1980.

15. Paterson, A.R.P., Jakobs, E.S., Harley, E.R., Cass, C.E. and Robins, M.J. Inhibitors of nucleoside transport as probes and drugs. In: Cheng, Y.-C., Goz, B. and Minkoff, M. (eds) Development of target-oriented anticancer drugs. Raven Press, Raven Press, New York, pp. 41-56,1983.

16. Paterson, A.R.P., Kolassa, N. and Cass. C.E. Transport of nucleosides in animal cells. Pharmac. Ther. 12:515-536,1981.

17. Jarvis, S.M. and Young, J.D. Photoaffinity labelling of nucleoside transporter polypeptides. Pharmac. Ther. 32:339-359,1987.

18. Gati, W.P. and Paterson, A.R.P. Nucleoside Transport. In: The Red Cell Membrane: Structure, Function and Clinical Implications. Agre, P. and Parker, J.C. Marcel Dekker, New York, in press.

19. Cabantchik, Z.I. and Ginsburg, H. Transport of uridine in human red blood cells: demonstration of a simple carrier mechanism. J. Gen. Physiol. 69:75-

96,1977.

20. Oliver, J.M. and Paterson, A.R.P. Nucleoside transport. I. A mediated process in human erythrocytes. Can. J. Biochem. 49:262-270,2977.

21. Cass, C.E. and Paterson, A.R.P. Mediated transport of nucleosides in human erythrocytes. J. Biol. Chem. 247:3314-3320,1972.

22. Stein, W.D. Transport and Diffusion Across Cell Membranes. Academic Press, New York, pp. 117-230, 1986.

23. Lieb, W.R. A kinetic approach to transport studies. In: Ellory, J.C and Young, J.D. Red Cell Membranes - A Methodological Approach. Academic Press, London, pp. 135-164,1982.

24. Jarvis, S.M. *Trans*-stimulation and *trans*-inhibition of uridine efflux from human erythrocytes by permeant nucleosides. Biochem. J. 233:295-297,1986.

25. Jarvis, S.M., Hammond, J.R., Paterson, A.R.P. and Clanachan, A.S. Nucleoside transport in human erythrocytes. A simple carrier with directional symmetry in fresh cells, but with directional asymmetry in cells from outdated blood. Biochem. J. 210:457-461,1983.

26. Plagemann, P.G.W. and Wohlhueter, R.M. Kinetics of nucleoside transport in human erythrocytes. Alterations using blood preservation. Biochim. Biophys. Acta 778:176-184,1984.

27. Cass, C.E. Gaudette, L.A. and Paterson, A.R.P. Mediated transport of nucleosides in human erythrocytes. Specific binding of the inhibitor nitrobenzylthioinosine to nucleoside transport sites in the erythrocyte membrane. Biochim. Biophys. Acta 345:1-10,1974.

28. Jarvis, S.M., Hammond, J.R., Paterson, A.R.P. and Clanachan, A.S. Species differences in nucleoside transport: a study of uridine transport and nitrobenzylthioinosine binding by mammalian erythrocytes. Biochem. J. 208:83-88,1982.

29. Agbanyo, F.R.. Cass, C.E. and Paterson, A.R.P. External location of sites on pig erythrocyte membranes that bind nitrobenzylthioinosine. Molec. Pharmacol. 33:332-337,1988.

30. Jarvis, S.M., McBride, D. and Young, J.D. Erythrocyte nucleoside transport: asymmetrical binding of nitrobenzylthioinosine to nucleoside permeation sites. J. Physiol.324:31-46,1982.

31. Jarvis, S.M., Janmohamed, S.N. and Young, J.D. Kinetics of nitrobenzylthioinosine binding to the human erythrocyte nucleoside transporter. Biochem. J. 216:661-667,1983.

32. Jarvis, S.M., Hammond, J.R., Paterson, A.R.P. and Clanachan, A.S. Nucleoside transport in human erythrocytes. A simple carrier with directional symmetry in fresh cells, but with directional

asymmetry in cells from outdated blood. Biochem. J. 210:457-461,1983.

33. Jarvis, S.M. Nitrobenzylthioinosine-sensitive nucleoside transport system: mechanism of inhibition by dipyridamole. Mol. Pharmacol. 30:659-665, 1986.

34. Jarvis, S.M. and Young, J.D. Nucleoside translocation in sheep reticulocytes and in erythrocytes from newborn lambs. A proposed molecular model for the nucleoside transporter. J. Physiol. 324: 47-66,1982.

35. Wu, J.S.R., Kwong, F.Y.P., Jarvis, S.M. and Young, J.D. Identification of the erythrocyte nucleoside transporter as a band 4.5 polypeptide. J. Biol. Chem. 258:13745-13751,1983.

36. Young, J.D., Jarvis, S.M., Robins, M.J. and Paterson, A.R.P. Photoaffinity labeling of the human eryth rocyte nucleoside transporter by N^6-(p-azidobenzyl)adenosine and nitrobenzylthioinosine. J. Biol. Chem. 258:2202-2208,1983.

37. Klip, A., Walker, D., Cohen, A. and Leung, C. Chemical and genetic comparison of the glucose and nucleoside transporters. Biochem. Cell Biol. 64:1170-1180,1986.

38. Steck, T.L. The organization of proteins in the human red blood cell membrane. J. Cell Biol. 62:1-19,1974.

39. Jarvis, S.M., Ellory, J.C. and Young, J.D. Radiation inactivation of the human erythrocyte nucleoside and glucose transporters. Biochim. Biophys. Acta 855:312-315,1986.

40. Kwong, F.Y.P., Tse, C.-M., Jarvis, S.M., Choy, M.Y.M. and Young, J.D. Purification and reconstitution studies of the nucleoside transporter from pig erythrocytes. Biochim. Biophys. Acta 904:105-116,1987.

41. Tse, C.-M., Wu, J.-S. R. and Young, J.D. Evidence for the asymmetrical binding of p-chloromercuriphenyl sulphonate to the human erythrocyte nucleoside transporter. Biochim. Biophys. Acta 818:316-24,1985.

42. Geisbuhler, T.P., Johnson, D.A. and Rovetto, M.J. Cardiac myocyte guanosine transport and metabolism. Am. J. Physiol. 253:C645-C651,1987.

43. Ford, D.A. and Rovetto, M.J. Rat cardiac myocyte adenosine transport and metabolism. Am. J. Physiol. 252:H54-H63,1987.

44. Heaton, T.P. and Clanachan, A.S. Nucleoside transport in guinea pig myocytes. Biochem. Pharmacol. 36:1275-1280,1987.

45. Plagemann, P.G.W. and Wohlhueter, R.M. Nitrobenzylthioinosine-sensitive and -resistant nucleoside transport in normal and transformed rat cells. Biochim. Biophys. Acta 816:387-

395,1985.

46. Chello, P.L., Sirotnak, F.M. Dorick, D.M., Yang, C.-H. and Montgomery, J.A. Initial rate kinetics and evidence for duality of mediated transport of adenosine, related purine nucleosides and nucleoside analogues in L1210 cells. Cancer Res. **43**:97-103,1983.

47. Plagemann, P.G.W., Behrens, M. and Abraham, D. Metabolism and cytotoxicity of 5-azacytidine in cultured Novikoff rat hepatoma and P388 mouse leukemia cells and their enhancement by preincubation with pyrazofurin. Cancer Res. **38**:2458-2466,1978.

48. Wolhueter, R.M., Marz, R. and Plagemann, P.G.W. Thymidine transport in cultured mammalian cells: Kinetic analysis, temperature dependence and specificity of the transport system. Biochim. Biophys. Acta **553**:261-268,1979.

49. Cybuslski, R.L., Fry, D.W. and Goldman, I.D. Adenosine stimulation of uphill adenine transport in L1210 leukemia cells. J. Biol. Chem. **256**:4455-4459,1981.

50. Belt, J.A. Heterogeneity of nucleoside transport in mammalian cells. Molec. Pharmacol. **24**:479-484,1983.

51. Aronow, B. and Ullman, B. Role of the nucleoside transport function in the transport and salvage

of purine nucleobases. J. Biol. Chem. **261**:2014-2019,1986.

52. Plagemann, P.G.W. and Wohlhueter, R.M. S49 mouse lymphoma cells are deficient in hypoxanthine transport. Biochim. Biophys. Acta **855**:25-32,1986.

53. Slaughter, R.S. and Barnes, E.M., Jr. Hypoxanthine transport by Chinese hamster lung fibroblasts: Kinetics and inhibition by nucleosides. Arch. Biochem. Biophys. **197**:349-355,1979.

54. Belt, J.A. and Welch, A.D. Transport of uridine and 6-azauridine in human lymphoblastoid cells. Mol. Pharmacol. **23**:53-58,1983.

55. Dahling-Harley, E., Paterson, A.R.P., Robins, M.J. and Cass, C.E. Transport of uridine and 3-deazauridine in cultured human lymphoblastoid cells. Cancer Res. **44**:161-165,1984.

56. Sixma, J.J., Lips, J.P.M., Trieschnigg, A.M.C. and Holmsen, H. Transport and metabolism of adenosine in human blood platelets. Biochim. Biophys. Acta. **443**:33-48,1976.

57. Plagemann, P.G.W. and Estensen, R.D. Cytochalasin B. VI. Competitive inhibition of nucleoside transport by cultured Novikoff rat hepatoma cells. J. Cell Biol. **55**:179-185,1972.

58. Mizel, S.B. and Wilson, L. Nucleoside transport in mammalian cells. Inhibition by colchicine. Biochem. **11**:2573-2578,1972.

59. Lemkin, J.A. and Hare, J.D. Nucleoside transport in normal and polyoma-transformed cells: Kinetic differences following adenosine and serum or insulin stimulation. Biochim. Biophys. Acta **318**:113-122,1973.

60. Loike, J.D. and Horwitz, S.B. Effects of podophyllotoxin and UP-116-213 on microtubule assembly *in vitro* and nucleoside transport in HeLa cells. Biochem. **15**:5435-5443,1976.

61. Gati, W.P., Wiebe, L.I., Knaus, E.E. and Paterson, A.R.P. [^{125}I]- Iodohydroxynitrobenzylthioinosine: a new high-affinity nucleoside transporter probe. Biochem. Cell Biol. **65**:467-473,1987.

62. Dahling-Harley, E., Eilam, Y., Paterson, A.R.P. and Cass, C.E. Binding of nitrobenzylthioinosine to high affinity sites on the nucleoside transport mechanism of HeLa cells. Biochem. J. **200**:295-305,1981.

63. Belt, J.A. and Noel, L.D. Nucleoside transport in Walker 256 rat carcinosarcoma and S49 mouse lymphoma cells. Biochem. J. **232**:681-688,1985.

64. Hammond, J.R. and Clanachan, A.S. Species differences in the binding of [^{3}H] nitrobenzylthioinosine to the nucleoside transport system in mammalian central nervous system membranes: evidence for interconvertible conformations of the binding

site/transporter complex. J. Neurochem. 45:527-535,1985.

65. Belloni, F.L., Liang, B.C. and Gerritsen, M.E. Effects of alkylxanthines and calcium antagonists on adenosine uptake by cultured rabbit coronary microvascular endothelium. Pharmacol. 35:1-15,1987.

66. Young. J.D. and Jarvis, S.M. Nucleoside transport in animal cells. Biosci. Rep. 3:309-322,1983.

67. Almeida, A.F., Jarvis, S.M., Young, J.D. and Paterson, A.R.P. Photoaffinity labelling of the nucleoside transporter of cultured mouse lymphoma cells. FEBS Lett. 176:444-448,1984.

68. Young, J.D., Jarvis, S.M., Belt, J.A., Gati, W.P. and Paterson, A.R.P. Identification of the nucleoside transporter in cultured mouse lymphoma cells. J. Biol. Chem. 259:8363-8365,1984.

69. Cass, C.E. and Hodgson, K.C. Effects of tunicamycin on interaction of nitrobenzylthioinosine with the nucleoside transporter of cultured L1210 leukemia cells. J. Cell Biol. 101:431a,1985.

70. Young, J.D. and Jarvis, S.M. The use of ligands in the study of the nucleoside-transport complex. Meth. Pharmacol. 8:181-190,1985.

71. Shi, M.M., Wu, J.-S.R., Lee, C.M. and Young, J.D. Photoaffinity labelling of high-affinity nitrobenzylthioinosine binding sites in rat and

guinea pig lung. Biochem. Biophys. Res. Commun. **118**:594-600,1984.

72. Kwan, K.F. and Jarvis, S.M. Photoaffinity labeling of adenosine transporter in cardiac membranes with nitrobenzylthioinosine. Am. J.Physiol. **246**:710-715,1984.

73. Wu, J.-S.R. and Young, J.D. Photoaffinity labelling of nucleoside-transport proteins in plasma membranes isolated from rat and guinea-pig liver. Biochem. J. **220**:499-506,1984.

74. Gati, W.P., Belt, J.A., Jakobs, E.S., Young, J.D., Jarvis, S.M. and Paterson, A.R.P. Photoaffinity labelling of a nitrobenzylthioinosine-binding polypeptide from cultured Novikoff hepatoma cells. Biochem. J. **236**:665-670,1986.

75. Kessel, D. and Shurin, S.B. Transport of two non-metabolized nucleosides, deoxycytidine and cytosine arabinoside, in a sub-line of the L1210 leukemia. Biochim. Biophys. Acta **163**: 179-187,1968.

76. Ungemach, F.R. and Hegner, D. Uptake of thymidine into isolated rate hepatocytes. Evidence for two transport systems. Hoppe-Seyler's Z. Physiol. Chem. **359**:845-856,1978.

77. LeHir, M. and Dubach, U.C. Sodium gradient-energized concentrative transport of adenosine in renal brush border vesicles. Pflugers Arch. **401**:58-

63,1984.

78. LeHir, M. and Dubach, U.C. Concentrative transport of nucleosides in brush border vesicles of rat kidney. Eur. J. Clin. Invest. 15:121-127,1985.

79. LeHir, M. and Dubach, U.C. Uphill transport of pyrimidine nucleosides in renal brush border vesicles. Pflugers Arch. 404:238-243,1985.

80. Angielski, S., LeHir, M. and Dubach, U.C. Transport of adenosine by renal brush border membranes. Pflugers Arch. 397:75-77,1983.

81. Kuttesch, J.F., Jr., Robins, M.J. and Nelson, J.A. Renal transport of 2'-deoxytubercidin in mice. Biochem. Pharmacol. 31:3387-3394,1982.

82. Kuttesch, J.F., Jr., and Nelson, J.A. (1982) Renal handling of 2'-deoxyadenosine and adenosine in humans and mice. Cancer Chemother. Pharmacol. 8:221-22,1982.

83. Bowman, W.C. and Rand, M.J. Textbook of Pharmacology. 2nd. ed. Blackwell Scientific Publications, Oxford, pp. 27.1-27.40,1980.

84. Schwenk, M., Hegazy, E. and Lopez del Pino, V. Uridine uptake by isolated intestinal epithelial cells of guinea pig. Biochim. Biophys. Acta 805:370-374,1984.

85. Jakobs, E.S. and Paterson, A.R.P. Sodium-dependent, concentrative nucleoside transport in cultured intestinal epithelial cells. Biochem. Biophys.

Res. Commun. 140:1028-1035,1986.

86. Spector, R. Thymidine accumulation by choroid plexus in vitro. Arch. Biochem. Biophys. 205:85-93,1980.

87. Spector, R. and Huntoon, S. Deoxycytidine transport and metabolism in choroid plexus. J. Neurochem. 40:1474-1480,1983.

88. Spector, R. Nucleoside transport in choroid plexus: mechanism and specificity. Arch. Biochem. Biophys. 216:693-703,1982.

89. Spector, R. and Huntoon, S. Specificity and sodium dependence of the active nucleoside transport system in choroid plexus. J. Neurochem. 42:1048-1052,1984.

90. Darnowski, J.W. and Handschumacher, R.E. Concentrative uridine transport by murine splenocytes: kinetics, substrate specificity and sodium dependence. Cancer Res. 47:2614-2619,1987.

91. Darnowski, J.W. and Handschumacher, R.E. Tissue uridine pools: evidence in vivo of a concentrative mechanism for uridine uptake. Cancer Res. 46:3490-3494,1986.

92. Gati, W.P., Stoyke, F.-W., Gero, A.M. and Paterson, A.R.P. Nucleoside permeation in mouse erythrocytes infected with Plasmodium yoelii. Biochem. Biophys. Res. Commun. 145:1134-1141,1987.

93. El Kouni, M.H., Diop, D. and Cha, S. Combination therapy of Schistosoma japonicum by tubercidin

and nitrobenzylthioinosine 5-monophosphate. Biochem. Pharmacol. 34:3921-3923,1985.

94. El Kouni, M.H., Messier, N.J. and Cha, S. Treatment of Schistosomiasis by purine nucleoside analogues in combination with nucleoside transport inhibitors. Biochem. Pharmacol. 36:3815-3821,1987.

95. Kang, G.-J. and Kimball, A.P. Dipyridamole enhancement of toxicity to L1210 cells by deoxyadenosine and deoxycoformycin combinations in vitro. Cancer Res. 44:461-466,1984.

96. Yang. J.L., Capizzi, R. and Contento, M. Sequential dipyridamole retards araC efflux and results in synergistic cytotoxicity. Proc. Amer. Assoc. Cancer Res. 24:346,1984.

97. Agarwal, R.P. Inhibitors of adenosine deaminase. Pharmac. Ther. 17:399-429,1982.

98. Henderson, J.F. and Paterson, A.R.P. Nucleotide metabolism. An introduction. Academic Press, New York and London,1973.

99. Fox, I.H. and Kelley, W.N. The role of adenosine and 2-deoxyadenosine in mammalian cells. Ann. Rev. Biochem. 47:655-686,1978.

100. Snyder, F.F and Henderson, J.F. Alternative pathways of deoxyadenosine and adenosine metabolism. J. Biol. Chem. 248:5899-5904,1973.

101. Fox, R.M., Kefford, R.F., Tripp, E.H. and Taylor, I.W. G_1-phase arrest of cultured human leukemic T-

cells induced by deoxyadenosine. Cancer Res. 41:5141-5150,1981.

102. Ullman, B., Gudas, L.J., Cohen, A. and Martin, D.W., Jr.Deoxyadenosine metabolism and cytotoxicity in cultured mouse T lymphoma cells: A model for immunodeficiency disease. Cell 14:365-375,1978.

103. Cass, C.E., Selner, M., Ferguson, P.J. and Phillips, J.R. Effects of 2'-deoxyadenosine, 9-beta-d-arabinofuranosyladenine and related compounds on S-adenosyl-L-homocysteine hydrolase activity in synchronous and asynchronous cultured cells. Cancer Res. 42:4991-4998,1982.

104. Hershfield, M.S. Apparent suicide inactivation of human lymphoblast S-adenosylhomocysteine hydrolase by 2'-deoxyadenosine. Cancer Res. 41:5141-5150,1981.

105. Bagnara, A.S. and Hershfield, M.S. Mechanism of deoxyadenosine induced catabolism of adenine ribonucleotides in adenosine deaminase-inhibited human T lymphoblastoid cells. Proc. Natl. Acad. Sci. U.S.A. 79:2673-2677,1982.

106. Hershfield, M.S. S-Adenosylhomocysteine hydrolase as a target in genetic and drug induced deficiency of adenosine demaminase. In: Berne, R.M., Rall, T.W. and Rubio, R. (eds.). Regulatory Function of Adenosine. Martinus Nijhoff, The Hague, pp. 171-178,1983.

107. Henderson, J.F., Scott, F.W. and Lowe, J.K. Toxicity of

naturally occurring purine deoxyribonucleosides. Pharmac. Ther. 8:573-604,1980.

108. Henderson, J.F. Mechanisms of toxicity of adenosine, 2'-deoxyadenosine and inhibitors of adenosine deaminase. In: Berne, R.M., Rall, T.W. and Rubio, R. (eds.). Regulatory Function of Adenosine. Martinus Nijhoff, The Hague, pp. 223-234,1983.

109. Kredich, N.M. and Hershfield, M.S. Immunodeficiency diseases caused by adenosine deaminase deficiency and purine phosphorylase deficiency. In: Stanbury, J.B., Wyngaarden, J.B., Fredrickson, D.S., Goldstein, J.L. and Brown, M.S. (eds.). The Metabolic Basis of Inherited Disease. Fifth ed., McGraw-Hill, New York, pp. 1157-1183,1983.

110. Pallavicini, M.G. Cytosine arabinoside: Molecular, pharmacokinetic and cytokinetic considerations. Pharmac. Ther. 25:207-238,1984.

111. Krenitsky, T.A., Tuttle, J.V., Koszalka, J.V., Chen, G.W., Chen, I.S., Beacham, L.M., Rideout, J.L. and Elion, G.B. Deoxycytidine kinase from calf thymus. J. Biol. Chem. 251:4055-4061,1976.

112. Chang, C.-H., Brockman, R.W. and Bennett, L.L., Jr. Purification and some properties of a deoxyribonucleoside kinase from L1210 cells. Cancer Res. 42:3033-3039,1982.

113. Miller, R.L., Adamczyk, D.L., Miller, W.H., Koszalka,

G.W., Rideout, J.L., Beacham, L.M., Chao, E.Y., Hagerty, J.J., Krenitsky, T.A. and Elion, G.B. Adenosine kinase from rabbit liver. II. Substrate and inhibitor specificity. J. Biol. Chem. 254:2346-2352,1979.

114. Verhoef, V., Sarup, J. and Fridland, A. Identification of the mechanism of activation of 9-beta-D-arabinofuranosyladenine in human lymphoid cells using mutants deficient in nucleoside kinases. Cancer Res. 41:4478-4483,1981.

115. Cohen, S.S. The lethality of aranucleotides. Med. Biol. 54:299-326,1976.

116. LePage, G.A Alterations in enzyme activity in tumors and implications for chemotherapy. Adv. Enzyme Regul. 8:323-332,1970.

117. Shewach, D.S. and Plunkett, W. Effect of 2'-deoxycoformycin on the biologic half-life of 9-beta-D-arabino-furanosyladenine 5'-triphosphate. Biochem. Pharmacol. 28:2404-2407,1979.

118. Brockman, R.W., Cheng, Y.-C., Schabel, F.M., Jr. and Montgomery, J.A. Metabolism and chemotherapeutic activity of 9-beta-D-arabinofuranosyl-2-fluoroadenine against murine leukemia L1210 and evidence for its phosphorylation by deoxycytidine kinase. Cancer Res. 40:3610-3615,1980.

119. El Dareer, S.M., Struck, R.F., Tillery, K.F., Rose, L.M., Brockman, R.W., Montgomery, J.A. and Hill,

D.L. Disposition of 9-beta-D-arabinofuranosyl-2-fluoroadenine in mice, dogs and monkeys. Drug Metab. Dispos. 8:60-63,1980.

120. Plunkett, W., Chubb, S., Alexander, L. and Montgomery, J.A. Comparison of the toxicity and metabolism of 9-beta-D-arabinofuranosyl-2-fluoroadenine and 9-beta-D-arabinofuranosyladenine in human lymphoblastoid cells. Cancer Res. 40:2349-2355,1980.

121. Satp, A., Montgomery, J.A. and Cory, J.G. Synergistic inhibition of leukemia L1210 cell growth in vitro by combinations of 2-fluoroadenine nucleosides and hydroxyurea or 2,3-dihydro-1H-pyrazole[2,3-a] imidazole Cancer Res. 44:3286-3290,1984.

120. Furth, J.J. and Cohen, S.S. Inhibition of mammalian DNA polymerase by the 5'-triphosphate of 1-beta-D-arabinofuranosylcytosine and the 5'-triphosphate of 9-beta-D-arabinofuranosyladenine. Cancer Res. 28:2061-2067,1968.

121. Struck, R.F., Shortnacy, A.T., Kirk, M.C. Thorpe, M.C., Brockman, R.W., Hill, D.L., El Dareer, S.M. and Montgomery, J.A. Identification of metabolites of 9-beta-D-arabinofuranosyl-2-fluoroadenine, an antitumor and antiviral agent. Biochem. Pharmacol. 31:1975-1978,1982.

122. White, E.L., Shaddix, S.C., Brockman, R.W. and Bennett, L.L., Jr. Comparison of the actions of

9-beta-D-arabinofuranosyladenine on target enzymes from mouse tumor cells. Cancer Res. 42:2260-2264,1982.

123. Dicioccio, R.A. and Sivrastava, B.I.S. Kinetics of inhibition of deoxynucleotide-polymerizing enzyme activities from normal and leukemic human cells by 9-beta-D-arabinofuranosyladenine 5'-triphosphate and 1-beta-D-arabinofuranosylcytosine 5'-triphosphate. Eur. J. Biochem. 79:411-418,1977.

124. Tseng, W.C., Derse, D., Cheng, Y.-C., Brockman, R.W. and Bennett, L.L., Jr. In vitro biological activity of 9-beta-D-arabinofuranosyl-2-fluoroadenine and the biochemical actions of its triphosphate on DNA polymerases and ribonucleotide reductase from HeLa cells. Mol. Pharmacol. 21:474-477,1982.

125. Kufe, D.W., Major, P.P., Munroe, D., Egan, M. and Herrick, D. Relationship between incorporation of 9-beta-D-arabinofuranosyladenine in L1210 DNA and cytotoxicity. Cancer Res. 43:2000-2004,1983.

126. Spriggs, D., Robbins, G., Mitchell, T. and Kufe, D.W. Incorporation of 9-beta-D-arabinofuranosyl-2-fluoro-adenine into HL-60 cellular RNA and DNA. Biochem. Pharmacol. 35:247-252,1986.

127. Helland, S. and Ueland, P.M. Interaction of 9-beta-D-arabinofuranosyladenine and 9-beta-D-arabino-

furanosyladenine 5'-triphosphate with S-adenosylhomocysteinase. Cancer Res. 41:673-678,1981.

128. Hershfield, M.S., Small, W.C., Premakumar, R., Bagnara, A.S. and Fetter, J.E. Inactivation of S-adenosylhomocysteine hydrolase: mechanism and occurence in vivo in disorders of purine nucleoside catabolism. In: Usdin, E., Borchardt, R.T. and Creveling, C.R. (eds) The Biochemistry of S-Adenosylmethionine and Related Compounds. McMillan, London, pp. 657-665,1982.

129. Young G.J., Hallam, L.J., Jack, I. and Van Der Weyden, M.B. S-adenosylhomocysteine hydrolase inactivation and purine toxicity in cultured human T- and B-lymphoblasts. J. Lab. Clin. Med. 104:86-95,1984.

130. Lynch, P.T., Lauzon, G.J., Naik, S.R., Cass, C.E. and Paterson, A.R.P. Inhibition of nucleoside uptake in HeLa cells by nitrobenzylthioinosinate. Biochem. Pharmacol. 27:1303-1304,1978.

131. Dunham, L.J. and Stewart, H.L. A survey of transplantable and transmissible animal tumors. J. Natl. Cancer Institute 13:1299-1377,1953.

132. Cass, C.E. and Au-Yeung, T.H. Enhancement of 9-beta-D-arabinofuranosyladenine toxicity to mouse leukemia in vitro by 2'-deoxycoformycin. Cancer Res. 36:1486-1491,1976.

133. Bennett, L.L., Jr., Bowdon, B.J., Shaddix, S.C.,

Dubois, N.F., Hughes, J. and Brockman, R.W. Resistance to 9-beta-D-arabinofuranosyladenine (AraA) in L1210 leukemia. Proc. Amer. Assoc. Cancer Res. 23:6,1982.

134. Cass, C.E., Tan, T.H. and Selner, M. Antiproliferative effects of 9-beta-D-arabinofuranosyladenine 5'-monophosphate and related compounds with adenosine deaminase inhibitors against mouse leukemia L1210/C2. Cancer Res. 39:1563-1569,1979.

135. Drack, J.C. and Novack, J.M. Some simple thin-layer chromatography systems for the separation of purines and purine nucleosides. Anal. Biochem. 52:633-636,1973.

136. Schwartz, P.M. and Drach, J.C Separation of arabinosyl, ribosyl and deoxyribosyl purine nucleotides by thin layer chromatography. J. Chromatogr. 106:200-203,1975.

137. Lauzon, G.J., Paran, J.H. and Paterson, A.R.P. Formation of 1-beta-D-arabinofuranosylcytosine diphosphate choline in cultured human leukemic RPMI 6410 cells. Cancer Res. 38:1723-1729,1978.

138. Kufe, D.W., Major, P.P., Egan, E.M. and Beardsley, G.P. Correlation of cytotoxicity with incorporation of araC into DNA. J. Biol. Chem. 255:8897-9000,1980.

139. Wallace, D.M. Large and small-scale phenol extrac tions. Meth. Enzymol. 152:33-41,1987.

140. Wallace, D.M. Precipitation of nucleic acids. Meth. Enzymol. 152:41-48,1987.

141. Chambers, J.A.A. and Rickwood, D. Separation of macromolecules by isopycnic centrifugation in dif ferent media. In: Rickwood, D. (ed) Centrifugation: A Practical Approach. Information Retrieval, London, pp. 119-133,1980.

142. Rose, L.M. and Brockman, R.W. Analysis by high-pressure liquid chromatography of 9-beta-D-arabinofuranosyladenine-5'-triphosphate levels in murine leukemia cells. J. Chromatogr. 133:335-343,1977.

143. Harley, E.R., Paterson, A.R.P. and Cass, C.E. Initial rates of transport of adenosine and tubercidin in cultured cells. Cancer Res. 42:1289-1295,1984.

144. Dulbecco, R. and Vogt, M. Plaque formation and isolation of pure lines with poliomyelitis viruses. J. Exp. Med. 99:167-182,1954.

145. Blackstock, E.J., Ellory, J.C. and Stewart, G.W. N-Methyl-D-glucamine as a cation replacement for human red-cell transport studies. J. Physiol. 358:90P,1985.

146. Smith, J.B., Cragoe, E.J., Jr. and Smith, L. Sodium/calcium antiport in cultured arterial smooth muscle cells. Inhibition by magnesium and other divalent cations. J. Biol. Chem. 262:11988-11994, 1987.

147. Pande, S.V. Liquid scintillation counting of aqueous samples using Triton-containing scintillants. Anal. Biochem. 74:25-34,1976.

148. Cohen, A., Ullman, B. and Martin, D.W., Jr. Characterization of a mutant lymphoma cell with deficient transport of purine and pyrimidine nucleosides. J. Biol. Chem. 254:112-116,1979.

149. Mitchell, B.S, Mejias, E., Daddona, P.E. and Kelley, W.N. Purinogenic immunodeficiency diseases - selective toxicity of deoxyribonucleosides for T-cells. Proc. Natl. Acad. Sci. U.S.A. 75:5011-5014,1978.

150. Iizasa, T., Kubota, M. and Carson, D.A. Modulation of adenine nucleoside excretion and incorporation in adenosine deaminase deficient human lymphoma cells. Biochem. Biophys. Res. Commun. 121:514-520,1984.

151. Ullman, B., Gudas, L.J., Cohen, A. and Martin, D.W. Deoxyadenosine metabolism and cytotoxicity in cultured mouse T lymphoma cells: A model for immunodeficiency disease. Cell 14:365-376,1978.

152. Bennett, L.L., Jr. and Hill, D.L. Structural requirements for activity of nucleosides as substrates for adenosine kinase: Orientation of substituents on the pentofuranosyl ring. Mol. Pharmacol. 11:803-808,1975.

153. Chang, C.-H., Brockman, R.W. and Bennett, L.L., Jr.

Purification and some properties of a deoxyribonucleoside kinase from L1210 cells. Cancer Res. 42:3033-3039,1982.

154. Henderson, J.F. and Paterson, A.R.P. Nucleoside Metabolism. An Introduction. Academic Press, New York and London, pp. 207-224, 1973.

155. Sugino, Y., Teraoka, H. and Shimono, H. Metabolism of deoxyribonucleosides. I. Purification and properties of deoxycytidine monophosphokinase of calf thymus. J. Biol. Chem. 241:961-969,1966.

156. Mourad, N. and Prks, R.E., Jr. Erythrocytic nucleoside diphosphokinase. J. Biol. Chem. 241:271-278,1966.

157. Gibson, W.B. and Drummond, G.I. Properties of 5'-nucleotidase from avia heart. Biochem. 11:223-229,1972.

158. Naito, Y. amd Lowenstein, I.M. 5'-Nucleotidase from rat heart. Biochem. 20:5188-5194,1981.

159. Pletsch, Q.A. and Coffey, J.W. Studies of 5'-nucleotidase of rat liver. Biochim. Biophys. Acta 276:192-205,1972.

160. Simmonds, H.A., Goday, A., Morris, G.S. and Brolsma, M.F.J. Metabolism of deoxynucleosides by lymphocytes in long-term culture deficient in different purine enzymes. Biochem. Pharmacol. 33:763-770,1984.

161. Graff, J.C., Wolhueter, R.M. and Plagemann, P.G.W. Effects of temperature and of cytochalasin B and

persantin on the non-mediated permeation of non-electrolytes into cultured rat Novikoff hepatoma cells. J. Biol. Chem. 252:4185-4190,1977.

162. Asano, T., Ochiai, Y. and Hiroyoski, H. Selective inhibition of separated forms of human cyclic nucleotide phosphodiesterase by platelet aggregation inhibitors. Mol. Pharmacol. 13:400-406,1977.

163. Chun, H.G., Leyland-Jones, B.R., Caryk, S.M. and Hoth, D.F. Central nervous system toxicity of fludarabine phosphate. Cancer Treat. Rep. 70: 1225-1228,1986.

164. Fludarabine phosphate (FAMP), NSC 312887. Annual Report to the Food and Drug Administration. Division of Cancer Treatment, National Cancer Institute, Bethesda, MD, 1986.

165. Stein, W.D. Transport and Diffusion Across Cell Membranes. Academic Press, Orlando, pp. 363-474,1986.

166. Kimmich, G.A. and Randles, J. Energetics of sugar transport by isolated intestinal epithelial cells: Effects of cytochalasin B. Am. J. Physiol. 237:C56-C63,1979.

167. Plagemann, P.G.W. and Wohlhueter, R.M. Nucleoside transport in cultured mammalian cells. Multiple forms with different sensitivity to inhibition by nitrobenzylthioinosine or hypoxanthine. Biochim. Biophys. Acta 773:39-52,1984.

168. Woffendin, C. and Plagemann, P.G.W. Interaction of [^{3}H] dipyridamole with the nucleoside transporters of human erythrocytes and cultured animal cells. J. Membr. Biol. 98:89-100,1987.

169. Plagemann, P.G.W. and Kraupp, M. Inhibition of nucleoside and nucleobase transport and nitrobenzylthioinosine binding by dilazep and hexobendine. Biochem. Pharmacol. 35:2559-2567,1986.

170. Hladky, S.B. and Rink, T.J. The use of ion transporters, pH measurements and light scattering with red blood cells. In: Ellory, J.C. and Young, J.D. (eds) Red Cell Membranes - A Methodological Approach. Academic Press, London, pp. 335-358,1984.

171. Pressman, B.C. Biological applications of ionophores. Ann. Rev. Biochem. 45:501-530,197

172. Gamble, G.J. and Lehninger, A.L. Transport of ornithine and citrulline accross the mitochondrial membrane. J. Biol. Chem. 248: 610-618,1973.

173. Fromter, E., Muller, C.W. and Wick, T. Permeability properties of the proximal tubular epithelium of the rat kidney studied with electrophysiological methods. In: Giebisch, G. (ed) Electrophysiology of Epithelial Cells. F.K. Schattauer, Sttutgart, pp. 119-146,1971.

174. Beck, J.C. and Sacktor, B. Energetics of the Na^+-

dependent transport of D-glucose in renal brush border membrane vesicles. J. Biol. Chem. 250:8674-8680,1975.

175. Weast, R.C. and Selby, S.M. (eds). Handbook of Chemistry and Physics. The Chemical Rubber Co., Cleveland, p. F124,1966.
of selective ionic effects on Michaelis parameters. J. Membr. Biol. 77:123-152,1984.

176. Asai, M., Hieda, H. and Shimizu, B. Studies on synthetic nucleosides. IV. Preparation of L-beta-ribonucleosides and L-beta-ribo-nucleotides. Chem. Pharm. Bull. 15:1863-1870, 1967.

177. Kinne, R., Murer, H., Kinne-Saffran, E., Thees, M. and Sachs, G. Sugar transport by renal plasma membrane vesicles. Characterization of the system in the brush-border microvilli and basal-lateral plasma membranes. J. Memb. Biol. 21:375-95,1975.

178. Schultz, S.G. and Curran, P.F. Coupled transport of sodium and organic solutes. Physiol. Rev. 50:637-718,1970.

179. Sanders, D. Hansen, U.P., Gradmann, D. and Slayman, C.L. Generalized kinetic analysis of ion-driven cotransport systems: A unified interpretation of selective ionic effects on Michaelis parameters. J. Membr. Biol. 77:123-152,1984.

180. Jacquez, J.A. Sodium-dependence of maximum flux, Jm, and Km of amino acid transport in Ehrlich ascites cells. Biochim. Biophys. Acta 318:411-425,1973.

181. McNamara, P.D., Pepe, Louise M. and Segal, S. Sodium gradient dependence of proline and glycine uptake in rat renal brush-border membrane vesicles. Biochim. Biophys. Acta 556:151-160,1979.

182. Nelson, P.J. and Rudnick, G. The role of chloride ion in platelet serotonin transport. J. Biol. Chem. 257:6151-6155,1982.

183. Turner, R.J. Stoichiometry of cotransport systems. Ann. N.Y.Acad. Sci. 456:10-25,1985.

184. Kimmich, G.A. Gradient coupling in intestinal cells. Fed. Proc. 40:2474-2479,1981.

185. Turner, R.J. and Moran, A. Stoichiometric studies of the renal outer cortical brush border membrane D-glucose transporter. J. Membr. Biol. 67:73-80,1982.

186. Fukuhara, Y. and Turner, R.J. The static head method for determining the charge stoichiometry of coupled transport systems. Applications to the sodium-coupleld D-glucose transporters of the renal proximal tubule. Biochim. Biophys. Acta 770:73-78,1984.

187. Geck, P. and Pfeiffer, B. $Na^+ + K^+ + 2Cl^-$ cotransport in animal cells. Its role in volume regulation. Ann. N.Y. Acad. Sci. 456:166-182,1985.

188. Grinstein, S., Goetz, J.D., Cohen, S., Rothstein, A. and Gelfand, E.W. Regulation of Na^+/H^+ exchange in lymphocytes. Ann. N.Y. Acad. Sci. **456**:207-219,1985.

189. Segel, I.H. Enzyme kinetics: behavior and analysis of rapid equilibrium and steady state enzyme systems. John Wiley & Sons, New York, pp. 346-403, 1975.

190. Turner, R.J. Kinetic analysis of a family of cotransport models. Biochim. Biophys. Acta **649**:269-280, 1981.

191. Skou, J.C. Enzymatic basis for active transport of Na^+ and K^+ across cell membrane. Physiol. Rev. **45**:596-617,1965.

192. Messner, G., Wang, W., Oberleithner, H. and Lang, F. Intracellular ion activities and cell membrane inhibition of Na^+/K^+ ATPase. In: Bronner, F. and Peterlink, M. (eds) Epithelial Calcium and Phosphate Transport: Molecular and Cellular Aspects. Alan Liss, Inc., N.Y., pp. 343-348,1984.

193. Lee, C.W., Cheeseman,C.I. and Jarvis, S.M. Amiloride inhibition of Na^+- and K^+-gradient-dependent uridine transport in rat renal brush border membrane vesicles. Molecular Aspects of Membrane Transport Symposium (Nucleoside Transport Workshop), Banff, Canada, p.18,1987.

194. Cook, J.S., Schaffer, C. and Cragoe, E.J., Jr. Inhibi-

tion by amiloride analagues of Na^+-dependent hexose uptake in LLC-PK_1/Cl_4 cells. Am. J. Physiol. 253:C199-C204,

195. Creighton, T.E. Proteins. Structures and Molecular Principles. W.H. Freeman, New York, pp. 2-60, 1983.

196. Strauss, W.L. Sulfhydryl grups and disulfide bonds: Modification of amino acid residues in studies of receptor structure and function. In: Venter, J.C. and Harrison, L.C. (eds) Receptor Biochemistry and Pharmacology, vol. 1, Alan Liss Inc., New York, pp. 85-97,1984.

197. Uehara, Y., Fusher, J.M. and Rabinovitz, M. Showdomycin and its reactive moiety, maleimide. A comparison in selective toxicity and mechanism of action *in vitro*. Biochem. Pharmacol. 29:2199-2204,1980.

198. Aronow, B., Allen, K., Patrick, J. and Ullman, B. Altered nucleoside transporters in mammalian cells selected for resistant to the physiological effects of inhibitors of nucleoside transport. J. Biol. Chem. 260:6226-6233,1985.

199. Aronow, B., Toll, D., Patrick, J., McCartan, K. and Ullman, B. Dipyridamole-insensitive nucleoside transport in mutant murine T lymphoma cells. J. Biol. Chem. 262:14467-14473,1986.

200. Cohen, A., Leung, C. and Thompson, E. Characterization

of mouse lymphoma cells with altered nucleoside transport. J. Cell. Physiol. 123:431-434,1985.

201. Thompson, L.H. and Baker, R.M. Isolation of mutants of cultured mammalian cells. Meth. Cell Biol. 6:209-281,1973.

202. Chang, T., Maschewske, E., Schneider, H., Croskey, L. Borondy, P. and Glazko, A.J. Metabolic disposition of adenine arabinoside (ara-A) and ara-A-5'-monophosphate (araAMP) in laboratory animals. Fed. Proc. 34:734-739,1975.

203. Weiss, G.R., Gaskill III, H.V. and Phillips, J.L. Pharmacological analysis of the ip administration of fludarabine phosphate in the swine. Cancer Treat. Rep. 70:499-502,1986.

204. Chang, T., Maschewske, E., Schneider, H., Croskey, L., Borondy, P. and Glazko. A.J. Metabolic disposition of adenine arabinoside (araA) and araA-5'-monophosphate (araAMP) in laboratory animals. Fed. Proc. 34:734-739,1975.

205. DeSouza, J.V., Grever, M., Neidhart, J.A., Neidhart, J.A. Staubus, A.E. and Malpeis, L.Comparative pharmacokinetics and metabolism of fludarabine phosphate (NSC 312887) in man and dog. Proc. Amer. Assoc. Cancer Res. 25:361,1984.

206. Plunkett, W., Alexander, L., Chubb, S. and Loo, T.L. Comparison of the activity of 2'-deoxycoformycin and erythro-9-(2-hydroxy-3-nonyl)adenine <u>in vivo</u>.

Biochem. Pharmacol. 28:201-206,1979.

207. Trotta, P.P., Ahland, M.P., Brown, G.F. and Balis, M.E. Studies on the effects of enzyme inhibitors on mouse adenosine deaminase. Mol. Pharmacol. 14:199-109,1978.

208. Trotta, P.P., Tedde, A. and Balis, M.E. In vivo effects of deoxycoformycin on mouse adenosine deaminase and nucleoside phosphorylase. Proc. Amer. Assoc. Cancer Res. 20:284,1979.

209. Hutton, J.J. Von Hoff, D.D., Kuhn, J., Phillips, J.H., Heish, M. and Clark, G. Phase I clinical investigation of 9-beta-D-arabinofuranosyl-2-fluoroadenine 5'-monophosphate (NSC 312887), a new purine antimetabolite. Cancer Res. 44:4183-4186, 1984.

210. Leiby, J.M., Grever, M.R., Staubus, A.E., Neidhart, J.A. and Malspeis, L.A. Phase I clinical investigation of fludarabine phosphate by loading dose/continuous infusion. Proc. Amer. Assoc. Cancer Res. 26:669,1985.

211. Fludarabine phosphate. National Cancer Institute Annual Report. Bethesda, Maryland, USA. August 1986.

212. Merkel, D.E., Griffin, N.L., Kagan-Hallet, K. and Von Hoff, D.D. Central nervous system toxicity with fludarabine. Cancer Treat. Rep. 70:1449-1450,1986.

213. Spriggs, D.R., Stopa, E., Mayer, R.J., Schoene, W. and Kufe, D.W. Fludarabine phosphate (NSC 312878) infusions for the treatment of acute leukemia: Phase I and neuropathological study. Cancer Res. 46:5953-5958,1986.

214. Kaplan, R.S. and Wiernik, P.H. Neurotoxicity of antineoplastic drugs. Semin. Oncol. 9:103-130,1982.

215. Skipper, H.E., Montgomery, J.A., Thomson, J.R. and Schabel, F.M., Jr. Structure-activity relationships and cross-resistance observed on evaluation of a series of purine analogs against experimental neoplasms. Cancer Res. 19:425-437,1959.

216. Avramis, V.I. and Plunkett, W. 2-Fluoro-ATP: A toxic metabolite of 9-beta-D-arabinosyl-2-fluoroadenine. Biochem. Biophys. Res. Commun. 113:35-43,1983.

217. Mahony, C., Wolfram, K.M., Cocchetto, D.M. and Bjornsson, T.D. Dipyridamole kinetics. Clin. Pharmacol. Ther. 31:330-338,1982.

218. Cornford, E.M. and Oldendorf, W.H. Independent blood-brain barrier system for nucleic acid precursors. Biochim. Biophys. Acta 394:211-219,1975.

219. Wu, P.H. and Phillis, J.W. Uptake of adenosine by isolated rat brain capillaries. J. Neurochem. 38:687-690,1982.

220. Stefanovich, V. Uptake of adenosine by isolated bovine cortex microvessels. Neurochem. Res. 8:1459-

1469,1983.

221. Morgan, P.F. and Marangos, P.J. Comparative aspects of nitrobenzylthioinosine and dipyridamole inhibition of adenosine accumulation in rat and guinea pig synaptosomes. Neurochem. Int. 11:339-346, 1987.

222. Thampy, K.G. and Barnes, E.M. Adenosine transport by primary cultures of neurons from chick embryo brain. J. Neurochem. 40:874-879,1983.

223. Thampy, K.G. and Barnes, E.M. Adenosine transport by cultured glial cells from chick embryo brain. Arch. Biochim. Biophys. 220:340-346,1983.

224. Bender, A.S. and Hertz, L. Similarities of adenosine uptake systems in astrocytes and neurons in primary cultures. Neurochem. Res. 11:1507-1524,1986.

225. Agarwal, R.P., Busso, M.E., Mian, A.M. and Resnick, L. Studies on the intracellular accumulation of 2',3'-dideoxyadenosine in human cells. Proc. Amer. Assoc. Cancer Res. 29:347,1988.

226. Placke, M.E., Mezza, L.E., Singer, A.W., Tomaszewski, J.E., and Grieshaber, C.K. 28-Day study of 2',3'-dideoxyadenosine in rats and dogs. Proc. Amer. Assoc. Cancer Res. 29:510, 1988.

227. Southern, P.J. and Berg, P. Transformation of mammalian cells to antibiotic resistance with a

bacterial gene under control of the SV40 early region promoter. J. Mol. Appl. Genet. 1:327-241, 1982.

228. Enquist, L.W., Van de Woude, G.F., Wagner, M., Smiley, J.R., and Summers, W.C. Construction and characterization of a recombinant plasmid encoding the gene for the thymidine kinase of Herpes simplex Type I virus. Gene 7:335-342,1979.

229. Gargus, J.J. Mutant isolation and gene transfer as tools in study of transport proteins. Am. J. Physiol. 252:C457-467,1987.

230. Thorpe, W. Reductionism vs. organicism. New Scientist, 635-638,1969.